

**BENCH MARKING
RAINFALL RUNOFF MODELS
WITHIN THE ANGLIAN REGION**

FINAL REPORT

A.R. Young

This report is an official document prepared under contract between the Environment Agency and the Natural Environment Research Council. It should not be quoted by third parties without permission of both the Environment Agency and the Institute of Hydrology.

Institute of Hydrology
Crowmarsh Gifford
Wallingford
Oxfordshire
OX10 8BB

Tel: 01491 838800
Fax: 01491 692424



ENVIRONMENT AGENCY

NATIONAL LIBRARY &
INFORMATION SERVICE

ANGLIAN REGION

Kingfisher House, Goldhay Way,
Orton Goldhay,
Peterborough PE2 5ZR

1997

Executive Summary

This report presents the work undertaken during the project "Bench marking of rainfall runoff models within the Anglian region" commissioned by the Anglian Region of the Environment Agency. The primary objective of the project has been to evaluate the utility of selected lumped rainfall runoff models as operational tools within the Anglian region of the Environment Agency.

From their experience in using a range of rainfall runoff models, staff in the Anglian Region have found that the accuracy of results is vary variable. This lack of consistency between the performance of different models, combined with wide variability in their ease of use, pose considerable difficulties in the use of these models in water resources planning and abstraction licensing decisions.

Within this study, the capability, scientific integrity and accessibility of available models has been reviewed. Based upon this assessment a short list of four models were selected in conjunction with Agency Staff. The four models selected as being broadly representative of the model classes reviewed were:

- Hydrological Simulation Model (HYSIM);
- Thames Catchment Model (TCM);
- Probability Distributed Model (PDM);
- Identification of Unit Hydrograph and Component Flows from Rainfall, Evaporation and Streamflow Data (IHACRES)

HYSIM is a traditional complex conceptual model in which the response of the conceptual representation of the hydrological processes is controlled by parameters, many of which the Author has sought to relate to physical catchment properties. The TCM is also a conceptual model, based on a simple Penman drying curve based loss module coupled with a series combination of a linear reservoir and a quadratic reservoir. Within the TCM the catchment can be modelled as one or two hydrological zones. The PDM is a fairly general conceptual rainfall -runoff model with a maximum of 14 calibration parameters. The PDM utilises a probability distributed soil moisture store in conjunction with combinations of linear and non linear storage reservoirs to route outflow from the soil moisture store through surface and groundwater storage. The version of IHACRES selected for this study is the PC implementation of the model, PC-IHACRES V1.0. The PC version of IHACRES comprises a non-linear empirical loss module in series with either a single linear unit hydrograph (UH) model or, alternatively, two linear unit hydrograph models in parallel or series.

These models have been evaluated within five representative, case study catchments within the Anglian region. This bench marking has been undertaken using criteria that not only reflect the scientific integrity of the models but also their appropriateness for addressing water resource issues. These criteria were applied to the model output over both calibration and evaluation periods of record.

The catchments selected were as follows:

- Babingley Brook above the Castle Rising gauging station (33054);
- Sapiston Brook above the Rectory Bridge gauging station (33013);
- River Nene above the Orton gauging station (32001);
- River Blackwater above Appleford Bridge (37010);
- River Box above Polstead Bridge (36003).

The results of the bench mark tests demonstrated that the the best model fits were consistently obtained for the Babingley Brook and the worst for the River Box. The model fits for the Blackwater were consistently fourth. During the calibration periods the model fits were better for the Nene than the Sapiston, however over the evaluation period better model fits were obtained for the Sapiston than for the Nene. It was not apparent from the analysis that particular models were more suitable than others for specific catchment types.

Considering individual models the PDM was the most consistent model across the calibration period followed by HYSIM, IHACRES and then the TCM. HYSIM gave better results over the evaluation period than the PDM and, when jointly considering the performance in the calibration period and the departure from that performance in the evaluation period, HYSIM was the most consistent of the four models. The PDM was the second most consistent model overall, followed by IHACRES and the TCM in that order.

In conclusion, this report recommends that HYSIM is the most suitable model for adoption by the Anglian region of the Environment Agency. This recommendation is subject to the proviso that the model is very complex and that the use of default values for many of the parameters within the model must raise the question of whether this level of complexity is warranted. Furthermore the strong structural interrelationships observed during calibration between the primary parameters must be a cause for concern regarding parameter identifiability.

The PDM and IHACRES are recommended as models worthy of future consideration for use. The former, although a mature model is not sufficiently matured as a daily flow modelling package for operational use, whilst the latter would benefit from having alternative loss module configurations included in the package. The Wilby implementation of the Thames Catchment Model is not recommended as an operational model. This is not a reflection of the model itself, but rather the limitations of the model package.

Contents

1.	INTRODUCTION AND MODEL SELECTION	1
1.1	The requirement for robust rainfall runoff models within the Anglian region	1
1.2	Model selection	2
1.2.1	Model Classification	2
1.2.2	Selection of bench mark models	6
2.	SELECTED REPRESENTATIVE RAINFALL RUNOFF MODELS	9
2.1	The Hydrological Simulation Model (HYSIM)	9
2.1.1	Overview	9
2.1.2	Snow and interception stores	10
2.1.2	Soil Moisture Store	10
2.1.3	The Groundwater Store	13
2.1.4	The Minor Channels Store and Hydraulic Routing	13
2.1.3	The package	15
2.2	The Thames Catchment Model	17
2.2.1.	Overview	17
2.2.2	The soil moisture store	17
2.2.3	The linear store	18
2.2.4	The non-linear store	18
2.2.5	The Package	22
2.3	The Probability Distributed Model	23
2.3.1	Overview	23
2.3.2	Soil moisture store	23
2.3.3	Surface and subsurface storages	31
2.3.4	The Package	32
2.4	Identification of unit Hydrographs And Component flows from Rainfall, Evaporation and Stream flow data (IHACRES)	34
2.4.1	Overview	34
2.4.2	The non-linear (loss) module	34
2.4.3	The linear (UH) module	36
2.4.3	Model calibration and the package	39
3.	APPLICATION OF THE MODELS WITHIN THE CASE STUDY CATCHMENTS	41
3.1	Catchment descriptions	41
3.2	Climatic data	43
3.3	Application of the models within the case study catchments.	45
3.3.1	HYSIM	45
3.3.2	IHACRES	46
3.3.3	Thames Catchment Model	47
3.3.4	Probability Distributed Model	48
4.	EVALUATION OF MODEL PERFORMANCE WITHIN THE CASE STUDY CATCHMENTS.	50
4.1	Evaluation criteria	50
4.2	Evaluation of model performance within the case study catchments	51
4.2.1	The Babingley Brook at Castle Rising	51

4.2.2	The Sapiston at Rectory Bridge	53
4.2.3	The Nene at Orton	55
4.2.4	The Blackwater at Appleford Bridge	56
4.2.5	The Box at Polstead Bridge	57
4.3	Inter-catchment and model comparisons	58
4.3.1	Inter-catchment comparison	59
4.3.2	Inter-model comparisons	61
5.	CONCLUSIONS	63
6.	REFERENCES	65

1. Introduction and Model Selection

1.1 THE REQUIREMENT FOR ROBUST RAINFALL RUNOFF MODELS WITHIN THE ANGLIAN REGION

The primary objective of the project has been to evaluate the utility of selected lumped rainfall runoff models as operational tools within the Anglian region of the Environment Agency. Rainfall runoff models are used to simulate river flows from climatic data using a mathematical description of the runoff generating processes for the management of water resources and flood events. The complexities of model classification are discussed in the subsequent section.

Daily mean flows (and to a lesser extent mean flows of longer duration) measured at gauged locations are the principal basic source of data for resource analysis. Lumped rainfall runoff models are extensively used within water resources to infill missing periods within gauged flow records, to simulate naturalised time series of flows, for extending short historical flow records and for evaluating the impact of existing and proposed water resources schemes and levels of demand/return.

The basic requirements of a rainfall runoff model are that the model should reliably simulate actual evaporation losses (extremely important in East Anglia as annual rainfall and evaporation are of similar magnitude within the region) and the routing of effective precipitation through the catchment. Ideally the model should also be able to simulate the impacts of artificial influences (including ground water abstractions where appropriate) although the number of models that meet this latter requirement are limited as, historically, this type of model has been developed for flood analysis where these influences constitute a small part of the water balance. To enable a model to be used as an operational water resource tool the model must also be user friendly and easy to apply.

From their experience in using a range of rainfall runoff models, staff in the Anglian Region have found that the accuracy of results is vary variable. This lack of consistency between the performance of different models, combined with wide variability in their ease of use, pose considerable difficulties in the use of these models in water resources planning and abstraction licensing decisions.

Within this study, the capability, scientific integrity and accessibility of available models has been assessed. Based upon this assessment a short list of four models were selected in conjunction with Agency Staff. These models have been evaluated within five representative, case study catchments within the Anglian region. This bench marking has been undertaken using criteria that not only reflect the scientific integrity of the models but also their appropriateness for addressing water resource issues.

The criteria used for short listing models and the selection of the four models is presented in the following section. The four short listed models and associated modelling packages are presented in greater detail in Chapter 2. The case study catchments and the application of the models within these case study catchments is presented in Chapter 3. The evaluation of the

models within the case study catchments is presented in Chapter 4. In this chapter the goodness of fit criteria used to evaluate the models are presented, model performance within individual catchments is discussed and the application of a ranking scheme for making inter-catchment and inter-model comparisons is presented. In the conclusions (Chapter 5) to the study recommendations are made as to the suitability of the models for operational application within the Anglian Region. These recommendations are made in the context of whether it is practicable to definitively conclude that one model is "better" than the next.

1.2 MODEL SELECTION

1.2.1 Model Classification

As discussed in section 1.1 the primary objective of rainfall runoff modelling is to simulate river flows from climatic data using a mathematical description of the runoff generating processes for the management of water resources and flood events. Secondary objectives may include the enhancement of knowledge about hydrological processes controlling runoff generation and recharge. These broad aims have led to a proliferation of models and modelling philosophies. As a general rule; the complexity of the model, and associated data requirements, increase rapidly when seeking to understand the catchment hydrological processes.

Many Authors have provided classification schemes for modelling philosophy; Hughes (1995) draws a distinction between models based upon the level of detail included in the representation of catchment processes and the time and space resolutions of the model. He quotes that models range in complexity from fully distributed, fine time interval models, which include detailed representations of catchment hydrological processes based upon physical laws, to models based upon a coarse time interval which are lumped or semi-distributed and where catchment processes are represented conceptual storages linked by empirical transfer functions. Todini (1988) developed a four class system based upon the degree of prior knowledge, this classification is summarised in Figure 1.1. The system differentiates between models on the initial basis of whether processes are represented statistically or physically and then how these processes are distributed and solved mathematically across the catchment.

Singh (1995) recognised the large number of possible permutations that can be obtained by classifying a model according to the spatial and temporal resolution of the application and the representation of physical processes. He proposed that models may be classified according to:

- process description;
- space and time scales;
- method of solution.

These three classifications are described schematically in Figure 1.2.

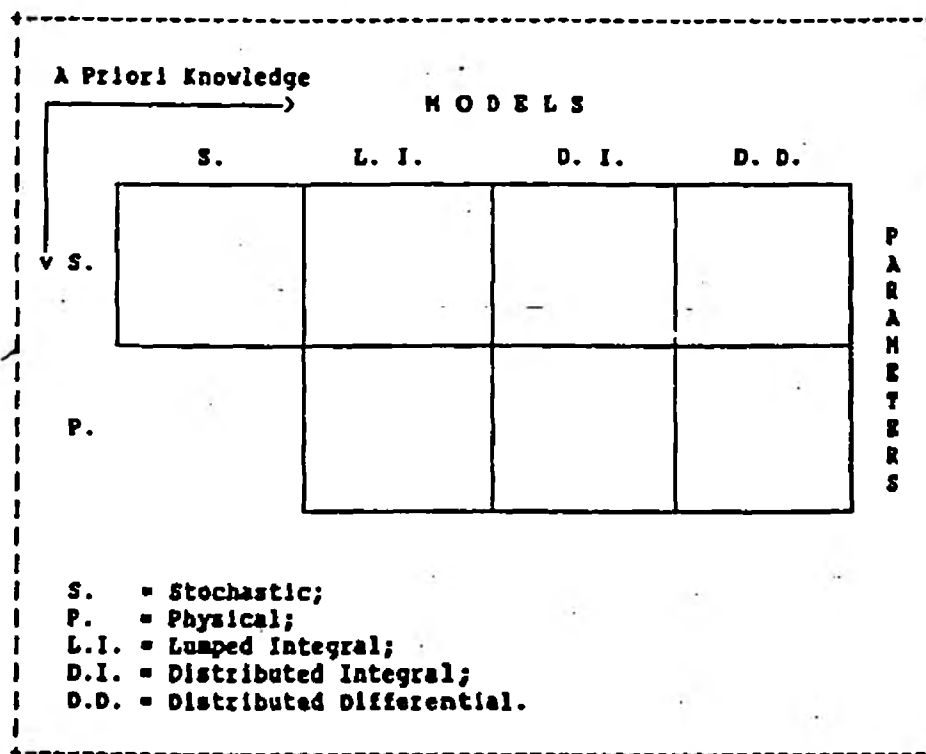


Figure 1.1: Classification based on level of prior knowledge (Todini, 1988)

However, in reality the boundaries between classifications and between the individual boxes within a classification are not clearly defined. Many models are essentially hybrid with constituent parts drawing from stochastic and deterministic components. The deterministic components may seek to describe the physics of the process, commonly called physically based, or may use a conceptual representation of the physical processes. Physically based models, tend to be distributed in nature (although not always) in that the model equations include space co-ordinates. Additionally, stochastic techniques are now commonly used when formulating the catchment implementation of deterministic model components; for example, the semi-distributed soil moisture module of the ARNO model (Todini, 1995). Singh in his 1995 paper states:

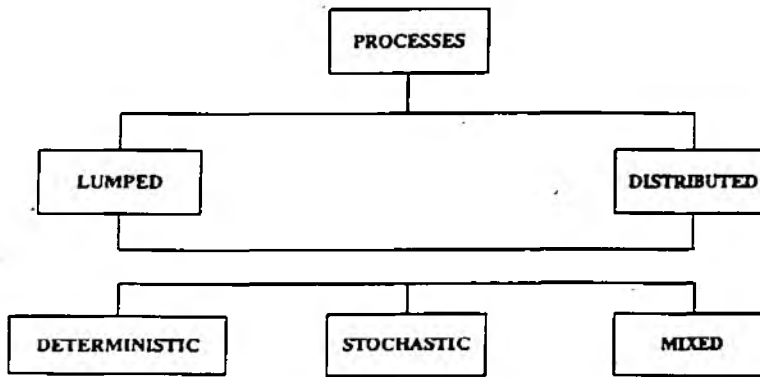
“A vast majority of the (available) models are deterministic, and virtually no model is fully stochastic. In some cases, only some parts of the model are described by the laws of probability, and other parts are fully deterministic. It is then fair to characterise them as quasi-deterministic or quasi-stochastic.”

An argument can be constructed that no model components are truly physically based. Any mathematical description of a process is a model of that process and thus is always conceptualisation. However the important factor is that the parameters of a physically based model can be determined independently from the model and therefore the model should not require calibration.

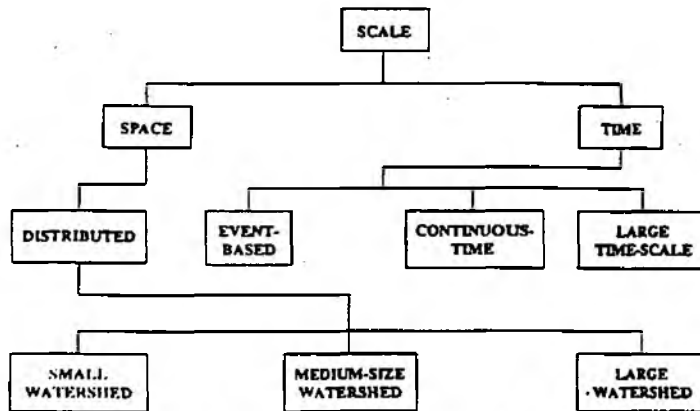
The preservation of the physicality of physically based deterministic model components can also be called into question in the application of the model. The uncertainty in input climatic data and field measurement of parameter values data will generally mean that the model will require calibration to compensate for these uncertainties. Catchment rainfall, whether represented as distributed values or as a catchment average, is the classic example of this. The spatial distribution of rainfall is derived by means of an interpolation procedure based on point measurements, sometimes with altitude corrections. The resultant distribution is thus an approximation to the true catchment rainfall. When calibrating parameters within a hydrological model the value of the parameters will be a function of the model structure, the uncertainty in the rainfall data, the objective function(s)/criteria used to determine goodness of fit and the calibration techniques employed. Hence the true physicality of the model is compromised.

In the context of this study a model is considered to be "lumped" if the input data, output data and model equations do not include a spatial description. This definition does not make a distinction between stochastic or deterministic formulations. However, it is implicit that models which use numerical techniques, such as finite element or finite difference schemes, to represent the spatial component of a deterministic formulation will always be distributed in nature as, regardless of the nature of the input/output data, these models utilise georeferenced, distributed catchment characteristic data.

(a) Classification of models on process description



(b) Classification of models based on space and time scales



(c) Classification of models based on method of solution

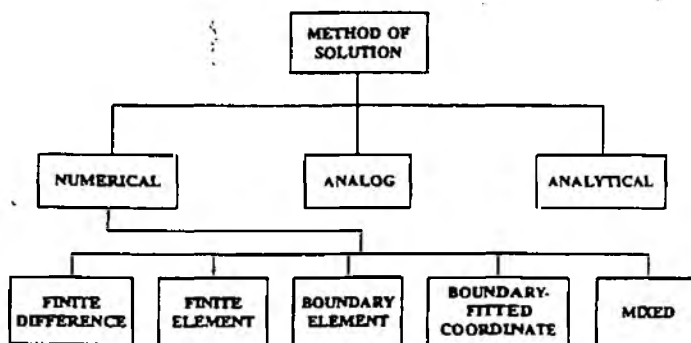


Figure 1.2: Model Classifications defined by Singh (1995)

1.2.2 Selection of bench mark models

A literature review of lumped, or semi distributed rainfall runoff models suitable for continuous simulation of daily mean flows has been undertaken. The review considered the following questions:

- Is there peer reviewed evidence of the models capabilities ?
- Is the model commercially available, public domain or published in full within the literature?
- What are the input data requirements ?
- Can the mode incorporate the impact of artificial influences on the flow regime ?
- Is the model stochastic, deterministic or hybrid ?
- If determinist, are the model conceptualisations physically based or empirical in nature ?
- What are the nature of the parameters used within the model ?
- How complex is the model (a subjective decision made on the basis of the number of parameters and the complexity of the input data requirements) ?
- If automatic calibration schemes exist for a model, what optimisation routines and associated objective functions are employed within the schemes ?
- If the model is packaged, what analysis functions are available ?
- If the model is packaged, what is the target operating platform(s)?

The review identified 19 distinct models which ranged from models published in refereed journals through public domain packaged models to packaged models marketed by the authoring organisations as commercial products. These are summarised in Table 1.1. From this review the following four models were selected as being broadly representative of the model classes reviewed:

- Hydrological Simulation Model (HYSIM);
- Thames Catchment Model (TCM);
- Probability Distributed Model (PDM);
- Identification of Unit Hydrograph and Component Flows from Rainfall, Evaporation and Streamflow Data (IHACRES)

HYSIM (Manley, 1978) is a traditional complex conceptual model in which the response of the conceptual representation of the hydrological processes is controlled by parameters, many of which Author has sought to relate to physical catchment properties. The development history of HYSIM dates back to the 1970s. When developing HYSIM, the Developer had the primary objective of producing a flexible model with physically significant model parameters.

The TCM (Greenfield, 1984) is also a conceptual model, based on a simple Penman drying curve based loss module coupled with a series combination of a linear reservoir and a quadratic reservoir. Within the TCM the catchment can be modelled as one or two

hydrological zones.

The PDM (Moore, 1985) is a fairly general conceptual rainfall -runoff model with a maximum of 14 calibration parameters. The PDM utilises a probability distributed soil moisture store in conjunction with combinations of linear and non linear storage reservoirs to route outflow from the soil moisture store through surface and groundwater storage. The catchment soil moisture store is conceptualised as a store of finite storage capacity but with different points within the catchment having different storage capacities. The spatial variation of this capacity is described by a probability distribution. The PDM has been applied as either a lumped model or a semi-distributed model.

The version of IHACRES selected for this study is the PC implementation of the model, PC-IHACRES V1.0, which has been packaged by the Institute of Hydrology as a commercial product. The IHACRES methodology (Jakeman et al.,1990; Littlewood & Jakeman, 1994) has been developed collaboratively by the Institute of Hydrology and the Centre for Resource and Environmental Studies at the Australian National University (CRES at ANU). The PC version of IHACRES comprises a non-linear empirical loss module in series with either a single linear unit hydrograph (UH) model or, alternatively, two linear unit hydrograph models in parallel or series. The response of the usual configuration of the loss model in series with two parallel UH models is controlled by six parameters.

These models are presented in greater detail in Chapter 2.

Table 1.1: Models reviewed

Model	Author	Reference
Hydrological Rainfall RunOff Model (HYRRROM)	Institute of Hydrology	Blackie & Eeles, 1985
Probability Distributed Model (PDM)	Institute of Hydrology	Moore, 1985
ARNO	Inst. Hyd. Con. Univ. Bologna, IT	Todini, 1995
Hydrological, Simulation Model HYSIM	R.E. Manley, Cambridge	Manley, 1978
Thames Catchment Model	B. Greenfield, Thames EA	Greenfield, 1984, NRA R&D Note 268
TANK Model	M.Sugawara Tokyo	Sugawara, 1995
UBC	Univ. Brit. Colombia. CA	Quick, 1995
Precipitation - Runoff Modelling System (PRMS)	USGS-Wat. Resources. Div.	Leavesly & Stannard, 1995
Sacramento Catchment Model	US-Dept. Of Commerce. Nat. Weather Service.	Burnash, 1995
Streamflow Synthesis and Reservoir Regulation (SSARR)	Hydrologic Engineering Center - US Army Corp	Speers 1995
The HBV Model	Swedish Met. & Hydrol. Institute	Bergström & Forsam 1973
NAM (inc. into MIKE II)	Marketed by DHI	Nielson & Hansen, 1973
IH-ACRES	Institute of Hydrology/CRES-Australia	Institute of Hydrology, 1997
Great Ouse Resource Model GORM	WRc	WRc., 1990.
SFB	Boughton	Boughton, 1984
MODHYDROLOG	Univ. Melbourne	Chiew & McMahon, 1991
STANFORD IV	NOAA, NWS	Crawford & Linsley ,1966
XINANJIANG	East China College of Hydraulic Engineering	Zhao et al, 1980
CREC	N/A	Servat & Dezetter, 1991
VTI-HYMAS GR3	Rhodes University CEMAGREF, France	Hughes& Sami, 1994 Edijatno & Michel, 1989

2. Selected representative rainfall runoff models

This chapter presents the detail of the four rainfall runoff models selected for evaluation in the bench mark catchments. The chapter concentrates on the structure of the models and a summary of the package details focussing on the calibration procedures. To aid the discussion of mathematical formulations, a distinction is made between explicit and implicit functions and their solution. An explicit function is one in which the variable of interest is a function of (n) independent variables. An implicit function occurs when the variable of interest cannot be expressed as a function of independent variables. The response function for a linear reservoir is an example of this where the outflow at time t is a function of the water in storage at time t. However the water in storage is a function of both the inflow and the outflow at time t. Implicit functions require solution using iterative numerical schemes.

In the case of the linear reservoir, as will be demonstrated, an explicit formulation can be obtained for this implicit solution, when applied on discretised data, by considering continuity over a time step and solving for the mean outflow over the time step and the outflow at the end of the time step. To apply the explicit solution assumes that the change in storage over the time step is small in comparison with the total volume of water in storage and thus the outflow in time step t is a function of the storage at the end of the previous time step. Explicit solutions generally require a smaller time step so that the variables on the right hand side of the equation are changing slowly. It is more difficult to spot instability because it is almost always possible to achieve a solution although may not be valid. One way to avoid the time step limitation is to apply the explicit solution recursively within a time step. In this application the value of the dependent variable at the end of the time step has been calculated using values for the variables on the right hand side of the solution that have been computed from within the time step. The recursive application of an explicit solution can be considered to be an implicit solution.

2.1 THE HYDROLOGICAL SIMULATION MODEL (HYSIM)

2.1.1 Overview

HYSIM is a commercial package authored by R.E. Manley. The origins of the model date back to the 1970s, however the commercial PC version of HYSIM, written in MicroSoft Visual Basic for DOS, was released in 1992. HYSIM is a seven store conceptual model coupled to a simple hydraulic routing model. This structure is summarised in Figure 2.1. When developing the model the author had the primary requirement that the parameters of the model should be physically significant (Manley, 1978). This discussion on HYSIM is predominantly based on the information published in the user and technical guides (Manley 1992a, 1992b).

HYSIM can be applied to single or multiple sub-catchments, each of which should be homogeneous with respect to soil type and climate. The model can receive input of five distinct data types, of which none are compulsory. These are:

- catchment average precipitation time series;
- catchment average potential evapotranspiration;
- catchment average potential melt rate for snow;
- nett effluent/ surface water abstraction rate;
- total groundwater abstraction rate.

The time step for these data can be monthly, daily or sub-daily although there are constraints on mixing data of differing time steps. The model has been coded so that the hydraulic and hydrological components can also be run on different time steps.

2.1.2 Snow and interception stores

If the incident precipitation is in the form of snow (as defined in the input data) it enters a semi - infinite store. If there is snow in storage at time step i the outflow is equal to the input melt rate within the time step. The interception store represents detention of water on vegetation. The capacity of the interception store (C_i) has a maximum capacity defined by the maximum depth of the store (I_{max}) and the impermeable fraction of the catchment:

$$C_i = I_{max} \times \frac{[1-IMPERMEABLE AREA]}{TOTAL AREA} \quad 2.1.1$$

The store receives water from precipitation and snow melt (if any) and loses water by evaporation, which takes place at the potential rate. Excess precipitation (EP) from the interception store is partitioned between the upper soil horizon and minor channel storage according to the fractional extent of the impermeable area of the catchment.

2.1.2 Soil Moisture Store

The soil moisture store consists of two stores; the Upper Soil Horizon (USH) and the Lower Soil Horizon. The USH represents moisture held in the top soil (the A soil horizon) whilst the LSH represents moisture below the USH but still within the rooting depth (the B and C soil horizons). The USH has a finite capacity given by:

$$C_{USH} = D_{USH} \times f_{USH} \quad 2.1.2$$

where D is the depth of the zone (mm) and f is the mean porosity of the zone.

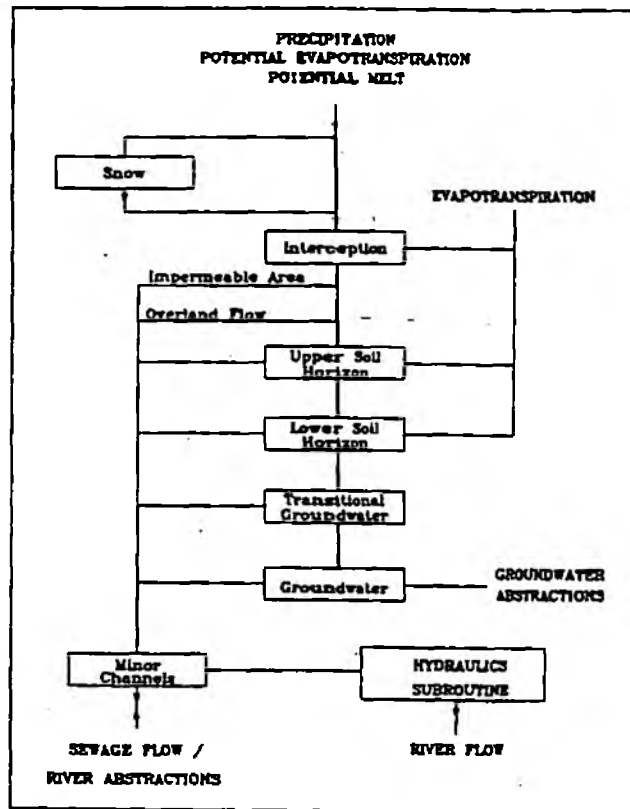


Figure 2.1: The Structure of HYSIM

The maximum rate at which the store can accept EP is determined by an approximation to the Philip's infiltration equation (Philip, 1957). Manley (1977) demonstrated that Philip's equation can be approximated by:

$$x = (2k_1 P.t)^{0.5} + k_1 t \quad 2.1.3$$

where x is the distance travelled downwards by the wetting front (mm), k_1 is the saturated permeability at the top of the horizon (mm/hr), t is the duration of the time step and P is the capillary suction (mm. H_2O).

This relationship facilitates the calculation of the maximum, or potential, infiltration rate across the time step. EP routed to the USH in excess of this limiting rate is routed to the minor channels store as overland flow. It has been demonstrated that P can be expressed as:

$$P = \frac{P_b}{S_e^{1/\gamma}} \quad 2.1.4$$

Where P_b is the bubbling pressure (mm/hr), γ is the pore size distribution index and S_e the

effective saturation. S_e is defined as:

$$S_e = \frac{m - S_r}{1.0 - S_r} \quad 2.1.5$$

Where m is the saturation at the beginning of the time step and S_r is the residual saturation which is the minimum saturation that can be obtained by de-watering the soil under increasing suction. Evapotranspiration takes place from the USH at the potential rate (minus any loss from the interception storage) if P is less than 15 atmospheres. If P is greater than 15 atmospheres evaporation takes place at a rate reduced in proportion to the remaining depth of water in storage.

The next transfer of moisture is via inter flow. The conceptualisation of inter flow is based on the Brookes and Corey empirical model for the effective permeability of porous media. Inter flow is calculated using:

$$\text{Interflow} = Rfac_1 (S_e)^{(2+3\gamma)/\gamma} \quad 2.1.6$$

where $Rfac_1$ is defined as the inter-flow run-off from the USH at maximum saturation. The power function of S_e is used to modulate $Rfac_1$ when the saturation is lower than the maximum. This reflects that, conceptually, lateral permeability will be less when the soils are not fully saturated. The final transfer of moisture is by percolation from the USH to the LSH, where percolation is estimated in an analogous way to inter flow using :

$$\text{Percolation} = K_b (S_e)^{(2+3\gamma)/\gamma} \quad 2.1.7$$

where K_b is saturated permeability at the horizon boundary. By combining the equations for inter flow and percolation the change in storage can be estimated using:

$$\frac{ds}{dt} = I - (Rfac_1 + k_b) S_e^{(2+3\gamma)/\gamma} \quad 2.1.8$$

Where I is the net inflow rate. This ordinary differential equation cannot be solved explicitly as the value of S_e is a function of the water in storage. However, an analytical approximation is found if the inflow over a time step is constant and the total change in storage over a time step is small in comparison to the total depth of water in storage at the start of the time step. This latter assumption means that S_e can be taken as being constant over the time step being considered. Within HYSIM the change in storage is constrained to lie between an upper and lower limit. The upper limit is defined by the level of storage at which the rate of outflow is equal to the rate of inflow. The lower limit results from setting $I=0$. It is not clear whether this approximate solution ensures that mass is conserved.

The percolation from the USH forms the input to the lower soil horizon (LSH). The LSH is configured in a similar way to the USH where the infiltration of percolation is controlled by

the ability of the LSH to accept percolation from the USH. Percolation in excess of the infiltration capacity is routed to the minor channels store. Loss from the LSH through inter flow and percolation to the groundwater is controlled by similar equations to the USH. Evaporation potential that is not met by the USH is met from the LSH, subject to the same suction pressure constraint that operated in the USH.

2.1.3 The Groundwater Store

The groundwater store is subdivided into two infinite linear reservoirs; the transitional groundwater and deep groundwater stores. The transitional groundwater store which receives percolation from the LSH, is taken to represent the first stage of groundwater storage where direct discharge to surface waters may occur via fissure flow, etc. The outflow from the transitional groundwater store is partitioned between the minor channels store and the deep groundwater store. The deep groundwater store discharges to the minor channels. It is from this groundwater store that ground water abstractions can be made. The functions defining the outflow, q , from a linear reservoir are given by:

$$q = \frac{1}{k} s, \quad 2.1.9$$

where s is the volume of water in storage and k is a constant (with units of time). This explicit formulation neglects that within a timestep the instantaneous value of s is dependent on the function of the outflow q . Combining this power equation with the equation of continuity:

$$\frac{ds}{dt} = u - q \quad 2.1.10$$

where u is the inflow over the time period yields:

$$\frac{dq}{dt} = \frac{1}{k} q(u - q) \quad 2.1.11$$

which is the linear representation of the Horton-Izzard model (Dooge, 1973). Rearranging 2.1.11 and integrating over the time period $(t, t+\tau)$ gives the explicit recursive solution for q as:

$$Q_{(t+\tau)} = e^{-\frac{\tau}{k}} q_t + u \left(1 - e^{-\frac{\tau}{k}} \right) \quad 2.1.12$$

A useful summary of the mathematical formulation of non-linear reservoirs (of which the linear reservoir is a special case) is presented in Moore et al, 1993. It is not clear whether this solution is implemented recursively within a time step in HYSIM, or whether the explicit form is used where the change in storage is assumed to be small over the entire time step compared with the total volume of water in storage. The mean output over the time period is given by the integral of this solution for q over the time step divided by the duration of the time step.

2.1.4 The Minor Channels Store and Hydraulic Routing

The minor channels store conceptually represents the routing of flows in minor streams, ditches and, if the catchment is saturated, ephemeral streams. This store uses a triangular Instantaneous Unit Hydrograph (IUH), with the time base equal to 2.5 times the time to peak. The time to peak is estimated using the Flood Studies Report equation (NERC, 1975):

$$T_p = 2.8 \left(\frac{L}{\sqrt{S}} \right)^{0.47} \quad 2.1.13$$

Where T_p is the time to peak, L is the stream length (km) and S is the stream slope (m/km). The time base of the IUH response to influent volume, $V_i = q_i \cdot t$, in time step (t) will be defined by:

$$T_L = 7 \left(\frac{L}{\sqrt{S}} \right)^{0.47} \quad 2.1.14$$

where T_L is the time base of hydrograph, and q_i is equal to zero at $\tau = 0$ and $\tau = T_L$. The maximum flow rate (q_{max}) occurs at T_p and is given by:

$$q_{max} = \frac{q_i \cdot t}{1.25 T_p} \quad 2.1.15$$

The "main" river within HYSIM is represented as a number of hydraulically homogenous reaches. Velocity of water along a reach is described by the kinematic wave approximation to the Saint Venant equations:

$$V_w = \frac{Q}{A} \quad 2.1.16$$

Where ΔQ and ΔA are the incremental changes in velocity along the reach and hydraulic cross-sectional area. The kinematic wave approximation is used as the Saint Venant equations cannot be solved explicitly. An empirical model is used within HYSIM for estimating cross-sectional area. The approximation takes into account that most channels lie between the two extremes of a rectangular channel and triangular channel. The form of this approximation is as follows:

$$Q = CA^{1.5} \quad 2.1.17$$

where C is a coefficient of proportionality. If out of bank flows can occur the manual advises the user to develop site specific coefficients which HYSIM will use under these conditions. The manual also advises the development of two such sets; the first for use when the flood plain is filling and the second for when the flood plain is full. HYSIM has facilities for using the hydraulic sub model to link together a number of sub catchment models in series, thus enabling the model to be used in a semi-distributed mode. The hydrological and hydraulic parameters controlling the response of HYSIM are summarised in Tables 2.1 and 2.2.

2.1.3 The package

HYSIM has facilities for pre-processing input data, which are described in detail within the HYSIM user manual. Calibration of HYSIM may be undertaken manually or automatically using either the Newton Raphson method of successive approximation for individual parameters or the Rosenbrock local search technique (Rosenbrock, 1960) for the simultaneous optimisation of several parameters. For the Newton Raphson method the objective function is the difference between simulated and observed mean flow. For the Rosenbrock methods the objective function can be selected from a choice of:

- The Proportional Error of Estimate (P.E.E); given by

$$P.E.E. = \frac{F - F_R}{F_R^2} \times \frac{1}{n-1} \quad 2.1.18$$

where F is the simulated daily flow, F_R is the recorded daily flow and n the number of days used for the calibration. In the P.E.E errors are normalised by the recorded flow and thus the model parameter set will be biased to ensuring low flows are simulated correctly as errors at low flows are likely to be proportionally bigger than those at high flows.

- The Reduced Error of Estimate (R.E.E.); given by:

$$R.E.E. = \left[\frac{F - F_R^2}{F - F_m^2} \right]^{0.5} \quad 2.1.19$$

Where F_m is the recorded mean flow. This function gives equal weight to all errors.

- iii) The Extremes Error of Estimate (E.E.E); given by:

$$E.E.E. = \left[\left(\frac{|F - F_R| \times |F - F_m|}{F_R \times F_m} \right) \times \frac{1}{n-1} \right]^{0.5} \quad 2.1.20$$

This function gives much greater weight to the extremes and is therefore a general purpose objective function.

HYSIM also allows the user to constrain the above objective functions by setting a maximum allowed difference between both the mean and standard deviations of the simulated and recorded flows over the calibration period. Manley suggests that maximum differences of 5% for the means and 10% for the standard deviations are acceptable.

The post processing facilities enable the user to analyse time series output from the model either graphically or numerically through output to file. The graphical display options are: simulated and recorded flow, moisture storage, moisture transfers and general. The plotting facilities can be used to analyse time series data associated with any of the stores within the model.

Table 2.1: Hydrological Parameters within HYSIM

No.	Hydrological response parameter
1.	Interception storage maximum depth
2.	Impermeable fraction of the catchment
3.	Time to peak (minor channels store)
4.	Total soil moisture storage depth
5.	Proportion of soil moisture in the USH
6.	Permeability at the top of the USH
7.	Permeability at the base of the LSH
8.	Permeability at the horizon boundary
9.	Porosity
10.	Bubbling pressure
11.	Discharge coefficient – Transitional groundwater
12.	Discharge coefficient – Groundwater
13.	Proportion of outflow from transitional groundwater that becomes runoff
14.	Inter flow runoff from the upper horizon at saturation
15.	Inter flow runoff from the lower horizon at saturation
16.	Precipitation correction factor
17.	Potential Evaporation Correction Factor
18.	Evaporation from Interception Factor
19.	Snowfall factor
20.	Ratio of Groundwater contributing area to Surface catchment area
21.	Ratio of area not contributing to groundwater to surface catchment area
22.	Pore Size Distribution Index

Table 2.2: Hydraulic parameters within HYSIM

No.	Hydraulic Parameters (for each of n reaches)
1.	In bank coefficient of proportionality
2.	In bank exponential coefficient
3.	Out of bank coefficient of proportionality (flood plain filling)
4.	Out of bank exponential coefficient (flood plain filling)
5.	Out of bank coefficient of proportionality (flood plain full)
6.	Out of bank exponential coefficient (flood plain full)

2.2 THE THAMES CATCHMENT MODEL

2.2.1. Overview

The Thames Catchment Model was originally developed by Greenfield (1984). It has been implemented within the Thames Environment Agency risk assessment and drought management system (Moore et al 1989) and has also been used to model the relative impact of weather, land use and groundwater abstraction on low flows in case study catchments across England and Wales. The latter work has been published as the National Rivers Authority R&D Note 268 (Wilby, 1994). Several versions of the model exist however the one considered for this study was developed by Wilby based on Greenfield's original model. This version of the model is available, in an unsupported format, as part of the R&D Note 268 and forms a component of a larger modelling suite, written in MicroSoft Quick Basic, called CLAM. The description of the model presented here is based on those of Greenfield, Moore (1993) (with regard to the solution of the storage-outflow functions for non-linear reservoirs) and Wilby.

The structure of the Thames Conceptual Model, or TCM, is based on the subdivision of a basin into different response zones representing, for example, runoff from aquifer, clay, riparian and paved areas and sewage effluent sources. Within the CLAM implementation the number of zones allowed is restricted to two and the total number of years of record that can be modelled to 21. These are restrictions forced by the programming environment rather than the model structure. The zones share the same model structure but have different, appropriate parameter sets. The zonal flows are combined to yield the total catchment runoff. A response zone may be considered to represent a combination of sub-areas within a catchment having similar hydrological characteristics. In some catchments a single geographical area will account for most or all of a zone. The conceptual representation of a hydrological response zone in the TCM is illustrated in Figure 2.2. Each zone consists of a two stage soil moisture store, a linear reservoir, or store, and a non linear reservoir, or store, connected in series.

2.2.2 The soil moisture store

Within a given zone, water movement in the soil is controlled by the Penman storage model (Penman, 1949) in which a near-surface storage, of depth equal to the rooting depth of the associated vegetation (the root constant depth), drains only when full into a lower storage of infinite capacity. The Penman model has been modified such that this drying curve has been redefined as two straight lines, Figure 2.3. Evaporation occurs at the Penman potential rate, P.E, whilst the upper store contains water and at a lower, actual rate, A.E, when only water from the lower store is available. The threshold deficit at which this lower rate evaporation is initiated is optimised though calibration. This threshold deficit can be thought of as the mean rooting constant for the catchment vegetation types. The A.E rate is set to $0.3P.E$ rather than $0.08P.E.$, as in the original Penman model based on the work of Hyoms (1980) during the 1976 drought. The Penman stores are replenished by rainfall, but a fraction called direct percolation D_p (typically 0.15) is bypassed to contribute directly as percolation to the linear store which may be conceptualised as unsaturated storage. Percolation occurs from the Penman stores only when the total soil moisture deficit has

been made up. The operational logic of the soil moisture store is presented in Figure 2.4.

2.2.3 The linear store

Within each zone, the total percolation forms the input to the linear store that can be conceptualised as representing unsaturated storage. The outflow from this store is proportional to the water held within the store. This outflow acts as the input to the non linear storage. Greenfield does not assign general physical meaning to the linear and non linear stores but he does state that in some applications, where permeable catchments are being modelled, that the linear store can be conceptualised as representing the unsaturated soil zone and the non-linear store as the groundwater zone below the phreatic surface within the aquifer. As a consequence the model has been structured so that groundwater abstractions can be made from the discharge (termed recharge) from the linear store to the non-linear store. The functions defining outflow from a linear reservoir are summarised in the description of the HYSIM model in section 2.1.. In both the original Greenfield code and the Wilby code the explicit solution is applied across the entire time step. To obtain a volumetric flow rate it is necessary to multiply the outflow from the linear reservoir by the area of the zone being considered.

2.2.4 The non-linear store

A quadratic storage function is used to represent the response of the saturated zone. The quadratic form of the Horton- Izzard equation corresponds to the 75% turbulent flow case using the Hortonian turbulence index. The outflow, Q , is related to the storage of water, S , through the relation:

$$Q = \frac{1}{K} S^2 \quad 2.2.1$$

where K is a non-linear storage constant (with units of volume time). The net inflow, I , into this storage is the difference between mean outflow from the linear reservoir and any groundwater abstraction. The Wilby implementation of the model is restricted to accepting a constant groundwater abstraction rate. It is possible to derive analytical solutions for the outflow Q_t at the end of a time interval $(t-T, t)$, during which the net inflow is I_t (assumed constant over the interval) and the initial outflow is Q_{t-T} .

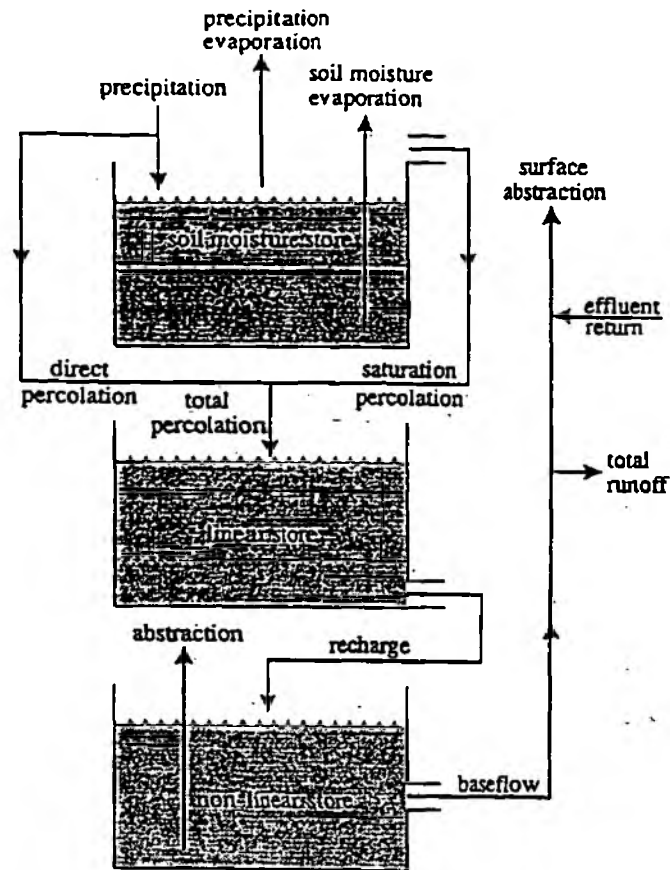


Figure 2.2: The Structure of the Thames Catchment Model

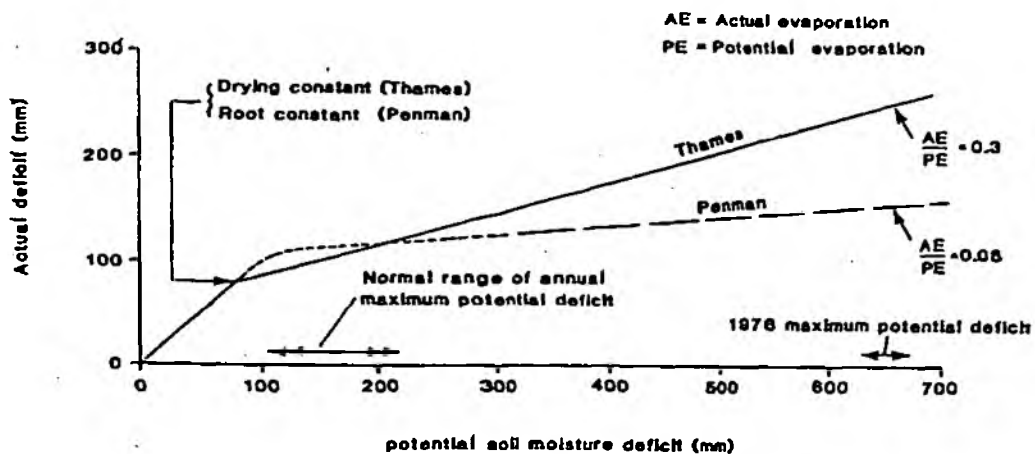


Figure 2.3: Penman and Thames catchment Model Drying Curves

RF daily rainfall
 PE potential evaporation
 D MAX 1 maximum deficit in zone 1
 D MAX 2 maximum deficit in zone 2 } in mm
 DC drying constant
 AE actual evaporation
 EPE excess potential evaporation
 PER percolation
 D1, D2 deficit in a zone
 W1, W2 water in a zone
 DP direct percolation %
 RER remaining rainfall
 F1, F2 actual evaporation/potential evaporation factor for a zone

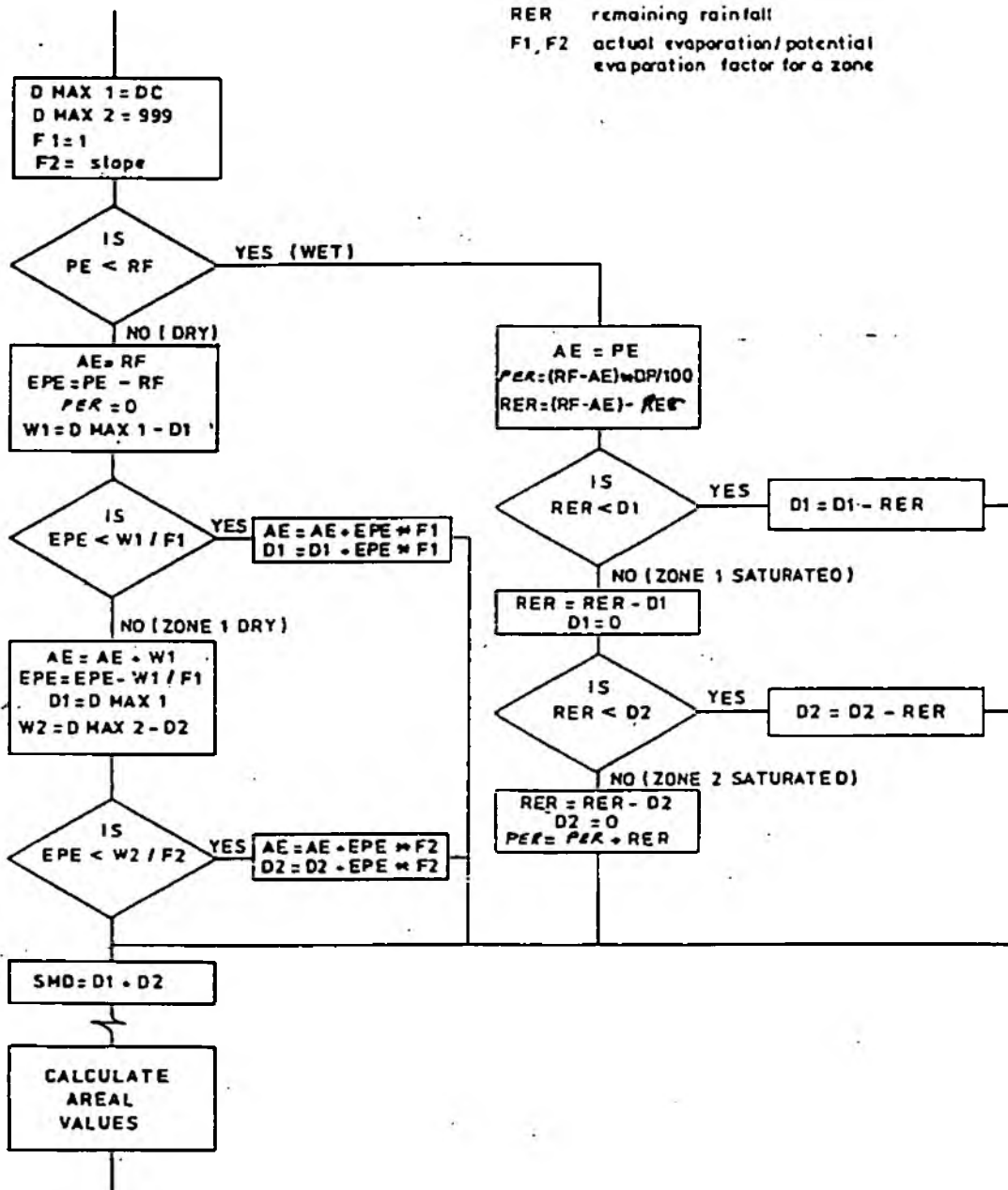


Figure 2.4: The operational logic of the soil moisture store

To find Q_t , the differential equation to be solved is

$$\frac{dS}{dt} = I - \frac{S^2}{K} \quad 2.2.2$$

Using the transformed variable, $v = S/\sqrt{IK}$, 2.2.2 may be written as

$$\frac{1}{1-v^2} dv = \sqrt{I/K} dt,$$

with solution

$$\tanh^{-1} v_t = \tanh^{-1} v_{t-T} + \frac{\sqrt{I_t}}{K} T,$$

where $v_t = S_t/\sqrt{IK} = \sqrt{Q_t/I_t}$. Taking hyperbolic tangents, and letting $\tau = \sqrt{I/K}T$ gives the result

$$Q_t = I_t \left(\sqrt{Q_{t-T}/I_t + \tanh \tau} \right)^2 / \left(1 + \sqrt{Q_{t-T}/I_t} \tanh \tau \right)^2 \quad 2.2.3$$

If I_t is negative due to abstractions exceeding recharge then a valid solution may be sought using the transformed variable $v = S/\sqrt{-IK}$, which gives the differential equation

$$\frac{1}{1+v^2} dv = -\sqrt{-I/K} dt,$$

with solution:

$$\tan^{-1} v_t = \tan^{-1} v_{t-T} - \sqrt{-I_t/K} T,$$

where $v_t = S_t/\sqrt{-IK} = \sqrt{Q_t/(-I_t)}$. This yields the result:

$$Q_t = I_t \tan^2 \left\{ \tan^{-1} \sqrt{Q_{t-T}/(-I_t)} - \sqrt{-I_t/K} T \right\} \quad 2.2.4$$

Note that in this case flow will cease at time

$$T' = \sqrt{K/(-I_t)} \tan^{-1} \sqrt{Q_{t-T}/(-I_t)} \quad 2.2.5$$

when the expression in curly brackets in the equation for Q_t falls below zero and a volume deficit begins to build up, which at the end of the interval $(t-T, t)$ is:

$$V_t = I_t (T - T') \quad 2.2.6$$

The solution for $I = 0$ is obtained by solving the differential equation

$$\frac{dS}{dt} = -\frac{S^2}{K}$$

which yields the result

$$Q_t = (1/\sqrt{Q_{t-T}} + t/\sqrt{K})^2 \quad 2.2.7$$

Within the Thames Catchment Model the explicit solutions for the mean and end of time step flows are applied across the entire time step. The Author hence, does not advise applying the model using time steps longer than a day.

The model parameters used in the Thames Catchment Model are presented in Table 2.3. The nomenclature adopted for the soil moisture model is that of Greenfield used in Figure 2.2 whilst, for consistency with the other models, the nomenclature adopted for the linear and quadratic stores is that of Moore 1993.

Table 2.3 Parameters in the Thames Conceptual Model

Parameter name	Unit	Description
<i>Zone parameters</i>		
A	km ²	Area of hydrological response zone
DC	none	Drying rate in lower soil zone (usually Dc=0.3)
DMAX1	mm	Depth of upper soil zone (drying or root constant)
DMAX2	mm	Depth of lower soil zone (notionally infinite)
DP	none	Direct percolation factor (proportion of rainfall bypassing soil storage)
K	hours	Linear reservoir time constant
K	mm hours	Quadratic reservoir time constant
q _c	m ³ s ⁻¹	Abstraction rate surface waters
RET	none	Effluent return (% of q _c)
Td	hours	Time delay

2.2.5 The Package

The Wilby implementation of the TCM is written in the Microsoft Quick Basic programming language as a module within the Climate, Land-use and Abstraction Model (CLAM). CLAM is menu driven and, although not supported, has a brief user guide as an appendix to Wilby, 1994. Calibration is achieved manually with a graphical presentation of the observed

and simulated hydrographs. The hydrographs can be analysed numerically through display of the ratio of the simulated and observed volumes of water over the calibration period, the mean error between the simulated and observed, the square of the serial correlation coefficient and the Nash Sutcliffe efficiency criteria which is calculated as:

$$\text{Efficiency} = 1 - \frac{\sum (q_s - q_o)^2}{\sum (q_s - \bar{q}_o)^2} \quad 2.2.8$$

Initially the model is calibrated on a single zone configuration. The software has the option of plotting the residual hydrograph. Making the assumption that this residual hydrograph represents the contribution from a second zone enables the user to calibrate a second zone to calibrate this residual hydrograph.

2.3 THE PROBABILITY DISTRIBUTED MODEL

2.3.1 Overview

The Probability Distributed Model or PDM was authored by R.J. Moore at the Institute of Hydrology (Moore, 1985). The description of the model presented here is essentially that of Moore et al (1993). Figure 2.5 illustrates the general form of the model. Runoff production at a point in the catchment is controlled by the absorption capacity of the soil to take up water: this can be conceptualised as a simple store with a given storage capacity. By considering that different points in a catchment have differing storage capacities and that the spatial variation of capacity can be described by a probability distribution, it is possible to formulate a simple runoff production model which integrates the point runoffs to yield the catchment surface runoff into surface storage. Groundwater recharge from the soil moisture store passes into subsurface storage. The outflow from surface and subsurface storages, together with any fixed flow representing, say, compensation releases from reservoirs or constant abstractions, forms the model output. The components of the PDM model are described in more detail below.

2.3.2 Soil moisture store

Runoff production at any point within a river basin may be conceptualised as a single storage, or tank, of capacity c' , representing the absorption capacity of the soil column at that point. The storage takes up water from rainfall, P , and loses water by evaporation, E , until either the storage fills and spills, generating direct runoff, q , or empties and ceases to lose water by evaporation. Figure 2.6(a) depicts such a storage, whose behaviour may be expressed mathematically by:

$$q = \begin{cases} P - E - (c' - S_0) & P > c' + E \\ 0 & P \leq c' + E \end{cases} \quad 2.3.1$$

where S_0 is the initial depth of water in storage, and where P , E and q represent the depth

of rainfall, evaporation and the resulting direct runoff over the interval being considered. Now consider that runoff production at every point within a river basin may be similarly described, each point differing from another only with regard to the storage capacity. The storage capacity at any point, c , may then be considered as a random variate with probability density function, $f(c)$, so that the proportion of the river basin with depths in the range $(c, c + dc)$ will be $f(c)dc$.

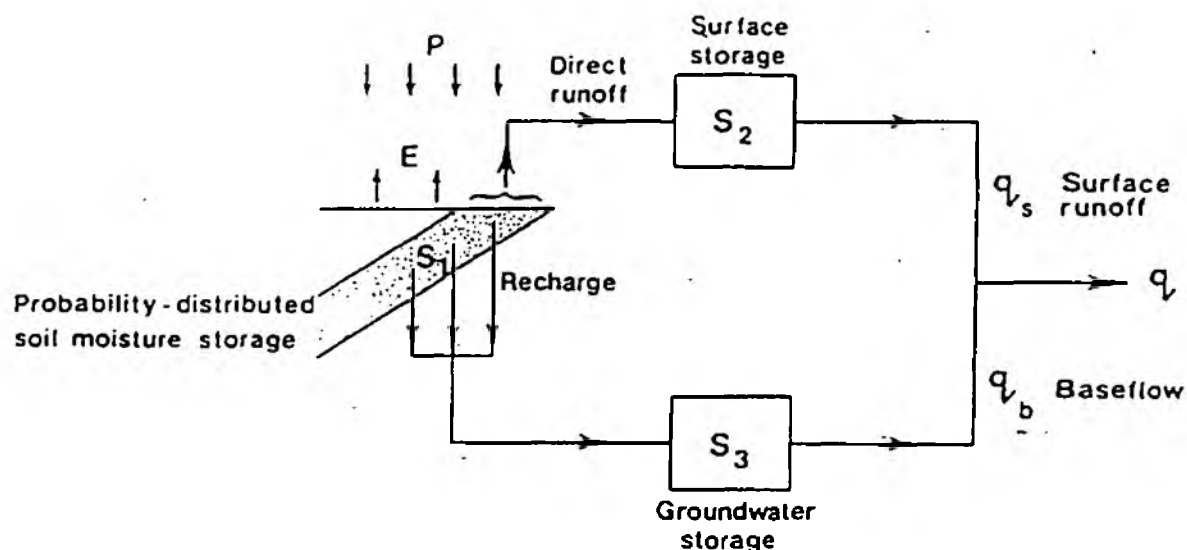


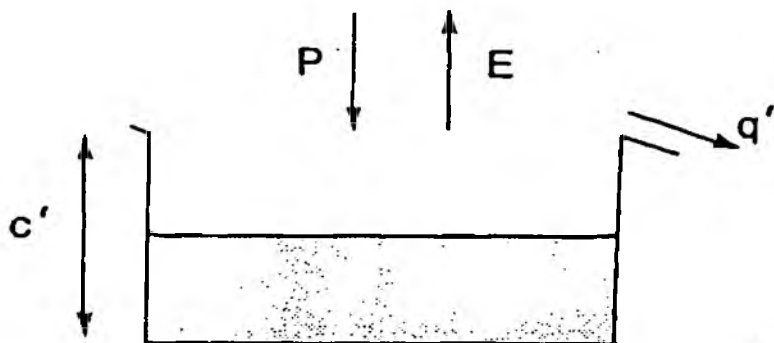
Figure 2.5 The Structure of the PDM rainfall-runoff model

The water balance for a river basin assumed to have storage capacities distributed in this way may be constructed as follows. First imagine that stores of all possible different depths are arranged in order of depth and with their open tops arranged at the same height: this results in a wedge-shaped diagram as depicted in Figure 2.6(b). If the basin is initially dry so that all stores are empty and rain falls at a net rate P for a unit duration, then stores will fill to a depth P unless they are of lesser depth than P when they will fill and spill. During the interval the shallowest stores will start generating direct runoff and at the end of the interval stores of depth P will just begin to produce runoff, so that the hachured triangular area denotes the depth produced from stores of different depth over the unit interval. Since, in general, there are more stores of one depth than another the actual runoff produced over the basin must be obtained by weighting the depth produced by a store of a given depth by its frequency of occurrence, as expressed by $f(c)$. Now, at the end of the interval stores of depth less than P are generating runoff: let this critical capacity below which all stores are full at some time t be denoted by $C^* = C^*(t)$ ($C^* = P$ in the present example). The proportion of the basin containing stores of capacity less than or equal to C^* is

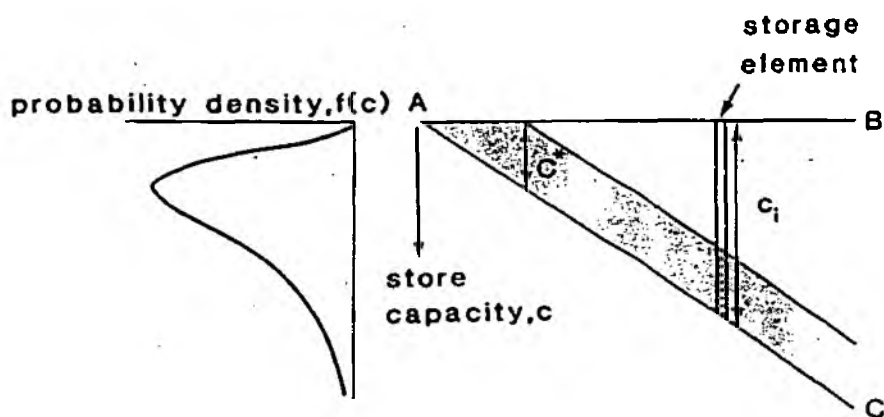
$$\text{prob}(c \leq C^*) = F(C^*) = \int_0^{C^*} f(c)dc.$$

2.3.2

(a) Point representation of runoff production by a single store



(b) Basin representation by storage elements of different depth and their associated probability density function



(c) Direct runoff production from a population of stores

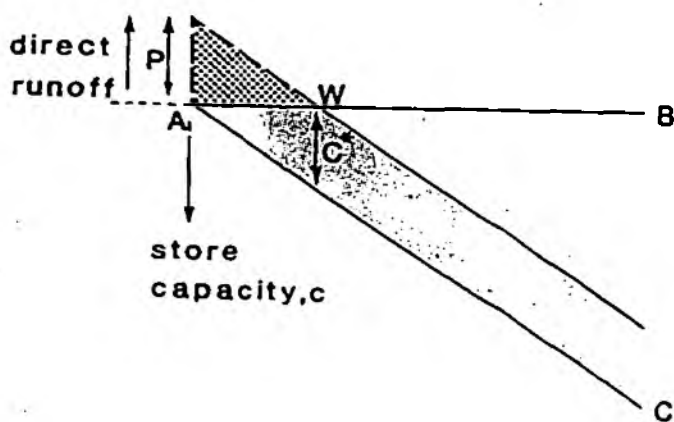


Figure 2.6 Definition diagrams for the probability-distributed interacting storage capacity component.

The function $F(\cdot)$ is the distribution function of store capacity and is related to the density function, $f(c)$, through the relation $f(c) = dF(c)/dc$. This proportion is also the proportion of the basin generating runoff, so that the contributing area at time t for a basin of area A is

$$A_c(t) = F(C^*(t)) A. \quad 2.3.3$$

The instantaneous direct runoff rate per unit area from the basin is the product of the net rainfall rate, $\pi(t)$, and the proportion of the basin generating runoff, $F(C^*(t))$; that is

$$q(t) = \pi(t) F(C^*(t)). \quad 2.3.4$$

During the i 'th wet interval, $(t, t+\Delta t)$, suppose rainfall and potential evaporation occur at constant rates P_i and E_i , so that net rainfall $\pi_i = P_i - E_i$. Then the critical capacity, $C^*(\tau)$, will increase over the interval according to

$$C^*(\tau) = C^*(t) + \pi_i (\tau - t) \quad t \leq \tau \leq t + \Delta t, \quad 2.3.5$$

The contributing area will expand according to (2.3.3), and the volume of basin direct runoff per unit area produced over this interval will be

$$V(t + \Delta t) = \int_t^{t+\Delta t} q(\tau) d\tau = \int_{C^*(t)}^{C^*(t+\Delta t)} F(c) dc. \quad 2.3.6$$

During dry periods potential evaporation will deplete the water content of each storage. It will be assumed during such depletion periods that water moves between storages of different depths so as to equalise the depth of stored water at different points within the basin. Thus at any time all stores will have a water content, C^* , irrespective of their capacity, unless this is less than C^* when they will be full: the water level profile across stores of different depths will therefore always be of the simple form shown in Figure 2.6(c). Particularly important is that a unique relationship exists between the water in storage over the basin as a whole, $S(t)$, and the critical capacity, $C^*(t)$, and in turn to the instantaneous rate of basin runoff production, $Q(t)$. Specifically, and referring to Figure 2.6(c), it is clear that the total water in storage over the basin is

$$\begin{aligned} S(t) &= \int_0^{C^*(t)} cf(c) dc + C^*(t) \int_{C^*(t)}^{\infty} f(c) dc \\ &= \int_0^{C^*(t)} (1 - F(c)) dc. \end{aligned} \quad 2.3.7$$

For a given value of storage, $S(t)$, this can be used to obtain $C^*(t)$ which allows the volume of direct runoff, $V(t+\Delta t)$, to be calculated using equations (2.3.6) together with (2.3.5).

The dependence of evaporation loss on soil moisture content is introduced by assuming the following simple function between the ratio of actual to potential evaporation, E_i/E_p , and soil moisture deficit, $S_{max} - S(t)$:

$$\frac{E_i}{E_p} = 1 - \left\{ \frac{S_{max} - S(t)}{S_{max}} \right\}^{b_e} \quad 2.3.8$$

either a linear ($b_e=1$ so $E_i=(S(t)/S_{max})E_p$) or quadratic form ($b_e=2$) is usually assumed. Here, S_{max} is the total available storage, and is given by

$$S_{max} = \int_0^\infty cf(c)dc = \int_0^\infty (1 - F(c)) dc = \bar{c}, \quad 2.3.9$$

where \bar{c} is the mean storage capacity over the basin.

Further loss as recharge to groundwater may be introduced by assuming that the rate of drainage over the interval, d_i , depends linearly on basin soil moisture content at the start of the interval i.e.

$$d_i = k_r (S(t) - S_i)^{b_r} \quad 2.3.10$$

where k_r is a drainage time constant with units of inverse time, b_r is an exponent (usually set to 1) and S_i is the threshold storage below which there is no drainage, water being held under soil tension. An alternative formulation is available which allows recharge to depend on both soil and groundwater storage for use in catchments where soil/groundwater interactions are important. Consider recharge into a groundwater store of maximum capacity S_g^{max} . Then a groundwater deficit ratio may be defined as

$$g(t) = \frac{S_g^{max} - S_g(t)}{S_g^{max}} \quad 2.3.11$$

where $S_g(t)$ denotes the groundwater storage at time t . This ratio can be used to define a groundwater demand factor between 0 and 1:

$$f(t) = \begin{cases} \left(\frac{g(t)}{\alpha} \right)^\rho & g(t) < \alpha \\ 1 & \text{otherwise} \end{cases} \quad 2.3.12$$

which achieves a maximum for values of the deficit ratio $g(t)$ in excess of α . It is then reasonable to suppose that the recharge depth over the interval, D_i , will increase with soil storage, $S(t)$, and with the groundwater demand factor, $f(t)$, according to

$$D_i = (D_{sat} + (S_{max} - D_{sat})f(t)) \frac{S(t)}{S_{max}} \quad 2.3.13$$

Here the maximum possible recharge depth $D_{sat} = q_{sat} \Delta t$, with q_{sat} the outflow from the groundwater storage when $S_g(t)$ equals S_g^{max} . Note that the drainage rate over the interval is

$d_i = D_i / \Delta t$. There are thus only three parameters: α , β and q_{\max} (with S_g^{\max} thereby implied from its storage function). It is seen that, for a saturated soil store, recharge is diminished when the groundwater demand factor is less than α , when the soil ceases to be freely draining. This formulation derives from a reparameterized form of percolation model used in the National Weather Service rainfall-runoff model (Burnash *et al.*, 1973; Gupta and Sarooshian, 1983).

A third recharge formulation is available which assumes that there is no soil drainage, d_i . Direct runoff is split between a fraction α which goes to make up surface runoff and a fraction $(1-\alpha)$ going to groundwater storage.

With both losses to evaporation and recharge, the net rainfall, π_i , may be defined in general as

$$\pi_i = P_i - E_i - d_i. \quad 2.3.14$$

During a period when no runoff generation occurs then, for this general case, soil moisture storage accounting simply involves the calculation

$$S(\tau) = S(t) + \pi_i (\tau - t) \quad t \leq \tau \leq t + \Delta t, \quad 0 \leq S(\tau) \leq S_{\max}. \quad 2.3.15$$

When runoff generation does occur then the volume of runoff produced, $V(t+\Delta t)$, is obtained using (2.2.6), and then continuity gives the replenished storage as

$$S(t + \Delta t) = \begin{cases} S(t) + \pi_i \Delta t - V(t + \Delta t) & S(t + \Delta t) < S_{\max} \\ S_{\max} & \text{otherwise} \end{cases} \quad 2.3.16$$

If basin storage is fully replenished within the interval $(t, t+\Delta t)$ then $V(t+\Delta t)$ should be computed from continuity as

$$V(t + \Delta t) = \pi_i \Delta t - (S_{\max} - S(t)). \quad 2.3.17$$

The above completes the procedure for soil moisture accounting and determining the value of runoff production according to a probability-distributed storage capacity model. Figure 2.7 provides a graphical representation of this procedure for a wet interval $(t, t+\Delta t)$ during which soil moisture storage is added to by an amount $\Delta S(t+\Delta t) = \pi_i \Delta t - V(t+\Delta t)$, and a volume of direct runoff, $V(t, \Delta t)$, is generated.

A specific application of the procedure can be developed for a given choice of probability density function. The Pareto distribution of storage capacity is the most widely used in practice and is used here to illustrate application of the method. The distribution function and probability density function for this distribution are:

$$F(c) = 1 - (1 - c / c_{\max})^b \quad 0 \leq c \leq c_{\max} \quad 2.3.18$$

$$f(c) = \frac{dF(c)}{dc} = \frac{b}{c_{\max}} \left(1 - \frac{c}{c_{\max}}\right)^{b-1} \quad 0 \leq c \leq c_{\max} \quad 2.3.19$$

where parameter c_{\max} is the maximum storage capacity in the basin, and parameter b controls the degree of spatial variability of storage capacity over the basin. These functions are illustrated in Figure 2.8: note that the rectangular distribution is obtained as a special case when $b=1$, and $b=0$ implies a constant storage capacity over the entire basin. The following relations apply for Pareto distributed storage capacities:

$$S_{\max} = c_{\max} / (b + 1), \quad 2.3.20a$$

$$S(t) = S_{\max} \left\{ 1 - (1 - C^*(t) / c_{\max})^{b+1} \right\} \quad 2.3.20b$$

$$C^*(t) = c_{\max} \left\{ 1 - (1 - S(t) / S_{\max})^{1/(b+1)} \right\} \quad 2.3.20c$$

$$v(t + \Delta t) = \pi \Delta t - S_{\max} \left\{ (1 - C^*(t) / c_{\max})^{b+1} - (1 - C^*(t + \Delta t) / c_{\max})^{b+1} \right\} \quad 2.3.20d$$

The relationship between rainfall and runoff implied by the above expressions, for given conditions of soil moisture, is presented in Figure 2.9.

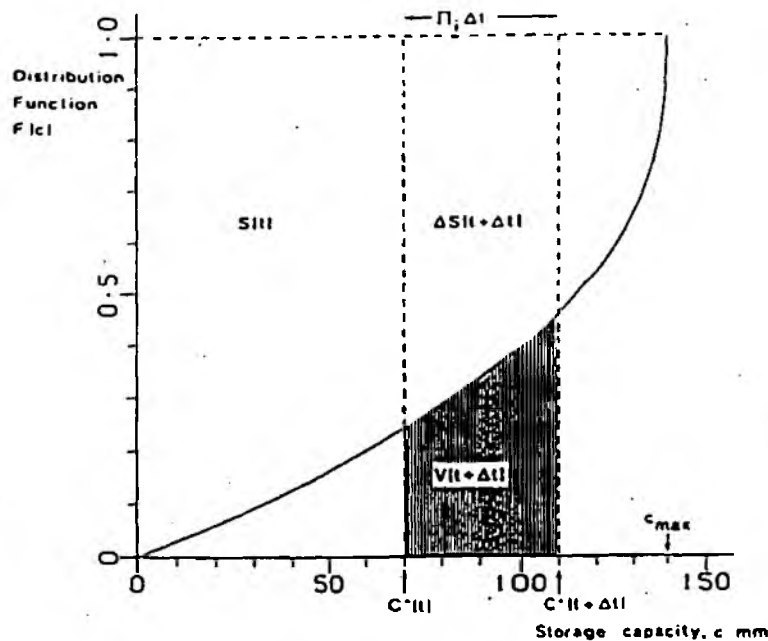


Figure 2.7 The storage capacity distribution function used to calculate basin moisture storage, critical capacity, and direct runoff according to the probability-distributed interacting storage capacity model.

(a) Probability density function

(b) Distribution function

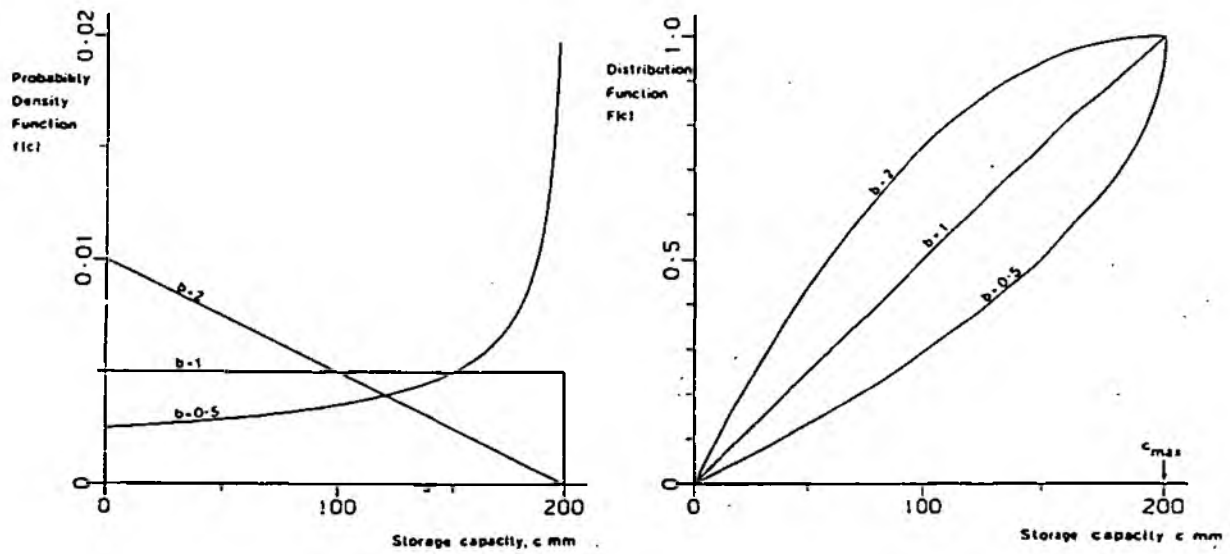


Figure 2.8 The Pareto distribution of storage capacity.

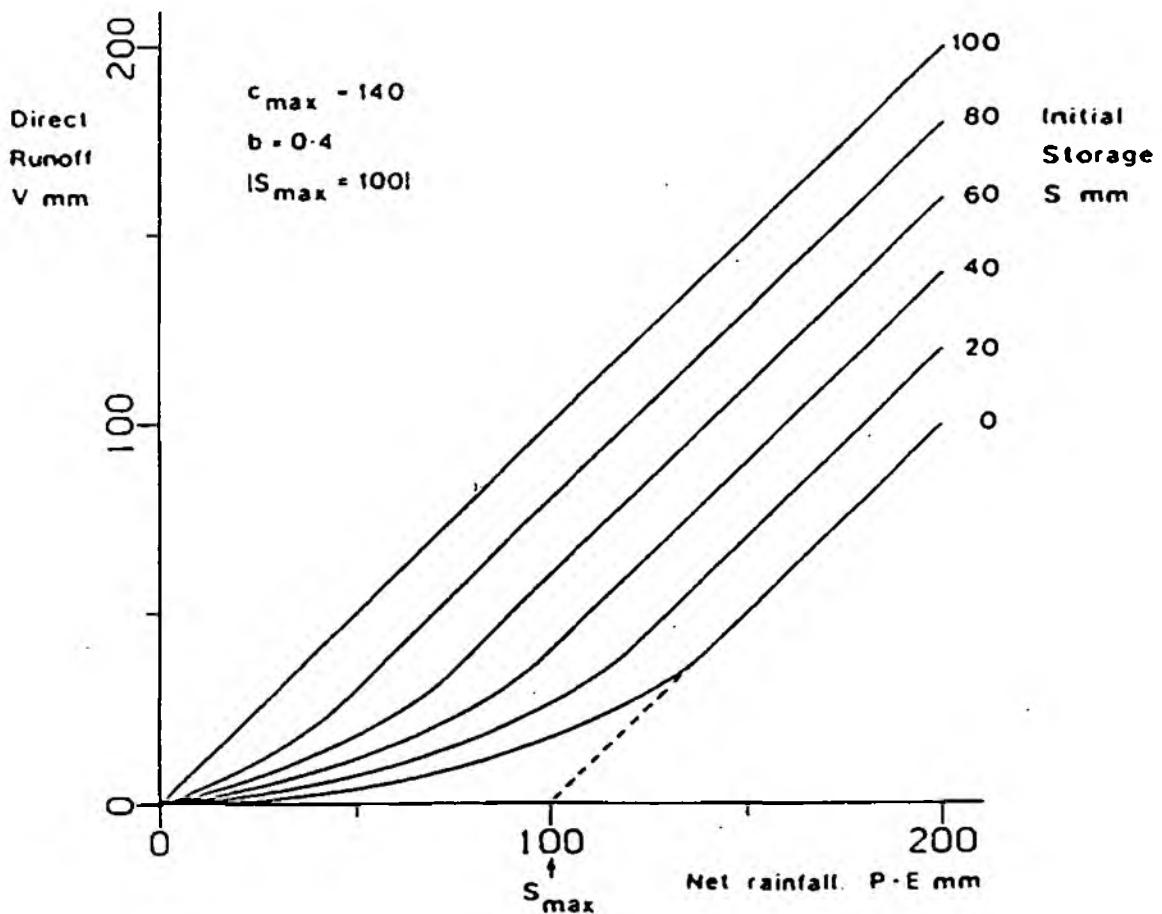


Figure 2.9 Rainfall-runoff relationship for the probability-distributed interacting storage capacity model, using the Pareto distribution of storage capacity.

2.3.3 Surface and subsurface storages

The probability-distributed store model partitions rainfall into direct runoff, groundwater recharge and soil moisture storage. Direct runoff is routed through surface storage: a "fast response system" representing channel and other fast translation flow paths. Groundwater recharge from soil water drainage is routed through subsurface storage: a "slow response system" representing groundwater and other slow flow paths. Both routing systems can be defined by a variety of non-linear storage reservoirs or by a cascade of two linear reservoirs (expressed as an equivalent second order transfer function model constrained to preserve continuity). The choice of non-linear storage includes the linear and quadratic storages, previously reviewed in the context of the TCM and HYSIM, together with exponential, cubic and general non-linear forms. A cubic form is usually considered most appropriate to represent the groundwater storage. In this case where $q = kS^3$ an approximate solution utilising a method due to Smith (1977) yields the following recursive equation for storage, given a constant input u over the interval $(t, t + \Delta t)$:

$$S(t + \Delta t) = S(t) - \frac{k}{3S(t)^2} \{ \exp(-3kS(t)^2 \Delta t) - 1 \} (u - kS(t)^2) \quad 2.3.21$$

Discharge may then be obtained simply using the non-linear relation

$$q(t + \Delta t) = kS(t + \Delta t)^3 \quad 2.3.22$$

When used to represent groundwater storage, the input u will be the drainage rate, d_i , from the soil moisture store and the output $q(t)$ will be the "baseflow" component of flow $q_b(t)$.

The most commonly used representation of the surface storage component is a cascade of two linear reservoirs, with time constants k_1 and k_2 , expressed as the discretely coincident transfer function model

$$q_i = -\delta_1 q_{i-1} - \delta_2 q_{i-2} + \omega_0 u_i + \omega_1 u_{i-1} \quad 2.3.23$$

with

$$\delta_1 = (\delta_1^* + \delta_2^*), \quad \delta_2 = \delta_1^* \delta_2^*, \quad \delta_1^* = \exp(\Delta t / k_1), \quad \delta_2^* = \exp(\Delta t / k_2)$$

$$\omega_0 = \frac{k_1(\delta_1^* - 1) - k_2 \delta_2^*}{k_2 - k_1} \quad k_1 \neq k_2$$

$$\omega_1 = \frac{k_2(\delta_2^* - 1) \delta_1^* k_1(\delta_1^* - 1) \delta_2^*}{k_2 k_1} \quad k_1 \neq k_2$$

2.3.24

$$\omega_0 = 1 - (1 + \Delta t / k_1) \delta_1^* \quad k_1 = k_2$$

$$\omega_1 = (\delta_1^* - 1 + \Delta t / k_1) \delta_1^* \quad k_1 = k_2$$

Here Δt is the time interval between times $t-1$ and t and it is assumed that the input u_i is constant over this interval. In this case the input is the volume of direct runoff, $V(t)$, generated from the probability-distributed soil moisture store and the output q_i will be the surface flow component of the total basin runoff, $q_s(t)$. The total basin flow is given by $q_s(t) + q_b(t)$, plus a constant flow, q_c , representing any returns or abstractions.

The parameter and structure options in the model are summarised in Table 2.4 below. Note that a rainfall factor, f_c , is incorporated in the model to allow conversion of a rainfall observation to rainfall, P , thereby compensating for effects such as lack of catchment representativeness.

2.3.4 The Package

The version of the PDM used in this study was that embodied within the suite of programs which form the Model Calibration facility of the River Flow Forecasting System (RFFS). It must be noted that the package, as it stands, is not marketed by IH as a stand alone package and as the title suggests, it is primarily directed at modelling at an hourly timestep. The package incorporates a modified Nelder & Mead simplex optimisation method and also has the facility for interactive parameter adjustment. The user interface is through a console application within Windows. This interface has the option for displaying graphically in a second window, the observed hydrograph and the modelled total flow and nonlinear storage outflow hydrographs. The configuration of the model, including the identification of which parameters are to be optimised and definition of the objective function to be used is controlled through an ASCII format control file. Both this file and the file containing the input climatic data and observed flow data (if any) for the period under consideration, have to be set up outside of the package.

Table 2.4 Parameters used in the PDM model for the present study

Parameter name	Unit	Description
f_c	none	rainfall factor
τ_d	hour	time delay
<i>Probability-distributed store</i>		
C_{min}	mm	minimum store capacity
C_{max}	mm	maximum store capacity
b	none	exponent of Pareto distribution
		controlling spatial variability of store capacity
<i>Evaporation function</i>		
b_e	none	exponent in actual evaporation function
<i>Recharge function</i>		
1: Standard		
k_g	hour mm^{b_g-1}	groundwater recharge time constant
b_g	none	exponent of recharge function
S_t	mm	soil tension storage capacity
2: Demand-based		
α	none	groundwater deficit ratio threshold
β	none	exponent in groundwater demand factor function
q_{sat}	$mm\ hr^{-1}$	maximum rate of recharge
3: Splitting		
α	none	runoff factor controlling the split of rainfall to surface and groundwater storage routing when no soil recharge is allowed
<i>Surface routing</i>		
k_s	hour	time constant of cascade of two equal linear reservoirs ($k_s = k_1 = k_2$)
<i>Groundwater storage routing</i>		
k_b	hour mm^{m-1}	baseflow time constant
m	none	exponent of baseflow non-linear storage
q_c	$m^3\ s^{-1}$	constant flow representing returns/abstractions

2.4 IDENTIFICATION OF UNIT HYDROGRAPHS AND COMPONENT FLOWS FROM RAINFALL, EVAPORATION AND STREAM FLOW DATA (IHACRES)

2.4.1 Overview

IHACRES has been developed collaboratively by the Institute of Hydrology and the Centre of Resource and Environmental Studies at the Australian National University (CRES at ANU), Canberra. The first published account of the IHACRES methodology and its application to two small research catchments in Wales is by Jakeman et al, 1990. IHACRES comprises a non-linear loss module in series with either a single linear unit hydrograph (UH) model or, alternatively, two linear unit hydrograph models in parallel or series. This description of IHACRES is based on the information published in the user guide (Littlewood & Parker, 1997) and published work (Jakeman et al, 1990, Jakeman & Hornberger, 1993 and Littlewood & Jakeman, 1994).

The input data requirements are restricted to time series of rainfall and stream flow, and a third variable by which evaporation effects can be approximated. The third variable is commonly temperature but estimates of potential evaporation may also be used. Data time steps that may be employed for stream flow and rainfall range from 1 minute to monthly. The time step has to be both consistent during a model run and has to be the same for rainfall and stream flow. The allowed time step for the third variable is constrained to be the same as that for the rainfall and stream flow data, either daily or monthly. However the time step must either be equal to or larger than that for the rainfall and stream flow data. The model comprises two modules, in series, as shown in Figure 2.10.

An assumption is made that there is a linear relationship between effective rainfall and stream flow (effective rainfall u_k for time step k is that part of rainfall r_k which eventually leaves the catchment as stream flow x_k). This allows the application of unit hydrograph theory in which the catchment is represented as a configuration of linear reservoirs acting in series and/or parallel. All of the non-linearity commonly observed between rainfall and stream flow is accommodated in the loss model which, although does not purport to conceptualise the physical behaviour of soil moisture, a comparison may be made between this model and the soil moisture stores considered within the preceding models.

Conceptualisation of spatially distributed processes in both the non-linear and linear modules of the IHACRES model is restricted. An advantage of the approach, however, is that the model requires only a small number of parameters. In the typical configuration of the non-linear loss module in series with two parallel linear modules there are three parameters in the non-linear loss module and another three in the linear module, making a total of six parameters overall.

2.4.2 The non-linear (loss) module

The loss module, which estimates effective rainfall, accounts for all of the non-linearity in the catchment-scale rainfall-runoff process. The underlying conceptualisation in this part of the model is that catchment wetness varies with recent past rainfall and actual evaporation. A

catchment wetness index, s_k (ideally, $0 < s_k < 1$) is computed at each time step k on the basis of recent rainfall and, optionally, the desired measure of evaporative effects, usually temperature. The catchment wetness index reflects that a catchment which is already wet will generate more stream flow than if it is previously dry. The percentage of rainfall which becomes effective rainfall in any time step varies linearly between 0% and 100% as s_k varies between zero and unity. An alternative conceptualisation of s_k is that it represents the proportion of the catchment area at time step k which contributes (eventually) to stream flow.

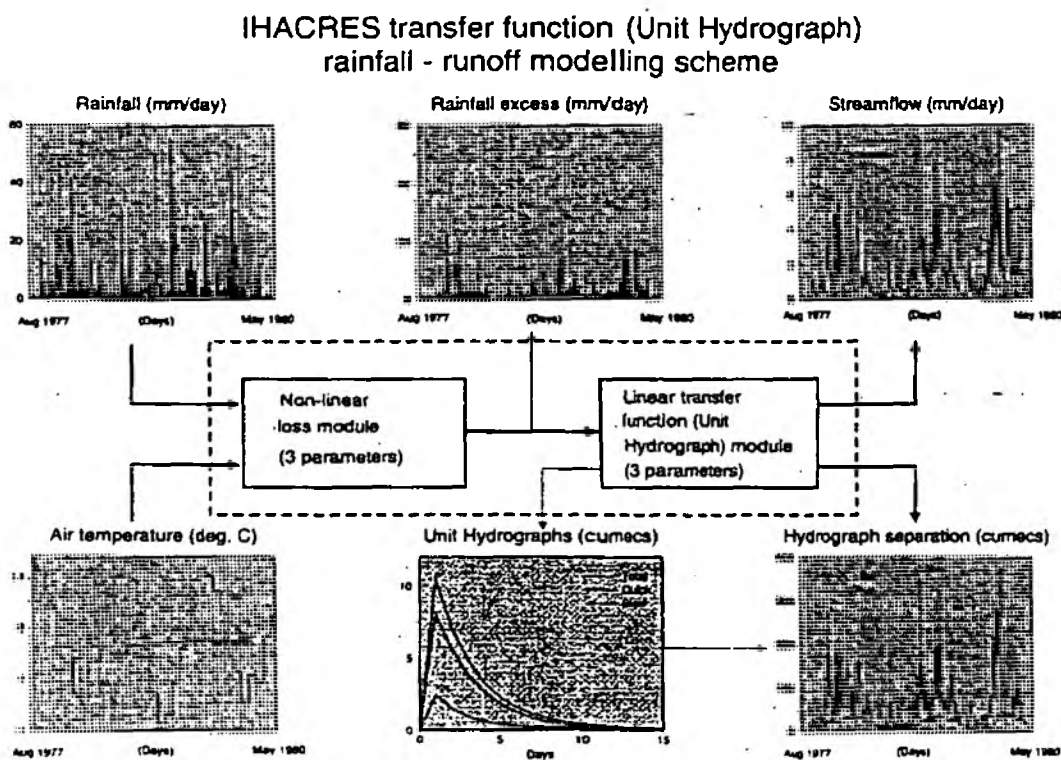


Figure 2.10 Schematic of the IHACRES modelling methodology

If input data to the loss model are restricted to those for rainfall the catchment wetness is calculated as:

$$s_k = Cr_k + (1 - 1/\tau_w)s_{k-1} \quad s_0 = 0 \quad 2.4.1$$

where r_k is the rainfall during the time step k , and τ_w is the time constant, or inversely, the rate at which the catchment wetness declines in the absence of rainfall. This time constant is termed the catchment drying constant. A larger value of T_w gives more weight to the effect of antecedent rainfall on catchment wetness than a smaller one. The parameter C is a constant of proportionality optimised during calibration so that the volume of excess rainfall is equal to the total stream flow volume over the calibration period, after adjustment for the change in catchment storage between the beginning and the end of the period. It is thus not really a free parameter but rather a normalising one. It is recommended, therefore, that model calibration periods are selected to start and finish at times of low flow (e.g. at suitable times near the end

of the regional water-year if modelling with daily data). Under these conditions it is assumed that the net change in catchment storage of water over the calibration period is close to zero. The excess or effective rainfall within the time step is calculated as:

$$u_k = r_k S_k \quad 2.4.2$$

To account for fluctuations in evaporation the catchment drying constant can be modulated by a function that relates this to the third variable, usually temperature:

$$\tau_w(t_k) = \tau_w \exp\{0.062f(R - t_k)\} \quad \tau_w(t_k) < 1 \quad 2.4.3$$

where t_k is the temperature in degrees Celsius during time step k , R is a reference temperature and f is a modulation factor which controls how sensitive the value of $\tau_w(t_k)$ is to departures from the reference temperature. In this context τ_w is the value of the catchment drying constant at the reference temperature and is replaced in equation 2.4.1 by $\tau_w(t_k)$. Parameters τ_w , f and C are termed the Dynamic Response Characteristics (DRC) for the loss model, DRCs are discussed in more detail in the following section.

2.4.3 The linear (UH) module

The continuous time convolution of rainfall excess $u(s)$ with an instantaneous unit hydrograph $h(t)$ to give continuous flow $q(t)$ is given by:

$$q(t) = \int_0^t h(t-s) \cdot u(s) ds \quad 2.4.4$$

Consider the simple discrete-time hydrograph such that *unit* effective rainfall over one data time step produces stream flow b (< 1) over the same time step (effective rainfall and flow have been zero in all preceding time steps and effective rainfall is zero in all subsequent time steps). In each subsequent time step, stream flow is a fixed proportion ($a < 1$) of what it was in the previous time step and thus the flow decays exponentially (at a rate determined by a). This scheme, including the resultant unit hydrograph, is shown in Fig. 2.11. The area under the UH (volume of flow) is given by the sum of the infinite geometric series ($b + ab + a^2b + a^3b + \dots$) and, by definition, this is one unit (1 mm over the catchment). With $0 < a < 1$, this infinite geometric series sums to $b/(1 - a)$, as given by equations 2.4.5a and 2.4.5b follows. The shape of this simple UH is completely defined, therefore, by one parameter (either a or b).

$$b(1 + a + a^2 + a^3 + \dots) = b / (1 - a) \quad 2.4.5a$$

$$b = 1 - a \quad 2.4.5b$$

Considering now the discretised version of equation 2.4.4 for the convolution of a time series of rainfall excess (u_j) up to and including time step k ($\dots, u_{k-3}, u_{k-2}, u_{k-1}, u_k$) with a unit hydrograph ($h_0, h_1, h_2, \dots, h_{ji}$) to estimate stream flow q_k at time step k is given by:

$$q_k = h_0 u_k + h_1 u_{k-1} + h_2 u_{k-2} + \dots + h_{k-1} u_1 + \dots + \zeta_k \quad 2.4.6$$

The error compensation term ζ_k , assumed to be normally distributed, represents all of the uncertainties arising from errors in both the model structure and the input data. Substituting a backwards shift operator such that $Z^{-i} X_k = X_{k-i}$, where X_k is any variable at time step k in 2.4.6 yields:

$$q_t = (h_0 + h_1 Z^{-1} + h_2 Z^{-2} + \dots + h_n Z^{-n} + \dots) + u_t + \zeta_t \quad 2.4.7$$

Representing the terms in 2.4.7 by the linear operator $H(Z^{-1})$ yields:

$$q_t = H(z^{-1})U_t + \zeta_t \quad 2.4.8$$

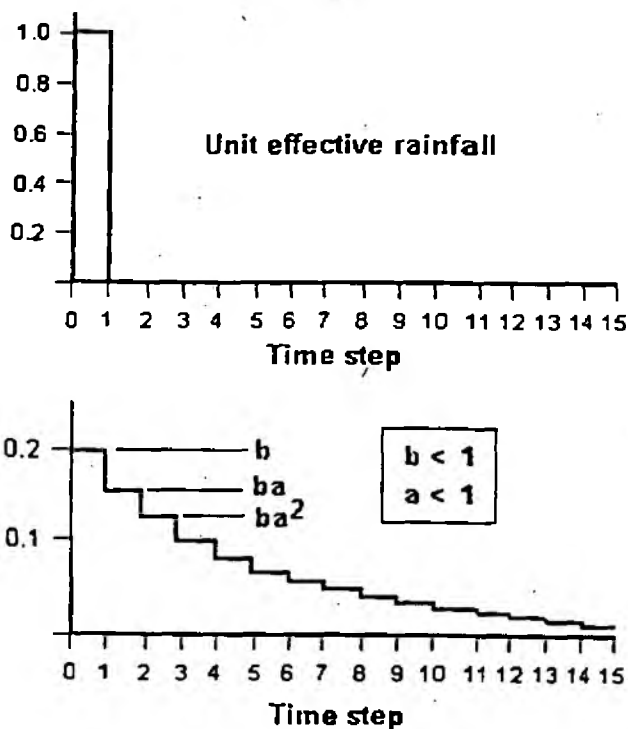


Figure 2.11 Definition of a single-storage UH in IHACRES

Thus $H(Z^{-1})$ is the noise free stream flow x_k . The coefficients of the polynomial are the ordinates of the UH total stream flow as opposed to those for the single event described above. Clearly the number of ordinates for such a UH can be large although, in practice, it has been found that the polynomial can be approximated closely by a rational transfer function of the form:

$$H(Z^{-1}) = \frac{B_n(Z^{-1})}{A_n(Z^{-1})} \quad 2.4.9$$

Where the polynomials $B_m(Z^{-1})$ and $A_n(Z^{-1})$ are defined as:

$$B_m(Z^{-1}) = b_0 + b_1 Z^{-1} + b_2 Z^{-2} + \dots + b_m Z^{-m}$$

$$A_n(Z^{-1}) = 1 + a_1 Z^{-1} + a_2 Z^{-2} + \dots + a_n Z^{-n}$$

with both n and m small. The expanded form of $x_k = H(Z^{-1})u_k$ is given by:

$$x_t = -a_1 x_{t-1} - a_2 x_{t-2} - \dots - a_n x_{t-n} + b_0 u_t + b_1 u_{t-1} + \dots + b_m u_{t-m} \quad 2.4.10$$

A pure time delay δ can be introduced into IHACRES by replacing all subscripts k in the right hand side of equation 2.4.10 with $k - \delta$.

The manual states that, in practice, subject to data quality and a suitable data time step, the IHACRES methodology indicates usually that two UHs in parallel, corresponding to the case $n=2$ and $m=1$ (the (2,1) transfer function) is the optimal configuration identifiable from the input data. The (2,1) transfer function is given by:

$$x_t = \left(\frac{b_0 + b_1 Z^{-1}}{1 + a_1 Z^{-1} + a_2 Z^{-2}} \right) u_t \quad 2.4.11$$

This second-order model can be written as the sum of two first-order (1,0) transfer functions:

$$x_t = \left(\frac{b^{(1)}}{1 + a^{(1)} Z^{-1}} \right) u_t + \left(\frac{b^{(2)}}{1 + a^{(2)} Z^{-1}} \right) u_t \quad 2.4.12$$

As presented graphically in Figure 2.11 an isolated unit input a first order (1,0) transfer function of the form $b/(1+az^{-1})$ will have a response of b during the time interval followed by a first order, or exponential decay, over the following time periods with a time constant τ given by:

$$\tau = \frac{-\Delta}{\ln(-a)} \quad \text{where } \Delta \text{ is the data time step.} \quad 2.4.13$$

The time constant is the time it takes the output of the IUH to decay to $\exp(-1)$ or approximately 37% of its peak value. The steady state gain, given a continuous unit input, is:

$$ssg = \frac{b}{1+a} \quad 2.4.14$$

By inspection it can be seen that the value of a is bounded between 0 and -1 and in equation 2.4.12 the first order transfer function with the value of a closest to -1 represents slow flow while the other first order transfer function represents quick flow. Coefficients of a and b will

henceforth be given super scripts of s and q to differentiate between quick and slow flow components. In this case, the rates of exponential decay for the two simple UHs are relatively quick (q) and slow (s), and the separate UHs sum to give a UH for *total* stream flow which has a mixed-exponential decay. Estimates of the quick and slow components of stream flow are given by recursive application of equations 2.4.15 and 2.4.16 respectively. Estimated total stream flow x_k is given by equation 2.4.17:

$$x_k^{(q)} = a^{(q)} x_{k-1}^{(q)} + b^{(q)} u_k \quad 2.4.15$$

$$x_k^{(s)} = a^{(s)} x_{k-1}^{(s)} + b^{(s)} u_k \quad 2.4.16$$

$$x_k = x_k^{(q)} + x_k^{(s)} \quad 2.4.17$$

In this instance the steady state gain of the (2,1) transfer function is given by:

$$1 = \left(\frac{b^{(q)}}{1+a^{(q)}} \right) + \left(\frac{b^{(s)}}{1+a^{(s)}} \right) \quad 2.4.18$$

and thus the response of the linear model is controlled by just three parameters (any three of $a^{(q)}$, $b^{(q)}$, $a^{(s)}$ and $b^{(s)}$). The area under the slow flow UH ($b^{(s)}/(1-a^{(s)})$) is a Slow Flow Index SFI which is comparable to the Base Flow Index BFI.

A central component of the IHACRES methodology is the use of the Simple Refined Instrumental Variable (SRIV) technique to estimate the parameters of the linear module for a given set of stream flow data and effective rainfall data received as output from the non-linear module. The detail of the SRIV technique is beyond the scope of this study, however the reader is referred to the work of Jakeman et al (1990) for further information.

2.4.3 Model calibration and the package

The whole model usually has six parameters; any three of $a^{(q)}$, $a^{(s)}$, $b^{(q)}$ and $b^{(s)}$ in the linear module plus f , T_w and C in the non-linear module. As discussed a pure time delay may also be incorporated.

For the (2,1) configuration the quick and slow flow components can be characterised by what are termed Dynamic Response Characteristics (DRCs):

$$\tau^{(q)} = \Delta / -\ln(a^{(q)}) \quad 2.4.19$$

$$\tau^{(s)} = \Delta / -\ln(a^{(s)}) \quad 2.4.20$$

Other DRCs are the relative volumetric throughputs for quick and slow flow ($v^{(q)}$ and $v^{(s)}$) given by equations 2.4.21 and 2.4.22 respectively (assuming both rainfall and stream flow are

in mm - in which case $v^{(s)} + v^{(q)} = 1$).

$$V^{(q)} = \frac{b^{(q)}}{1 - a^{(q)}} \quad 2.4.21$$

$$V^{(s)} = \frac{b^{(s)}}{1 - a^{(s)}} \quad 2.4.22$$

The DRC $v^{(s)}$ is the Slow Flow Index, mentioned already. Peaks of the quick and slow UHs, $l^{(q)}$ and $l^{(s)}$ are given by 2.4.23 and 2.4.24 respectively.

$$l^{(q)} = b_0^{(q)} \quad 2.4.23$$

$$l^{(s)} = b_0^{(s)} \quad 2.4.24$$

All of these DRCs are calculated and presented by the package. The calibration scheme, which is automated within the package, is based around searching the parameter space of the the loss module and optimising the parameters of the linear module (using the SRIV technique) for each selection of loss module parameters. Obviously the calibration scheme should be tried on differing configurations of the linear module to optimise the model structure. The fit of the model is optimised with primary references to two statistical measures, the coefficient of Determination, D, and the Average Relative Parameter Error (ARPE) (for the linear model) where:

$$D = \frac{\sum_{k=1}^N (\hat{y}_k - \bar{y}_k)^2}{\sum_{k=1}^N (\hat{y}_k - y_k)^2} \quad 2.4.25$$

$$ARPE = \frac{\sum_{i=1}^m \frac{\hat{\sigma}_i^2}{\hat{a}_i^2} + \sum_{i=1}^n \frac{\hat{\sigma}_{i+n+1}^2}{\hat{b}_i^2}}{m+n+1} \quad 2.4.26$$

Each $\hat{\sigma}_i$ within equation 2.4.26 is the estimated variance of the i th element in the set $(a_1, a_2, \dots, a_m, b_0, b_1, \dots, b_m)$; these variances are a by product of the SRIV algorithm. The selection of an optimal set of parameters is based around maximising the coefficient of determination whilst minimising the ARPE. Other statistics produced by the package which may also be used to select an optimal parameter set are a measure of bias, as represented by the mean of the model residuals and cross correlation coefficients between model residuals and stream flow and between model residuals and effective rainfall.

In addition to automated calibration facilities PC-IHACRES has extensive graphical facilities for viewing model input data, results and hydrographs of simulated total, quick and slow flow components.

3. Application of the models within the case study catchments

This chapter presents the five case study catchments and summarises the application of the four models within the catchments. The catchment selected were as follows:

- Babingley Brook above the Castle Rising gauging station (33054);
- Sapiston Brook above the Rectory Bridge gauging station (33013);
- River Nene above the Orton gauging station (32001);
- River Blackwater above Appleford Bridge (37010);
- River Box above Polstead Bridge (36003).

These catchments were selected to represent a broad cross section of catchment types across the Anglian region and are described in more detail within section 3.1. The objective of the exercise was to apply the models to the 22 year period of record between 1970 and the end of 1992, where available. The selection of the period of record was restricted by the availability of naturalised flow data for the Blackwater and the Nene. The three year period 1986-1988 was used as a calibration period and the period either side of the calibration period used for model evaluation. The period 1986-88 was selected for calibration as the flow variability within this period is broadly representative of that across the full 22 year period. The periods selected for the Babingley Brook and the Sapiston were respectively 1976-1992 and 1970-1990. The Castle Rising gauging station, which replaced an unreliable upstream gauge, became operational in 1976 whilst significant utilisation of the groundwater resources within the Sapiston catchment commenced post 1990.

The climate data used to drive the models and the application of the models is presented in sections 3.2 and 3.3. The evaluation of model performance is presented in Chapter 4.

3.1 CATCHMENT DESCRIPTIONS

- **The Babingley Brook above the Castle Rising gauging station (33054)**

The Babingley Brook above Castle Rising has a topographic catchment area of 47.7 km², however the mean groundwater catchment area is believed to be approximately 86 km². The gauging station is a triangular profile flow V crump weir and was assigned an A Grade for hydrometric quality at low flows by the Institute of Hydrology (Gustard et al, 1992).

The catchment average value of the Meteorological Office Standard Period 1961-90 Average Annual Rainfall (SAAR) is 670 mm/year and the catchment has a gauged runoff of 150-200 mm/yr. The catchment is predominantly unconfined Chalk and thus the flow regime is heavily dominated by groundwater discharge. The land use within the catchment is primarily arable. The artificial influences within the catchment are dominated by the utilisation of groundwater for public water supply which constitute 98% of the licenced abstractions. The abstraction time series over the period 1976-1992 have been accumulated at a monthly resolution as part of a naturalisation study undertaken by the Anglian Region of the Environment Agency in 1992 (Watts, 1994). This abstraction time series was included explicitly within the HYSIM and TCM simulations as these models have the facility for incorporating groundwater abstraction time series directly. For the other model simulations

the monthly influence series was partitioned to generate a daily series. The daily flow series at the gauging station were subsequently naturalised by adding in the abstraction time series. This was considered to be appropriate as the significant boreholes are close to the river channel and the abstraction time series demonstrates little seasonality.

- **The Sapiston Brook above the Rectory Bridge gauging station (33013);**

The Sapiston at Rectory Bridge is a rectangular thin-plate weir gauging an upstream catchment of 206 km² and was assigned an IH grade A for hydrometric quality at low flows. The catchment SAAR(61-90) is 590 mm/year and the gauged runoff is approximately 105 mm/year. Prior to 1990 the catchment was essentially natural with only minor abstraction for public water supply and agriculture. The catchment is agricultural in nature with a geology dominated by Chalk with Boulder Clay cover.

- **The Nene above the Orton gauging station (32001)**

The flow record for the Nene at Orton is a composite record. Flows below 17 m³s⁻¹ are measured at Orton. Flows above 17 m³s⁻¹ are derived by rescaling flows measured at Wansford, which lies some 12 km upstream from Orton. The structure at Orton consists of a series of sluices, weirs and a lock. The station was assigned a B grade for hydrometric quality under the IH grading system. The station is the lowest on the Nene and gauges an upstream catchment area of 1634km². The SAAR(61-90) across the catchment is 616 mm/year and the catchment has an gauged runoff of 180-190 mm/yr. The catchment is mainly clay and rural in nature.

The flow record is heavily artificially influenced by direct and indirect abstractions for public water supply, agricultural abstraction and effluent returns. The system is complicated by the abstraction at Wansford for Rutland Water which is used to supply towns within the catchment, such as Northampton that discharge back into the Nene. In 1992 the Anglian Region of the Environment Agency undertook a programme of naturalising the record flow through decomposition (Fawthrop, 1992). The resultant naturalised flows were used for this study.

- **The River Blackwater above Appleford Bridge (37010)**

The Blackwater above Appleford Bridge is a very rural catchment with a catchment area of 247.3 km². The gauging structure is a double throated trapezoidal flume assigned an A grade for hydrometric quality at low flows. The catchment SAAR(61-90) is 572 mm/year and the catchment has a gauged runoff of approximately 160mm/yr. The hydrogeology of the catchment is principally Boulder clay over London Clay with Chalk in the headwaters.

The majority of artificial influences on the flow record are associated with small abstractions for agricultural, public water supply and industrial purposes and small sewage treatment works discharges. The primary influence is water transferred from the Stour to the Blackwater as part of the Ely Ouse Transfer Scheme. The transferred water is discharged into the River Pant at Great Sampford in the headwaters of the river. During the 1970-1992 period considered within this study extensive transfers have been made in 1973/4, 1976 and 1989-

1992. Small but significant transfers have also been made during 1980, 1984, 1986 and during testing in 1971. The gauged flow record was naturalised by Young & Sekulin (1996). This naturalised record was used for the current study.

- **The River Box above Polstead Bridge (36003).**

The Box above Polstead is rural, natural catchment with a catchment area of 53.9 km². The gauging structure is a trapezoidal flume with a high flow rated spillway that rarely drowns. The structure was assigned an IH A grade for hydrometric quality. The catchment SAAR(61-90) is approximately 566mm/yr with a gauged runoff of 130 mm/yr. The catchment hydrogeology is dominated by London Clay with Chalk in the north, all overlain by superficial deposits. The minor artificial influences on the flow record are mainly associated with abstractions for agricultural purposes and sewage treatment plant discharges. The flow record was naturalised for the influence of these minor influences by Young & Sekulin (1996). This naturalised flow record was used for this study.

3.2 CLIMATIC DATA

- **Rainfall data**

The catchment average daily rainfall time series was generated for all catchments using the method of triangulation (Jones, 1983), applied to rain gauges held on the Meteorological Office rain gauge database using the IH catchment rainfall estimation facility. The method is applied on a 1 km² resolution grid. For each day, and for each cell in a grid that encloses the catchment boundary, the three closest rain gauges capable of forming an enclosing triangle around the centroid of each cell were identified. The distance from the centroid of the cell to the each rain gauge is then calculated and a weighted average of the rainfall measures at each gauge is then derived. The weight for an individual gauge is based on the inverse of the distance of the gauge from the centroid of the cell. This method ensures the generation of a smooth daily rainfall surface whose value at a gauge location is coincident with that of the gauge. This approach avoids the boundary discontinuities which occur with discrete domain based methods such as Thiessen polygons. Estimates of average annual rainfall generated using this method over the 61-90 standard period are presented in Table 3.1 for each of the case study catchments. Also presented are the SAAR(61-90) Met. Office estimates and the percentage difference between the two estimation procedures. The table clearly demonstrates the close correspondence between the estimation methods.

Table 3.1: A comparison of SAAR(61-90) and aggregated catchment daily rainfall estimates

Catchment	Triangulation based (61-90) SAAR mm/yr	SAAR(61-90) mm/yr	%diff.
33054	670	682	-2
33013	594	590	+1
32001	622	616	+1
37010	577	572	+1
37003	568	566	+0.1

- **Potential Evaporation and Temperature**

The PDM, HYSIM and TCM models all require a time series of catchment average potential evaporation as input to the model, whereas the PC version of IHACRES requires catchment average temperature time series data. Ideally a daily resolution would be used for these data. For this evaluation Met. Office MORECS weekly PE estimates for short grass and temperature estimates were utilised. These data are available for England, Wales & Scotland and are derived at a grid resolution of 40km². Where a catchment intersected more than one MORECS grid cell an area weighted average of cell values was taken. The MORECS grid cell and the extents intersected by each catchment are presented in Table 3.2. The resultant weekly time series were partitioned to give daily time series for input into the models.

Table 3.2: MORECS grid cells used in the estimation of catchment PE and Temperature

Catchment	MORECS grid cell (extent km ²)
33054	119(87)
33013	141(205)
32001	127 (304), 128 (256), 137(99), 138(945), 139(29)
37010	141(0.5), 152(159), 153(93)
37003	141(49.52), 153(16.92)

3.3 APPLICATION OF THE MODELS WITHIN THE CASE STUDY CATCHMENTS.

The evaluation of the model results is presented in Chapter 4. This section summarises the mode of application of each model.

3.3.1 HYSIM

The calibrated hydrological parameters are presented in Table 3.3. The hydraulic parameters are not presented as the default parameters suggested by the user guide were employed. In all catchments, the objective function used was the Extremes Error of Estimate, which is recommended for use as a general objective function. The other objective function formulations were found to make little difference to the fit of the model. Following the user guide the objective function was applied to the 1986-88 calibration period with an initial two years of data, from 1984-5 used to "warm up" the model. The recommended procedure for fitting the model, as discussed in the user guide, was adopted. Firstly default values were set for all parameters using the guidance given in the reference manual. The second step was to optimise the potential evaporation correction factor using the Newton-Raphson single parameter optimisation option to ensure mass is conserved over the calibration period. This step is of questionable value as the subsequent optimisation of soil moisture behaviour will modify the relationship between input potential and modelled actual evaporation. The third step was to use the Rosenbrock search algorithm, in conjunction with visual inspection and manual intervention, to optimise the remaining parameters in the model. The user guide recommends initially seeking a fit by modifying the following primary parameters:

- permeability at the horizon boundary;
- interflow runoff at saturation - upper horizon;
- interflow runoff at saturation- lower horizon;
- and in the case of groundwater, the permeability at the lower horizon boundary.

In practice it was found necessary to adjust all of these parameters to obtain a reasonable fit and in addition, in some catchments, it was necessary to adjust:

- impermeable fraction of the catchment to improve rapid response to summer storms;
- the recession rates (or time constants) of both groundwater stores to improve the fit of recession periods;
- the proportion of outflow from the transitional storage to increase the quick flow component of the modelled hydrograph.

Altering the remaining 14 parameters did not seem to noticeably improve the model fit.

Table 3.3: Calibrated hydrological parameters for HYSIM

Hydrological response parameter	37054	33013	32001	37010	36003
Interception storage maximum depth	1	2.0	2.2	2.0	2.0
Impermeable fraction of the catchment	0.022	0.02	0.16	0.016	0.02
Time to peak (minor channels store)	10	8.4	5.0	10.0	8.4
Total soil moisture storage depth	330	500.0	400	500	500.
Proportion of soil moisture in the USH	0.51	0.3	0.33	0.33	.3
Permeability at the top of the USH	1000	1000	1000.	1000.0	1000.0
Permeability at the base of the LSH	465.4	54.76	19.0	17.1	54.76
Permeability at the horizon boundary	557.3	57.84	14.1	27.1	57.83
Porosity	0.4	0.45	0.45	.48	0.45
Bubbling pressure	100	400	300	500	400
Discharge coefficient - Transitional g/water	0.736	0.736	0.651	0.733	0.736
Discharge coefficient - Groundwater	0.903	0.903	0.946	0.822	0.943
Proportion of outflow from transitional groundwater that becomes runoff	0.0	0.346	0.4	0	0.35
Inter flow runoff from the upper horizon at saturation	6.45	12.2	6.87	11.65	12.2
Inter flow runoff from the lower horizon at saturation	55.3	24.9	20.64	9.4	24.92
Precipitation correction factor	1.04	1.04	1.04	1	1.04
Potential Evaporation Correction Factor	0.9	1.01	0.813	.87	1.02
Evaporation from Interception Factor	1.0	1.0	1.0	1.	1.0
Snowfall factor	1.5	1.5	1.5	1.5	1.5
Ratio of Groundwater contributing area to Surface catchment area	1.0	0.903	1.0	1.0	0.903
Ratio of area not contributing to groundwater to surface catchment area	0.0	0.0	0	0.	0
Pore Size Distribution Index	.25	0.1	0.15	0.1	0.1

3.3.2 IHACRES

The approach for calibrating IHACRES is based around incremental searching through the parameter space of the loss model and the subsequent solving of the linear, routing model using the SRIV technique. The fit of the model is assessed through visual examination of the modelled flows, the coefficient of determination between observed and simulated flows and the uncertainty associated with the parameter values for the linear module. In the calibration procedure conservation of mass is ensured through the inclusion of a volume forcing coefficient in the loss module. For this study the full loss module was employed; in this the time constant, T_w , within a time step is modulated according to a temperature dependent function. In this configuration the response of the loss module is controlled by the volume forcing coefficient, C , the time constant, T_w , and f , the modulation constant which

determines how sensitive the modulation function is to temperature. A further term to be considered is a pure time delay between the nonlinear and linear modules. The model was calibrated over the period from October 1985 to October 1989. The manual recommends starting the simulation in October when runoff is generally low to minimise the error in estimating the volume forcing coefficient. The approach adopted for searching the parameter space in the loss module was to set the time delay to zero and search the parameter space defined by T_w and f for both the first and second order configurations of the linear module. Following the selection of an optimal pairing of T_w and f further simulations were undertaken to optimise the time delay. In all catchments the first order configuration was the optimal one. Where a viable second order solution was obtained the high associated ARPE values indicated that the additional complexity was not warranted. The parameter estimates for each catchment are presented in Table 3.4.

Table 3.4: Calibrated model parameters for IHACRES

Parameter	33054	33013	32001	37010	36003
T_D	0	1	1	1	0
F	2.4	1.5	3.5	2.0	2.0
C	0.008	0.002	0.007	0.002	0.004
T_w	3	21	16	34	10
A_1	-0.989	-0.751	-873	-0.686	-0.693
B_0	0.011	0.563	2.74	0.868	0.203

3.3.3 Thames Catchment Model

The Thames catchment model was the most problematical model to apply. The primary reasons for this is that it is a complicated model when more than one zone is used. This, coupled with the lack of an interactive or incremental parameter search facility, makes it very long winded to apply. The other consideration is that it was very difficult to assess the model fit using the evaluation statistics (Correlation coefficient, bias and Nash-Sutcliffe efficiency) when more than one zone was used as the statistics appear to apply to individual zones. Visual inspection of the observed and simulated hydrographs was therefore the major tool used to judge the goodness of fit. The strategy adopted was to set up a zone to model the slow flow component of the hydrograph coupled with a second, quick response zone to capture the residual variability. The model parameters for the case study catchments are presented in Table 3.5

Table 3.5 Calibrated model parameters for the Thames Catchment Model

Parameters	33054	33013	32001	37010	36003
A	86	90, 115	700, 950	80, 150	27, 30
DC (k)	0.2	0.3, 0.3	0.3, 0.2	0.3, 0.1	0.3, 0.3
DMAX1	20	100, 140	20, 70	30, 20	140, 75
DP	15	30, 10	30, 15	50, 30	40, 25
K (Cr)	0	0, 3	5, 2	5, 6	0, 2
K(Cq)	600	100, 0	150, 0	150, 0	150, 0

3.3.4 Probability Distributed Model

As described in chapter 2, the PDM may be used in many alternative configurations. The calibration manual advocates the use of the Pareto distribution for describing the variability in soil store depths in the loss model, the use of two identical linear reservoirs in series for the quick flow routing and a cubic non-linear reservoir for slow flow routing. - Regarding the partitioning of effective rainfall between the quick and slow flow routing paths it is recommended to use the demand based function in permeable catchments, and either the simple splitting function or the soil moisture driven (conventional) function for catchments where there is no appreciable groundwater. In practice it was found that either the direct split or the soil moisture based configurations gave the best results, as judged by visual inspection of the hydrographs and the value of the sum of squares objective function. The PDM offers the user the alternatives of using objectives functions based on the sum of squares with or without log10 or loge transformations. In practice it was found that the basic sum of squares gave the best results in terms of visual hydrograph fit. The calibration strategy was to use the automatic calibration facility in conjunction with manual intervention to obtain a best fit based on the value of the objective function, the reasonableness of parameter values which have a physical correspondence and visual inspection of the hydrograph. Following the guidance given in the calibration manual, the calibration focused on the Cmax, Kb, k1, kg (alpha when the direct split configuration was used), f, b, be, bg parameters aiming to achieve a fit using the earlier parameters in the list. The fits obtained with both effective rainfall partitioning approaches tended to be very similar in terms of the objective function value and hydrograph inspection. The decision as to which was adopted as the better fit was generally a subjective one made on reasonableness of the value of the Cmax and Be parameter values. In practice the calibration for simple split option was only selected for the Babingley and Box catchments. The parameter values for individual catchments are presented in Table 3.5.

Table 3.5: Calibrated model parameters for the PDM

Parameters	33054	33013	32001	37010	36003
Rainfac	0.89	0.79	1	0.63	1.0
Cmin	0	0	0	0	0
Cmax	93.7	175.9	151.6	160.0	177.8
B	0.79	0.48	0.39	0.5	0.79
Be	2.7	2	2	2	1
K1,k2	10.6	38.9	54.0	20.2	8.6
Kb	1097	72.5	73.1	448.7	32.76
Kg (theta)	(1.82)	76754	54484	23917	(0.86)
St (alpha)	(0.12)	0	0	0	(0.36)
Bg	-----	1.5	1.5	1.5	1.5
Qconst	0	0	0	0	0
Tdelay	0	0	0	0	0

4. Evaluation of model performance within the case study catchments.

4.1 EVALUATION CRITERIA

The objective of the evaluation exercise was to look at the performance of the individual models within each catchment and, from this analysis to identify whether any general statements can be made about the relative merits of the four models and their packages. The models were applied using the packaged objective functions and graphical displays. To make comparisons between the models it was necessary to use a set of common goodness of fit tests, these are presented in section 4.1. The individual catchment assessments undertaken using these goodness of fit tests are presented in section 4.2. A generalised ranking scheme was applied to draw out general statements about model performance across the five catchments. This ranking scheme and the application to case study catchments is presented in section 4.3.

As discussed in Chapter 2 all of the models under evaluation advocate the use of one or more mathematical descriptions, or objective functions, for comparing observed and simulated flow time series as part of the model calibration process. It is also generally recommended by the authors that visual inspection of the hydrograph should form part of the calibration process. This combination of quantitative and qualitative goodness of fit tests represents the classical approach employed when calibrating the goodness of fit. Both of these approaches focus on the similarity of the simulated and observed time series within individual time steps. Alternative objective functions, both quantitative and qualitative, can be constructed by looking to optimise the distributional fit of the simulated time series to the observed. Examples of quantitative distribution objective functions are the use of summary statistics, for example measures of central tendency such as the mean and median, and measures of variance such as the standard deviation. Qualitative measures include graphical representation such as flow duration curves and flow frequency curves.

Ideally, an optimal model calibration would be one that provides an un-biased good fit across the full range of observed flows. This is rarely achievable in practice. The one or more objective functions used to evaluate the goodness of fit of a model should be closely related to the objective of the modelling study. If the model is to predict the response of flood events the objective function should focus on ensuring that high flow extremes are fitted well. Conversely, if the objectives of the modelling study are water resource orientated, as in the case of this study, then it is important to ensure that mass is conserved, i.e. mean flow is accurately simulated and that low flow extremes are modelled correctly. The issue of whether the objective function accounts for the time series element of flow or whether it is distributional in nature is also influenced by the intended use of the model. If the results are to be summarised statistically then the precision of the sequencing may be less important, however if the sequencing is correct this gives much greater confidence to the validity of the model and thus there is a strong case for it always to be considered. For the purposes of evaluating the models the following measures were employed:

- bias expressed as the difference between observed and simulated mean flow, presented as

- a percentage of the observed mean flow;
- the correlation coefficient (R^2);
- the Nash-Sutcliffe efficiency criteria;
- graphical comparison of observed and simulated flow duration curves;
- graphical comparison of observed and simulated hydrographs;
- graphical analysis of summary statistics associated with key percentiles on the observed flow duration curve.

The last of these measures is presented in more detail. The flow duration curve is derived for the observed flow time series by ranking in order of size and calculating an exceedence percentile for each flow, whilst retaining the date associated with each flow. This is equivalent to assigning a flow exceedence percentile to each date. Twelve key percentile points were considered. For each percentile point, the observed flow data and associated dates falling within the data range of $\pm 0.5\%$ around the point were extracted. For each extracted date the corresponding flow was extracted from the simulated time series. This selection process yields $N/100$ simulated and observed pairs for each exceedence percentile, where N is the total number of data points in the period being considered.

The performance of the model at each percentile point is assessed by calculating the bias and Coefficient of Variance (CoV) across the $N/100$ pairs at each point. These are then plotted as a function of exceedence percentile. The bias plot provides information as to whether the model consistently under or over predicts at particular flows, whilst the CoV plot provides information as to the consistency of the model at particular flows, which can be regarded as a measure of model stability at the percentile point. The CoV is used to facilitate comparison between different parts of the flow regime. As the number of pairs for each percentile point is much smaller for the calibration period than for the validation period, direct comparison between the results of a model within the calibration period and the validation period should not be made.

4.2 EVALUATION OF MODEL PERFORMANCE WITHIN THE CASE STUDY CATCHMENTS

Within each catchment, the models were assessed both within the calibration period and across the modelled period either side of this period; termed the evaluation period. For each period graphs for the observed and simulated example hydrographs, flow duration curves, percentile bias and percentile CoV plots are presented by catchment in Appendix A. These plots and associated summary statistics are reviewed below on a catchment basis.

4.2.1 The Babingley Brook at Castle Rising

- **Calibration period**

From inspection of the observed and simulated hydrographs for 1988 (Figure A1.1) it appears that none of the models are simulating the winter storm events well and that general flow recession characteristics through the year are best modelled by IHACRES and the TCM. The rate of recession for the PDM and HYSIM is too low. HYSIM also fails to model the recovery of flows at the end of the year. None of the models seem to model the response to

summer storms well. The TCM does not respond at all whilst HYSIM over predicts the response to large summer storms and fails to pick up the smaller events. The recession rates for response to the summer events are too low for both the PDM and IHACRES. All models route the majority, if not all, of the effective rainfall through a single slow response reservoir. This explains the poor response of PDM, IHACRES and the TCM to summer storms. The origin of the behaviour of HYSIM to large summer storms is less clear, although the behaviour may be associated with the conceptualisation of interflow within the upper and lower soil horizons.

The flow duration curves presented in Figure A.1.2 demonstrate that the PDM and HYSIM are the closest in simulating the observed distribution of flows, whilst IHACRES tends to under estimate the extremes and the TCM is very poor in simulating the distribution of flow for observed flows below Q20. The plot of the mean error at percentile points (Figure A.1.3) demonstrates the poor performance of the TCM. IHACRES has the highest mean error at high flows where it underestimates and it consistently over predicts for observed flows below Q20 although it has the smallest mean error for observed flows at the 95th percentile. The PDM and HYSIM are broadly similar in that they both generally under predict for flows above Q50 and over predict for flows below Q50 with similar patterns. The CoV plot (Figure A.1.3) shows that the PDM consistently has the lowest CoV, followed by IHACRES. The TCM has a low CoV at low flows, whilst HYSIM has a high CoV which strongly fluctuates between 10 and 25%.

Table 4.1 presents summary bias, R^2 and efficiency statistics for models within the calibration and evaluation periods. In the calibration periods the highest R^2 and efficiency values were for the PDM, which corroborates the lower error CoV plot for the PDM. HYSIM had the lowest bias, whilst the TCM had the largest bias but has the same R^2 value as IHACRES.

Table 4.1: Summary statistics for the Babingley Brook

	PDM	IHACR ES	TCM	HYSIM
Calibration				
Bias	-1.97	2.73	-15.61	-0.76
R^2	0.95	0.88	0.88	0.86
Efficiency	0.87	0.72	0.67	0.73
Evaluation				
Bias	-2.11	1.58	-24.91	-2.46
R^2	0.93	0.89	0.66	0.88
Efficiency	0.68	0.78	0.27	0.75

- **Evaluation**

The observed and simulated hydrographs are presented for a dry year (1992) in Figure A.1.4.

The flows simulated by the TCM are consistently lower than the observed, with little or no response to either short term events or the onset of recharge in the September. HYSIM did not simulate the onset of recharge until November and also consistently underestimates the baseflow. Once again the "spiky" response to summer storms is observed. The PDM and IHACRES markedly overestimate the flows at the start of the year but correctly pick up the catchment response to recharge. For the majority of the time both the PDM and IHACRES also significantly over estimate the flows. The flow duration curve plots, Figure A.1.5, show that the gradient and hence the variance of the flow distribution simulated by the TCM is close to that of the observed, although the simulated flows are consistently lower than the observed. The distribution fits of both IHACRES and HYSIM simulated flows are good, The PDM underestimates the high flows and overestimates the low flows. The mean error plots (Figure A.1.6) are consistent with the flow duration plots although the CoV plots (Figure A1.7) demonstrate that the PDM is much more consistent in the predictive error than the other models . HYSIM and IHACRES are broadly similar with respect to consistency whilst the TCM has the largest CoV. The summary statistics over the evaluation period show that the PDM has the highest R^2 value whilst IHACRES has the lowest bias and the highest efficiency.

4.2.2 The Sapiston at Rectory Bridge

- **Calibration period**

From inspection of the 1988 observed and simulated hydrographs (Figure A2.1) it is apparent that the PDM and HYSIM are the most consistent in simulating the observed hydrograph. The TCM dramatically over estimates the winter flows whilst the rate of recession in IHACRES is too high, a consequence of the first order model. This is borne out by the summary statistics presented in Table 4.2, which show that the PDM and HYSIM have the highest R^2 and efficiency values. The TCM has a negative efficiency, which indicates the sum of squares would be smaller if the simulated flows were replaced by the observed mean flow. Interestingly, the PDM and HYSIM have the largest bias values whilst the TCM has the smallest.

The flow duration curve presented in Figure A2.2 demonstrate that the PDM is the closest in simulating the observed distribution of flows. The TCM is good at low flows but over estimates the upper tail of the distribution, whilst IHACRES and HYSIM underestimate the low flows. Looking at the mean simulation error at specific exceedence percentiles, Figure A2.3, the distinction between models is less clear, although it should be noted that all models show significant error at one or more percentile points and, from the CoV plot (Figure A2.4), all models show high variation at percentile points, particularly for the TCM at high flows and IHACRES at low flows.

- **Evaluation**

The observed and simulated hydrographs for 1976, presented in Figure A2.5, demonstrate that none of the models are effective in simulating the observed flows in this year. The base flow recession for both HYSIM and IHACRES are too high, whilst all models over estimate the catchment response to both small and larger events. Looking at the flow duration curve, Figure A2.6, the PDM, although it has a similar gradient to the observed curve, consistently overpredicts for percentiles greater than Q80. The gradient of the TCM curve is too low whilst both IHACRES and HYSIM markedly underestimate at low flows. The summary statistics show that whilst the PDM still has a higher R^2 and efficiency than the other models it has the second highest bias at a 19% overestimate. The TCM has the largest bias and the lowest R^2 value. This coupled with the poor R^2 and negative efficiency values indicate the model fit is not valid. IHACRES has the smallest bias but has a low model efficiency. HYSIM has the second lowest bias, and the second largest R^2 and efficiency values.

Table 4.2: Summary statistics for the Sapiston Brook

	PDM	IHACRES	TCM	HYSIM
Calibration				
Bias	7.49	-4.16	-2.50	-5.10
R^2	0.91	0.72	0.25	0.85
Efficiency	0.77	0.27	-0.30	0.67
Evaluation				
Bias	18.94	-6.90	-28.28	-11.50
R^2	0.84	0.71	0.16	0.82
Efficiency	0.65	0.17	-1.49	0.55

Looking at the mean and CoV of errors between the observed and simulated flows at key percentile points, Figures A2.7 and A2.8, HYSIM is the most consistent model in terms of both the magnitude of the mean error at percentile points and the range of error as represented by the CoV plots. The mean error for the PDM is consistently positive and increases greatly at flows below the Q70 observed flow. The mean error for IHACRES gradually changes from a significant under estimate at the Q(2) observed flow to a significant overestimate at the Q70 observed flow. The precision of the mean error of the PDM and IHACRES, as indicated by the CoV plot is very similar for individual percentile points but increases at the observed flow decreases. The plots for the TCM show that the stability of fit for the TCM is similar to those for the PDM and IHACRES at high flows, and is better at low flows. However, the mean error translates from a large under prediction at high flows to a large over prediction at low flows, indicating that the model is not fitting the data well; as indicated by the other analyses.

4.2.3 The Nene at Orton

- **Calibration period**

From inspection of the 1998 observed and simulated hydrographs (Figure A3.1) it appears that the PDM and HYSIM are again the most consistent in simulating the observed hydrograph. The TCM under estimates the high winter flows in late January and early February and over estimates the catchment response to other winter events and to summer events. IHACRES consistently underestimates the observed flows and fails to model the catchment response to winter rainfall. This is consistent with the summary statistics presented in Table 4.3, which demonstrate that the PDM and HYSIM have the highest R^2 and efficiency whilst the TCM and IHACRES have a negative efficiency. HYSIM and the PDM have relatively small bias errors whilst IHACRES and HYSIM both have a high bias.

Table 4.3 Summary statistics for the Nene at Orton

	PDM	IHACRES	TCM	HYSIM
Calibration				
Bias	-3.23	-32.27	-23.53	1.75
R^2	0.91	-0.09	0.33	0.89
Efficiency	0.81	-1.51	-0.55	0.76
Evaluation				
Bias	11.94	-1.69	-25.61	4.91
R^2	0.86	0.79	0.30	0.81
Efficiency	0.71	0.57	-0.59	0.61

The flow duration curves presented in Figure A3.2 demonstrate that the flows for the PDM, HYSIM and the TCM in the lower tail of the distribution are a close fit to those of the observed, whilst all models underestimate in the upper tail of the distribution. Looking at the mean simulation error at specific exceedence percentiles, Figure A3.3, the PDM and HYSIM are broadly similar with mean errors of generally less than $\pm 25\%$. The TCM and IHACRES have much larger mean error at high flows. At low flows the TCM is broadly similar to the PDM and HYSIM whilst IHACRES greatly over predicts. These patterns are generally repeated in the CoV plots (Figure A3.4) which show that the fit of the PDM and HYSIM is much more stable than that of the other models. IHACRES is particularly unstable at low flows.

- **Evaluation**

The observed and simulated hydrographs for 1992, Figure A3.5, demonstrate that none of the models simulate the observed flows well in this year. The figure also demonstrates that the Wansford flows have not been added to the observed flows at Orton. On closer investigation it was found that this problem was restricted to 1992 and was thus omitted from the subsequent statistical analysis. Looking at the flow duration curves, Figure A3.6, the pattern is similar to that over the calibration period. The summary statistics show that whilst the PDM still has a higher R^2 and efficiency than the other models it has the second highest bias at a 12% overestimate. The TCM has the largest bias and the lowest R^2 value. This coupled

with the negative efficiency value indicate that the model fit is not valid. IHACRES has the smallest bias and, interestingly both the R^2 and efficiency values are much better than over the calibration period. On the basis of these statistics the fit of IHACRES is very similar to that of HYSIM. Looking at the errors between the observed and simulated flows at key percentile points, Figures A3.6 and A3.7, IHACRES generally has lower mean errors than the PDM and HYSIM which are very similar, whilst the TCM underestimates at high flows and overestimates at low flows. As regards stability, as expressed by the CoV plots, all models are generally similar except at low flows where HYSIM appears to be more stable than the other models.

4.2.4 The Blackwater at Appleford Bridge

- Calibration period

From inspection of the observed and simulated hydrographs (Figure A4.1) it appears HSYIM is the most consistent model when modelling the observed flows. The PDM under-estimates at high flows while the TCM fails to simulate the high flows at the end of January, yet attempts to replicate the other winter high flow periods. The base flow response is adequately modelled by the TCM although the model consistently over estimates the catchment response to summer rainfall. IHACRES again over estimates high flows and under-estimates low flows. This is a consequence of the first order routing model. The summary statistics presented in Table 4.4 show that HYSIM has the highest R^2 and efficiency. The PDM has the second highest R^2 value, but has a negative efficiency. IHACRES has a lower R^2 value than the PDM yet has a positive efficiency. The R^2 and efficiency values for the TCM are low. Interestingly IHACRES and the TCM have the lowest bias at 2.4% and 3.5% respectively. Both the PDM and HYSIM have a high negative bias.

Table 4.4 Summary statistics for the Blackwater at Appleford Bridge

	PDM	IHACRES	TCM	HYSIM
Calibration				
Bias	-19.34	2.43	3.47	-20.90
R2	0.70	0.66	0.24	0.74
Efficiency	-1.61	0.29	-0.93	0.45
Evaluation				
Bias	-18.83	2.58	12.55	-10.66
R2	0.64	0.62	0.20	0.66
Efficiency	-2.12	0.16	-0.84	0.22

The flow duration curves presented in Figure A4.2 demonstrate that the best distributional fit is given by the TCM simulation. IHACRES and HYSIM underestimate flows in the lower tail of the distribution, with HYSIM predicting zero flows at the 98th percentile. The PDM over estimates in the lower end and under estimates in the upper tail. It is difficult to draw firm conclusions from the plots of mean simulation error at specific exceedence percentiles (Figure A4.3), except that, looking across the entire percentile range, the PDM and

IHACRES are broadly comparable. The TCM and HYSIM are comparable at high flows yet below the median flow the TCM over predicts whilst HYSIM under predicts. The CoV plots in Figure A4.4 demonstrate that the PDM is generally more stable across the flow regime than the other models. IHACRES is very unstable at low flows whilst the TCM and HYSIM are less stable in the middle of the flow regime.

- **Evaluation**

The observed and simulated hydrographs for 1992, presented in Figure A4.5. demonstrate that none of the models simulate the observed flows well in this year. Looking at the flow duration curves, Figure A4.6, the pattern is similar to that over the calibration period. The summary statistics show that HYSIM still has a higher R^2 and efficiency than the other models and that the bias has reduced by approximately 50%. The bias of the TCM has increased by a factor of approximately 3.5 and the low R^2 and negative efficiency value call the fit of the model into question. IHACRES has the smallest bias with only small decreases in both the R^2 and efficiency values. The PDM has a high negative bias and, although the R^2 value is still relatively high, the model efficiency is negative. Looking at the errors between the observed and simulated flows at key percentile points, Figure A4.7, HYSIM generally has lower mean errors than the other models. The PDM and IHACRES are broadly similar and the TCM underestimates at flows above the observed $Q(10)$ flow and greatly over estimates at all flows below $Q(10)$. As regards stability, as expressed by the CoV plots (Figure A4.8), the PDM is the most stable followed by HYSIM. IHACRES demonstrates a similar stability to that of HYSIM at flows above the $Q(30)$ flow but becomes increasingly unstable as the exceedence percentile increases. The TCM is generally less stable than the other models.

4.2.5 The Box at Polstead Bridge

- **Calibration period**

From inspection of the 1998 observed and simulated hydrographs (Figure A5.1) it appears that none of the models simulate the observed hydrograph well. HYSIM, IHACRES and the TCM all under predict baseflow and all models tend to over predict the catchment response to summer rainfall. Winter high flow events within the catchment are also poorly simulated by all models. The summary statistics presented in Table 4.5, show that the PDM, IHACRES and HYSIM all have a similar R^2 value of around 0.7. The TCM R^2 value is very much lower at 0.14. All models have low efficiency values, with the PDM and TCM values being negative. The PDM has the second highest R^2 value, yet has a negative efficiency. IHACRES has a lower R^2 value than the PDM yet has a positive efficiency. The R^2 and efficiency values for the TCM are low. IHACRES has an almost zero bias whilst the TCM and PDM have very large bias values of -50% and 29% respectively.

The flow duration curves presented in Figure A5.2 demonstrate that none of models particularly simulate the observed flow duration curve well. The PDM curve has a similar variance but is consistently higher than the observed curve. The TCM consistently under predicts, whilst IHACRES and HYSIM underestimate markedly at low flows and over estimate at flows above $Q(30)$. Looking at the mean simulation error at specific exceedence percentiles, Figure 5.3, it is difficult to draw distinctions with models performing better at

some percentiles than others. A similar behaviour is observed within the CoV plots (Figure A5.4) with the exception that the HYSIM is much more stable at the higher exceedence percentiles than the other models.

Table 4.5 Summary statistics for the Box at Polstead Bridge

	PDM	IHACRES	TCM	HYSIM
Calibration				
Bias	28.90	-0.66	-50.17	6.31
R2	0.70	0.70	0.14	0.68
Efficiency	-0.04	0.08	-1.48	0.27
Evaluation				
Bias	73.08	21.15	-2.88	24.52
R2	0.60	0.64	0.17	0.65
Efficiency	0.25	0.34	-2.64	0.42

• **Evaluation**

The observed and simulated hydrographs for 1992, in Figure A5.5, demonstrate that none of the models simulate the observed flows well in this year. Looking at the flow duration curves, Figure A5.6, the pattern is similar to that over the calibration period with the exception of the TCM which fits relatively well across the entire percentile range. The summary statistics show that model efficiency has improved for the PDM, HYSIM and IHACRES. The PDM shows the biggest decrease in R² value of 15%. The TCM R² and efficiency values are still extremely low indicated a very poor model fit. The bias of the TCM has decreased from being the largest to being the smallest bias. The bias for all the other models has substantially increased, with the PDM showing the biggest absolute increase to 73%. Looking at the errors between the observed and simulated flows at key percentile points, Figures A5.7, IHACRES generally has a lower mean error than the other models. The PDM generally has the highest mean errors. HYSIM exhibits the biggest change from a mean over estimate of +50% at the Q(2) observed flow to a mean under estimate of -100% at the Q(98) flow. The TCM behaves in the opposite way to HYSIM with the largest underestimates at high flows and the largest over estimates at low flows. The CoV plots, Figure A5.8, shows that all the models are unstable right across the flow regimes with the exception of HYSIM which exhibits quite a low CoV at low flows.

4.3 INTER-CATCHMENT AND MODEL COMPARISONS

The discussion of the results from the case study catchments, presented in Section 3.3, demonstrate how difficult it is to draw firm conclusions about the performance of the individual models within the case study catchments with goodness of fit tests often providing conflicting, or inconclusive results. However the results of the exercise have proved that a reasonable distributional fit (as described by the flow duration curve) may be obtained when the time series fit may be very poor. This is of concern when evaluating model performance and as a consequence the flow duration statistics are not included in the comparison of model

performance across catchments. A generalised ranking scheme for target goodness of fit tests has been developed and used to assess:

- how amenable the flow regimes of the individual catchments were to modelling using simple lumped models;
- if any of the models could be identified as performing more consistently better than others.

The application of the ranking scheme in these contexts is presented below. The goodness of fit test statistics used within the ranking scheme were:

- Bias
- R^2
- Efficiency
- Mean percentile error (the average of the dimensionless error for the 5, 10, 15, 20, 30, 50, 70, 80, 90 and 95 exceedence percentiles)
- Stability (the average of the CoV of the dimensionless error for the 5, 10, 15, 20, 30, 50, 70, 80, 90 and 95 exceedence percentiles)

These last two test statistics, whilst not statistically rigorous, attempt to numerically summarise the information presented graphically and discussed for individual catchments. In the ranking scheme analysis three scenarios were considered:

- Goodness of fit over the calibration period
- Goodness of fit over the evaluation period
- Goodness of fit over the calibration period and the change in goodness of fit between the calibration and evaluation periods.

For the third scenario the sum of the modulus of the departure from a perfect fit in the calibration period and the modulus of the difference between the fit in the calibration period and the evaluation period was used to summarise the performance of the individual goodness of fit tests over the two periods.

4.3.1 Inter-catchment comparison

This comparison exercise was undertaken to assess, relatively, how well the flow regimes of the catchments could be represented by lumped rainfall runoff models. The application of the ranking scheme in this comparison is discussed with respect to one scenario. For each model the goodness of fit was assessed in each catchment according to each of the test statistics and the catchments ranked according to the value of the test statistic. The average rank across the four models was then taken to give an overall catchment rank for each test statistic. An example for the efficiency statistic over the calibration period is shown in Table 4.6.

Table 4.6 Example ranking of catchments by model

Efficiency PDM	Calibration Period			Mean Rank
	IHACRES	TCM	HYSIM	
Babingley	1.00	1.00	1.00	1.00
Sapiston	3.00	3.00	2.00	2.00
Nene	2.00	5.00	3.00	2.00
Blackwater	5.00	2.00	4.00	3.00
Box	4.00	4.00	5.00	4.00

The average ranks for each test statistic were then collated for each scenario. These are presented in Table 4.7.

Table 4.7 Ranking of catchments by model and scenario

	Calibration				
	Babingley	Sapiston	Nene	Blackwater	Box
Bias	1	2	3	3	5
Efficiency	1	2	2	3	4
R ²	1	3	2	4	5
Mean % err.	1	3	2	4	5
Stability	1	2	2	5	4
Overall	1	3	2	4	5
	Evaluation				
	Babingley	Sapiston	Nene	Blackwater	Box
Bias	1	4	2	3	5
Efficiency	1	3	2	4	5
R ²	1	2	3	4	5
Mean % err.	1	2	3	4	5
Stability	1	2	3	4	5
Overall	1	2	2	4	5
	Combined				
	Babingley	Sapiston	Nene	Blackwater	Box
Bias	1	4	3	2	5
Efficiency	1	3	2	4	5
R ²	1	2	3	4	5
Mean % err.	1	2	3	4	5
Stability	1	2	4	3	4
Overall	1	2	3	4	5

The overall picture produced by this ranking scheme shows that for all scenarios the best model fits were obtained for the Babingley Brook and the worst for the River Box. The Blackwater was consistently fourth. The Nene had an over all rank of 2 over the calibration and evaluation periods and the Sapiston a rank of 3, however when considering the goodness of fit in the calibration period and the stability of that goodness of fit between the calibration period and the evaluation period (scenario 3) the rank places changed over for these latter

catchments.

4.3.2 Inter-model comparisons

A similar approach to the inter-catchment comparisons was adopted for the inter-model comparisons. For each catchment the goodness of fit was assessed for each model according to each of the test statistics and the models ranked according to the value of the test statistic. The average rank across the five catchments was then taken to give an overall model rank for each test statistic. An example for the efficiency statistic over the calibration period is shown in Table 4.8

Table 4.8 Example ranking of models by catchment

Efficiency	PDM	Calibration		Period	
		IHACRES	TCM	HYSIM	mean rank
Babingley	1.00	1.00	1.00	2.00	1.00
Sapiston	3.00	3.00	2.00	3.00	2.00
Nene	2.00	5.00	3.00	1.00	2.00
Blackwater	5.00	2.00	4.00	4.00	3.00
Box	4.00	4.00	5.00	5.00	4.00

The average ranks for each test statistic were then collated for each scenario. These are presented in Table 4.9. Within the calibration phase the PDM scores the highest overall rank followed by HYSI, IHACRES and the TCM in that order. With the exception of the bias statistics the scorings for individual test statistics is very consistent. The bias rankings reflect that both IHACRES and HYSIM include calibration factors to ensure that mass is conserved over the calibration period.

Over the evaluation period HYSIM scores the highest overall rank followed jointly by IHACRES and the PDM with the TCM scoring the lowest rank. The scorings for individual statistics are consistent with the calibration period for HYSIM and the TCM. The promotion of HYSIM to rank 1 for the mean error and stability indices is a consequence of the degradation of the PDM scores for these indices. IHACRES retains the highest rank for the bias statistics demonstrating the utility of calibrating to ensure mass is conserved.

When looking at the rankings for the combined score, HYSIM scores the highest rank. This is consistent across all statistics, with the exception of bias, where IHACRES has the highest combined rank. The PDM scores the second highest rank and, with the exception of bias, the PDM is ranked either second or joint first with HYSIM. IHACRES is ranked third and the TCM is ranked fourth. The overall ranks for the models are very consistent with the ranks for the individual test statistics for scenario 3.

Table 4.9 Ranking of models by catchment model and scenario

Calibration				
	PDM	IHACRES	TCM	HYSIM
Bias	3	1	4	2
Efficiency	2	3	4	1
R ²	1	3	4	2
mean % err.	1	3	4	2
Stability	1	3	3	2
overall	1	3	4	2
Evaluation				
	PDM	IHACRES	TCM	HYSIM
Bias	3	1	3	2
Eff.	3	2	4	1
R ²	1	3	4	2
mean % err.	3	2	4	1
Stability	2	4	3	1
overall	2	2	4	1
Combined				
	PDM	IHACRES	TCM	HYSIM
Bias	3	1	4	2
Eff.	2	3	4	1
R ²	1	3	4	1
mean % err.	2	3	4	1
Stability	1	3	3	1
overall	2	3	4	1

5. Conclusions

Looking at the calibration and evaluation periods the best model fits were consistently obtained for the Babingley Brook and the worst for the River Box. The model fits for the Blackwater were consistently fourth. During the calibration periods the model fits were better for the Nene than the Sapiston, however over the evaluation period better model fits were obtained for the Sapiston than for the Nene. It was not apparent from the analysis that particular models were more suitable than others for specific catchment types.

During the period of record considered the Sapiston and Box catchment were relatively natural. When the Ely Ouse scheme is not operating the Blackwater catchment is essentially natural and, given the transient nature of the schemes operation, the errors in the naturalised flow records associated with the Ely Ouse transfer scheme will not have a major impact upon the quality of the flow record. Without further investigations, and given the good hydrometric quality of the flow record it is difficult to see why the performance of the models should be worse in these catchments than the other catchments.

The Nene is subject to some complex artificial influences and, given the poor data quality associated with the majority of influences and the temporal variability of the quality, it is quite likely that time dependent artifacts of the influences remain within the naturalised flow record. This may account for why, generally, the quality of the model fits were much better in the calibration period than the evaluation period.

The case study catchments are amongst some of the driest gauged catchments within the United Kingdom. The treatment of evaporation and the modelling of actual evaporative losses is a primary issues when modelling these catchments. Modelling in these dry catchments is thus a good test of the performance of the loss modules within rainfall runoff model. However the issue of errors in the input data must not be ignored. In these dry catchments the gauged runoff is in the order of 100-150 mm/yr, the consequence of relatively small errors in the estimation of catchment rainfall and evaporation/temperature may result in quite major errors in the modelled runoff. For example, taking a crude water balance a 5% error in an estimated rainfall of 600mm/yr may result in a water balance error of up to 30% in the gauged runoff.

Obviously the model parameters derived during optimisation will tend to compensate for any errors within the input data, including stream flow data. However this may lead to structural problems within the model which, coupled with the likely random nature of errors in the input data, will reduce the quality of the model fit.

It is important to draw the distinction between the model structure and the packaged optimisation procedures and associated objective functions. The performance of the model will be strongly influenced by the choice of objective function and the efficiency of the optimisation scheme will be strongly influenced by how identifiable unique model parameters are, which is a function of the model structure. All of the aforementioned will be influenced by input data quality. On the basis of these considerations it is not possible to definitively say that one model is better than another model.

From a technical viewpoint the ranking scheme adopted demonstrated that the PDM was the most consistent model across the calibration period followed by HYSIM, IHACRES and then the TCM. HYSIM gave better results over the evaluation period than the PDM and when jointly considering the performance in the calibration period and the departure from that performance in the evaluation period HYSIM was the most consistent of the four models. The PDM was the second most consistent model overall, followed by IHACRES and the TCM in that order.

On the issue of ease of use HYSIM and IHACRES were the easiest models to use. Both of these models came with comprehensive documentation and clear tutorial exercises. The user interfaces for these models, whilst a little cumbersome, were found to be easy to use and data import was found to be straightforward. The PDM and the TCM packages did not come with adequate documentation, but it must be stated that these models are not marketed as standalone commercial packages in the same way that HYSIM and IHACRES are. The user interfaces for both the PDM and TCM are fairly basic but ergonomically easy to use. Both models suffered from poorly documented data import facilities. The complexity of the TCM interface was not commensurate with the relatively complex nature of the model, which made it difficult to find adequate model fits.

In conclusion, this report recommends that HYSIM is the most suitable model for adoption by the Anglian region of the Environment Agency. This recommendation is subject to the proviso that the model is very complex and that the use of default values for many of the parameters within the model must raise the question of whether this level of complexity is warranted. Furthermore the strong structural interrelationships between the primary parameters must be a cause for concern regarding parameter identifiability.

The PDM and IHACRES are recommended as models worthy of future consideration for use. However, the former, although a mature model is not sufficiently matured as a daily flow modelling package for operational use, whilst the latter would benefit from having alternative loss module configurations included in the package. The Wilby implementation of the Thames Catchment Model is not recommended as an operational model. This is not a reflection of the model itself, but rather the limitations of the model package.

6. References

- Bergström S. & Forsam A., 1973. Development of a conceptual deterministic rainfall-runoff model. *Nordic Hydrology* 4, 1973, 141-170
- Blackie J.R. & Eeles C.W.O, 1985. Lumped Catchment models. In *Hydrological Forecasting* (edited by M.G. Anderson & T.P. Burt). John Wiley & Sons Ltd.
- Boughton, W.C. 1966. A mathematical model for relating runoff to rainfall with daily data. *Civil Eng. Trans., I.E. Aust.* Vol. CE8, No. 1, 83-93
- Brooks R.H. and Corey A.T. Hydraulic properties of porous media. Colorado State University, Hydrology Paper No. 3.
- Burnash R.J.C., 1995. The NWS River Forecast System-Catchment modelling. Chapter 10, *Computer Models of Watershed Hydrology*. Editor V.J. Singh, Water Resources Publications, Colorado, USA.
- Burnash R.J.C., Ferral, R.L. & McGuire, R.A., 1973. A generalised streamflow simulation system: conceptual modelling for digital computers, Report of the Joint Federal State River Forecast Centre, U.S. National Weather Service and California Department of Water Resources, Sacramento.
- Chiew F.H.S. & McMahon T.A., 1991. Improved modelling of the groundwater processes in MODHYDROLOG. *Proc. Hydrol. And Water Resources Symp.*, Perth, Western Australia, October 1991
- Crawford N.H. & Linsley R.K., 1966. Digital Simulation on Hydrology: Stanford Watershed Model IV. Stanford University Technical Report No. 39. Stanford University, Palo Alto.CA.
- Dooge J.C.I., 1973. Linear Theory of hydrologic systems. Tech. Bull. 1468. Agric. Res. Service, US Dept. Agric., Washington.
- Fawthrop N., 1992. Naturalisation of the Orton River Flow Record. National Rivers Authority. Anglian Region.
- Greenfield B., 1984. The Thames Catchment Model. Unpublished Report. Thames Water Authority.
- Gupta V.K. & Sarooshian S., 1983. Uniqueness and observability of conceptual rainfall-runoff parameters: The percolation process examined. *Water Resources Research* 19(1), 269-276.
- Hughes D.A. & Sami K., 1994. A semi-distributed, variable time interval model of catchment hydrology – structure and parameter estimation procedures. *J. Hydrol.*, 155, 265-291.

Hughes D.A., 1995. Monthly rainfall-runoff models applied to arid and semiarid catchments for water resource estimation purposes. *Hydrol. Sci. Journ.* 34(1), 63-78.

Hyoms C.M. 1980. Development of a Soil Moisture Model for the Estimation of Percolation. Unpublished M.Phil thesis, The City University.

Jakeman A.J. & Hornberger G.M., 1993. How much complexity is warranted in a rainfall runoff model? *Water Resources Research*, 29(8), 2637-2649.

Jakeman A.J., Littlewood, I.G., Whitehead, P.G. , 1990. Computation of the instantaneous unit hydrograph and identifiable component flows with application to two small upland catchments. *Journal of hydrology*, 117, 275-300.

Leavesly G.H. & Stannard L.G., 1995. The Precipitation-Runoff Modelling System-PRMS. Chapter 9, *Computer Models of Watershed Hydrology*. Editor V.J. Singh, Water Resources Publications, Colorado, USA.

Littlewood I.G. & Jakeman A.J., 1994. A new method of rainfall runoff modelling and its applications in catchment hydrology. In P.Zanetti (ed) *Environmental Modelling (Volume II) Computational Mechanics Publications*, Southampton, UK, 141-171.

Littlewood I.G. & Parker J., 1997. *PC-IHACRES User Guide*. Institute of Hydrology

Manley R.E., 1977. The soil moisture component of mathematical catchment simulation models., *J.Hydrol.* 35, 341-356.

Manley R.E., 1978. The use of a hydrological model in water resources planning. *Poc.Instrn Civ. Engrs*, Part 2, 1978, 65, 223-235.

Moore R.J, 1985. The probability-distributed principle and runoff production at point and basin scales. *Hydrological Sciences Journal*, 30(2), 273-297.

Moore R.J., Austin R.M. & Carrington D.S. 1994. Evaluation of FRONTIERS and Local Radar Rainfall Forecasts for Use in Flood Forecasting Models. National Rivers Authority R&D Note 225.

Moore R.J., Jones D.A. & Black K.B. 1989. Risk assessment and drought management in the Thames basin. *Hydrological Sciences Journal*, 34(6), 705-717.

NERC, 1975. *Flood Studies Report*.

Nielson S.A. & Hansen E., 1973. Numerical simulation of the rainfall-runoff process on a daily basis. *Nordic Hydrology* 4, 171-190.

Penman H.L., 1949. The dependence of transpiration on weather and soil conditions. *Journal of Science*, 1, 74-89.

Philip J.R., 1957. The theory of infiltration, 1 The infiltration equation and its solution. *Soil*

Sci., 83, 345-357.

Quick M.C., 1995. The UBC watershed model. Chapter 8, Computer Models of Watershed Hydrology. Editor V.J. Singh, Water Resources Publications, Colorado, USA.

Rosenbrock H.H., 1960. "An Automatic method of finding the greatest or least value of a function. Computer Journal, 3, 175-184.

Servat E. & Dezetter A, 1991. Selection of calibration objective functions in the context of rainfall runoff modelling in a sudanese savannah area.

Singh V.P. 1995. Watershed Modelling. Chapter 1, Computer Models of Watershed Hydrology. Editor V.J. Singh, Water Resources Publications, Colorado, USA.

Smith J.M., 1977. Mathematical modelling and Digital Simulation for Engineers and Scientists. John Wiley & Sons Ltd.

Sorooshian and Gupta, 1995. Model calibration. Chapter 2, Computer Models of Watershed Hydrology. Editor V.J. Singh, Water Resources Publications, Colorado, USA.

Speers D.D., 1995. SSARR Model. Chapter 11, Computer Models of Watershed Hydrology. Editor V.J. Singh, Water Resources Publications, Colorado, USA.

Sugawara M., 1995. The Tank Model. Chapter 6, Computer Models of Watershed Hydrology. Editor V.J. Singh, Water Resources Publications, Colorado, USA.

Todini, E. 1996. The Arno rainfall-runoff model., J.Hydrol. 175, 339-382.

Todini, E., 1988. Rainfall-Runoff modelling: past, present and future. J. Hydrol., 100, 341-352.

Watts G, 1994. Naturalisation of the Babingley Flows. Internal Report. National Rivers Authority – Anglian Region.

Wilby R.L., 1994. Modelling the Relative Impact of Weather, Landuse and Groundwater Abstraction on Low Flows. National Rivers Authority R&D Note 268.

WRc, 1990. A Resource Model of the Great Ouse River System. Report No. CO 2504-M.

Young A.R. & Sekulin A.E. 1996. Naturalised River Flow Records of the Essex Region, Phase III Final Report. Institute of Hydrology Client Report to the Anglian region of the Environment Agency.

Zhao, R.J., Zhuang, Y., Fang L.R., Lin X.R. & Zhang Q.S., 1980. The Xinanjiang model. In: hydrological forecasting (Proc. Oxford Symp., April 1980) IAHS Publ. No. 129.

Appendix A: Model evaluation graphs

A1 The Babingley Brook at Castle Rising

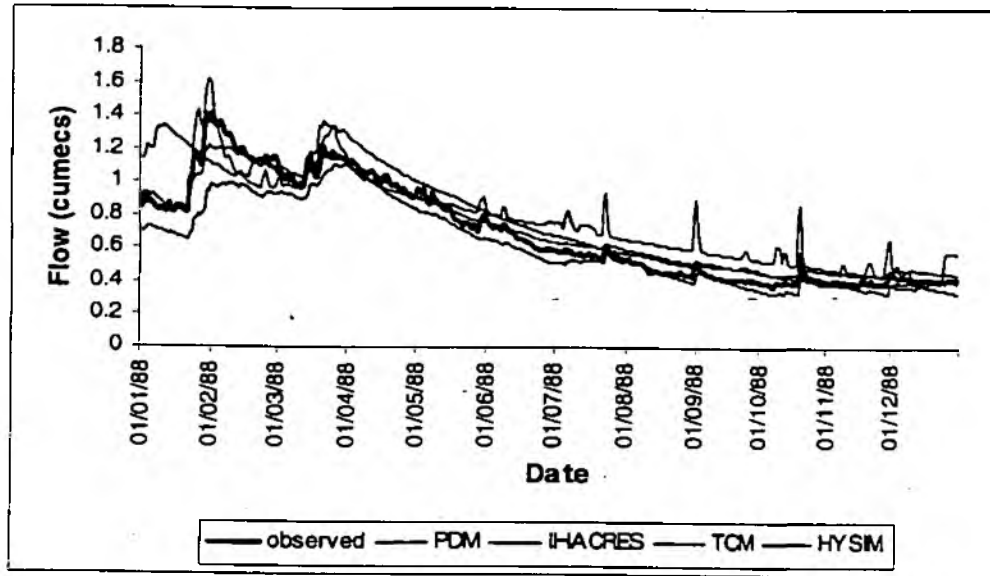


Figure A1.1: Calibration period: observed and simulated hydrographs for 1988

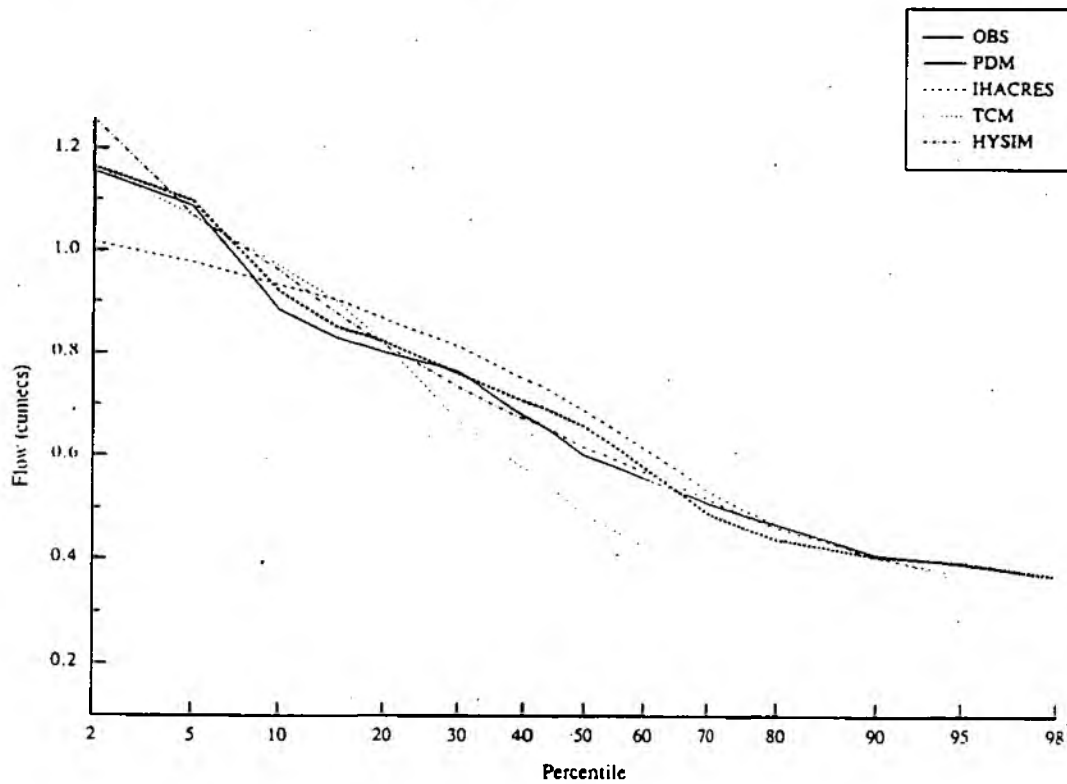


Figure A1.2: Calibration period: simulated and observed flow duration curves

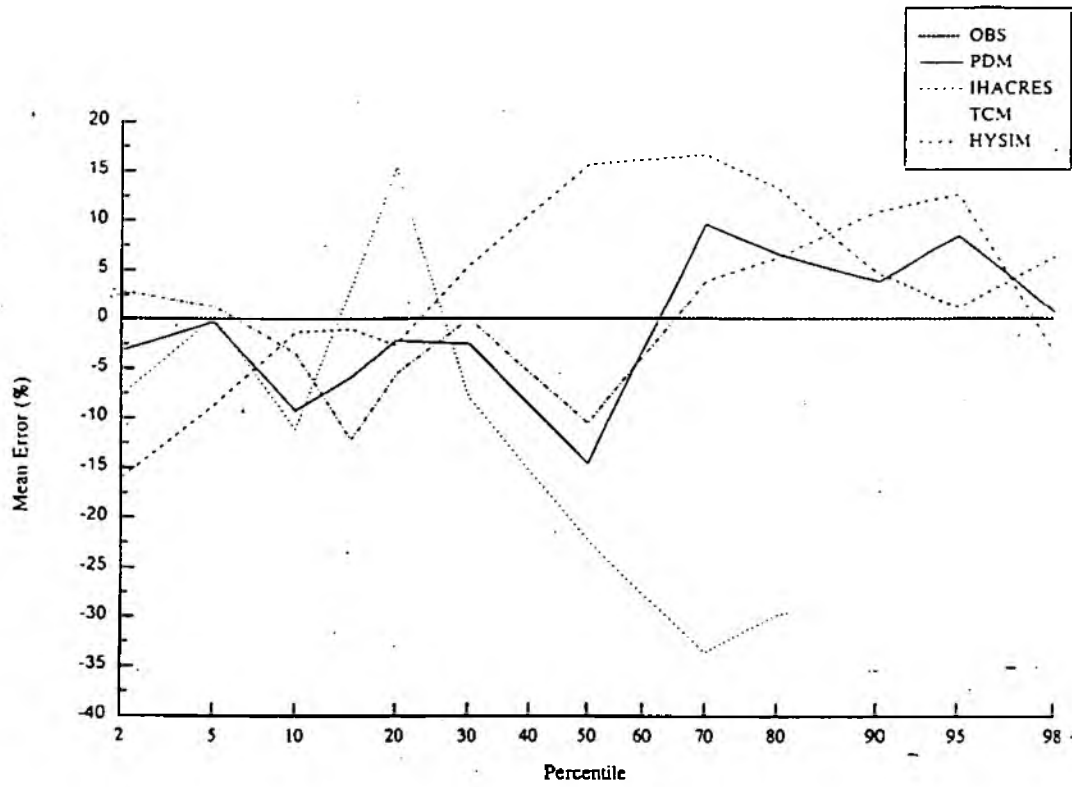


Figure A1.3: Calibration period: mean simulation errors at observed percentile points

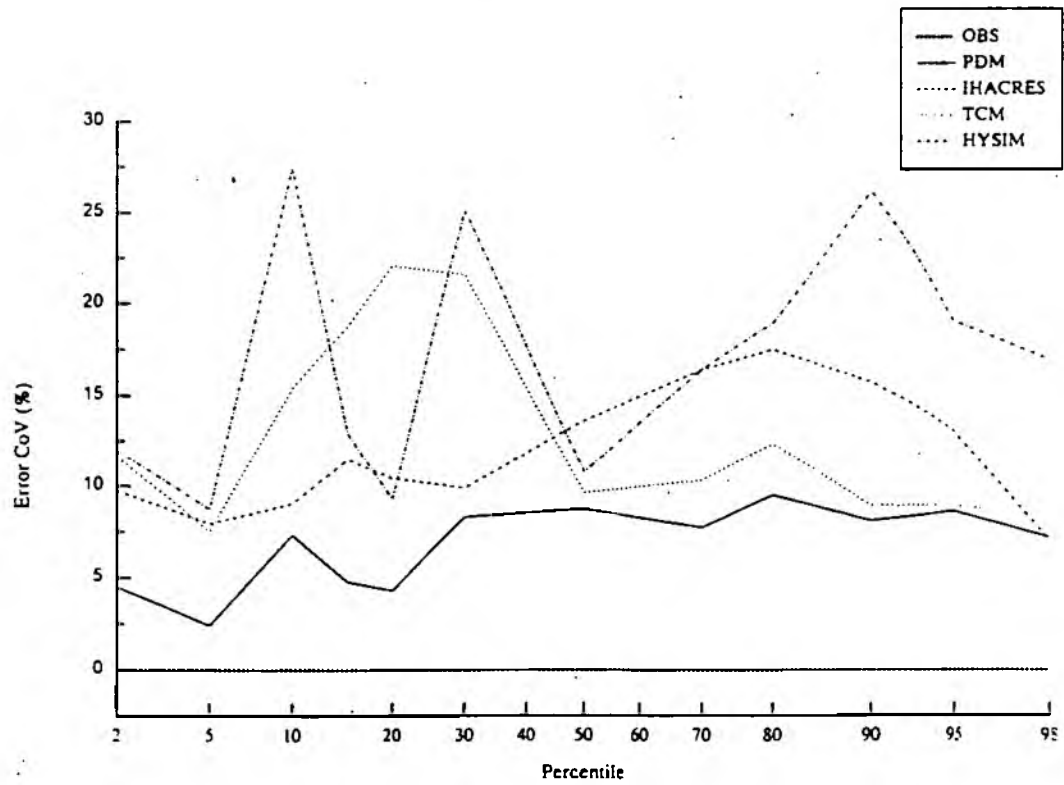


Figure A1.4: Calibration period: CoV for simulation errors at key percentile points

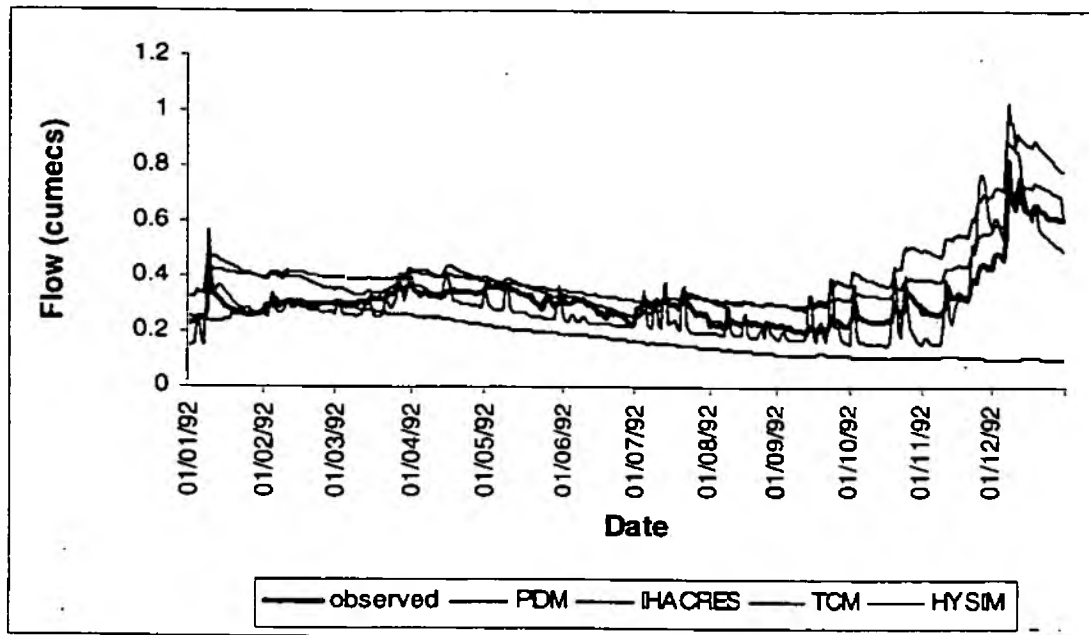


Figure A1.5: Evaluation period: observed and simulated hydrographs for 1976

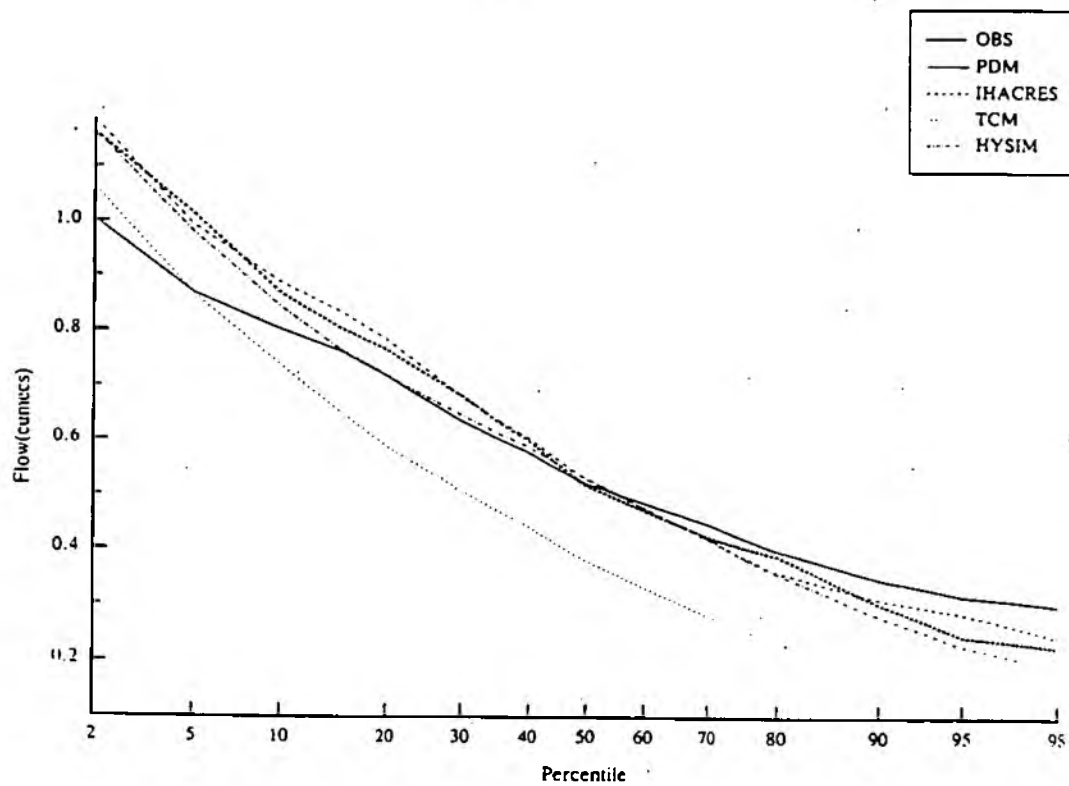


Figure A1.6: Evaluation period: simulated and observed flow duration curves

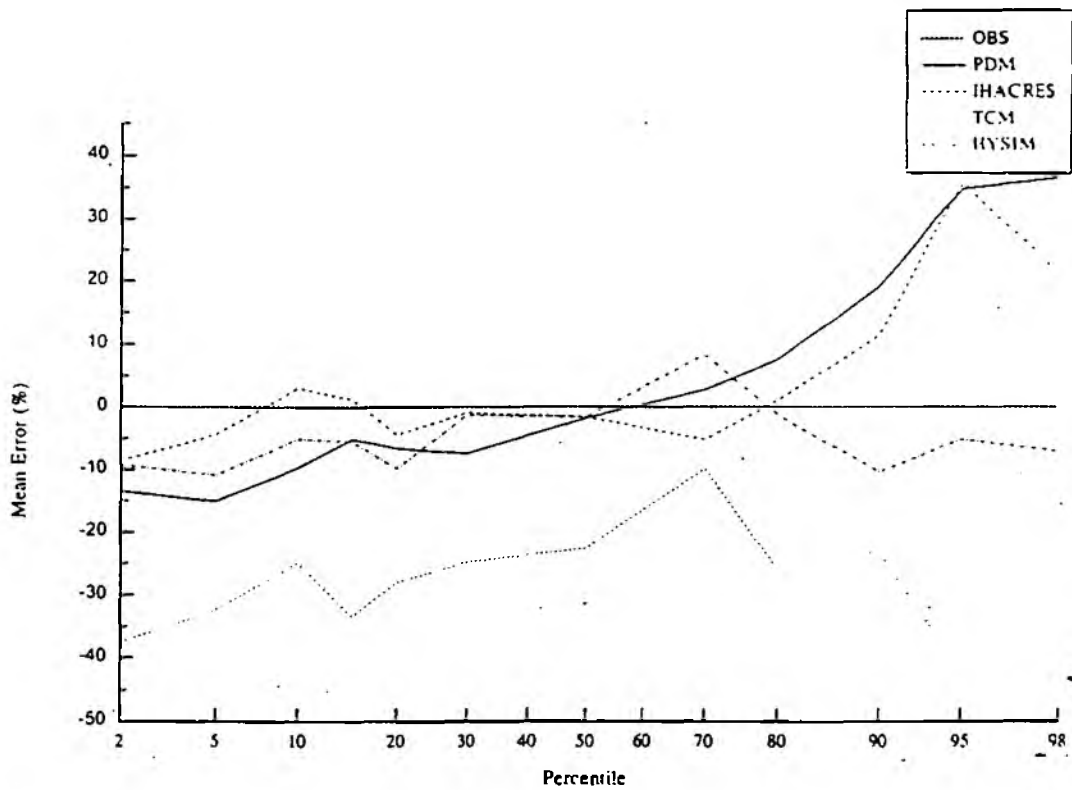


Figure A1.7: Evaluation period: mean simulation errors at observed percentile points

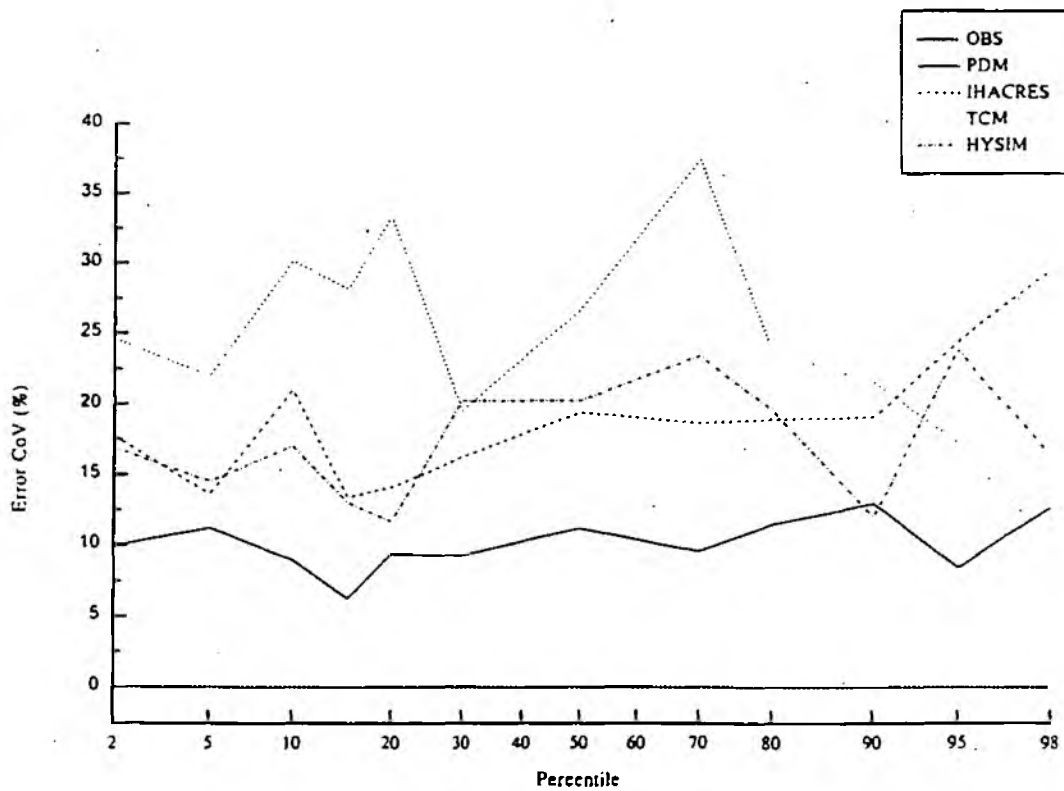


Figure A1.8: Evaluation period: CoV for simulation errors at key percentile points

A2 The Sapiston at Rectory Farm

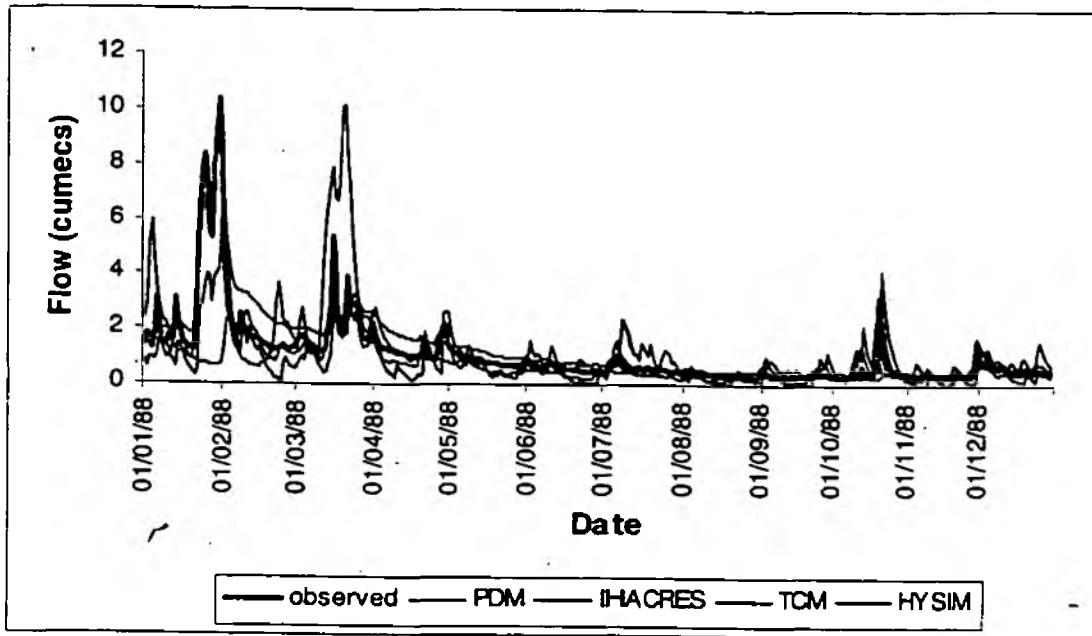


Figure A2.1: Calibration period: observed and simulated hydrographs for 1988

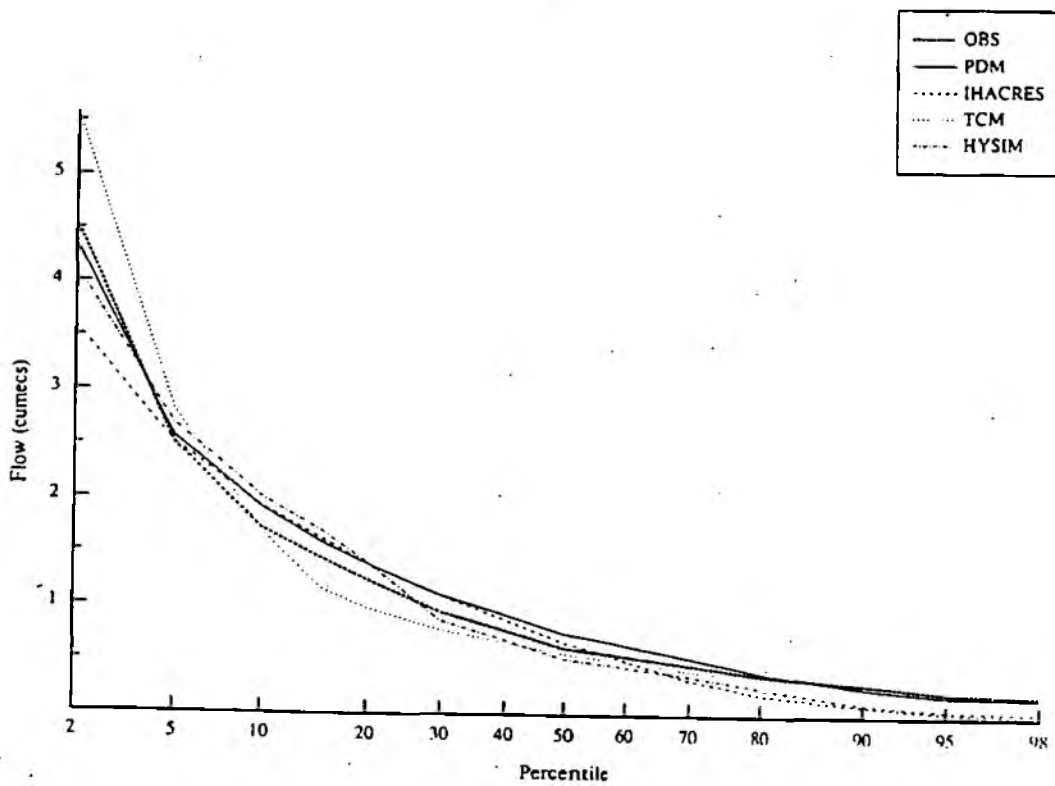


Figure A2.2: Calibration period: simulated and observed flow duration curves

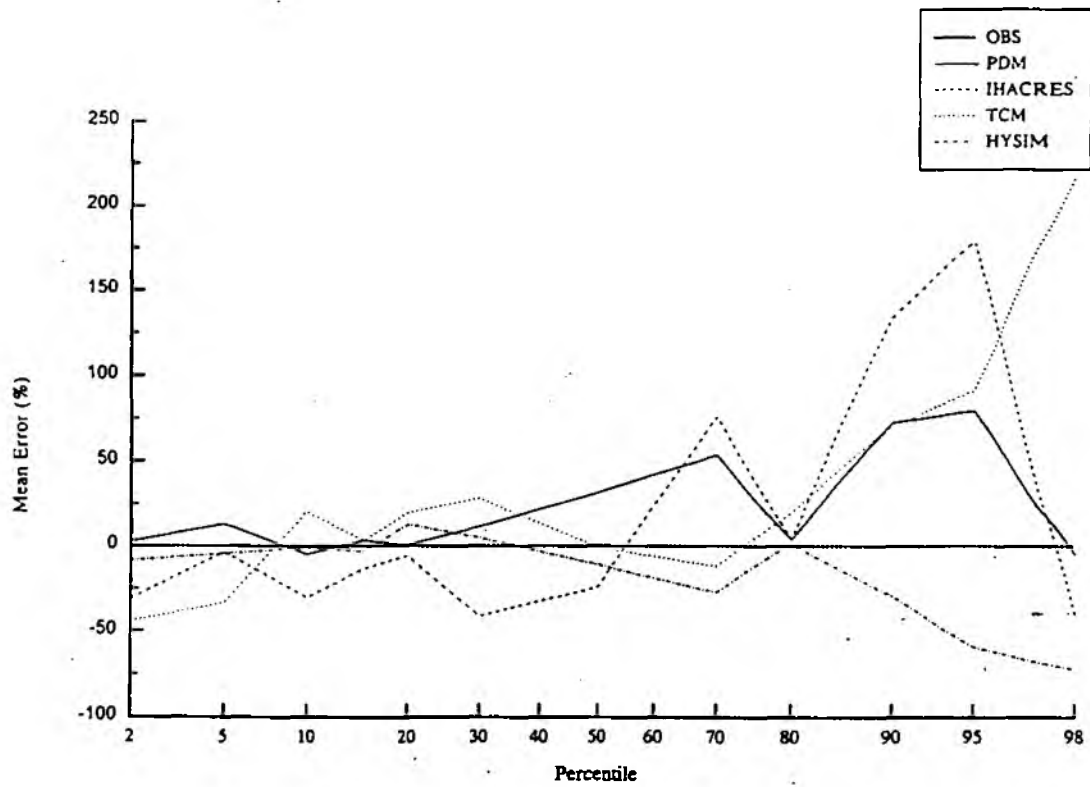


Figure A2.3: Calibration period: mean simulation errors at observed percentile points

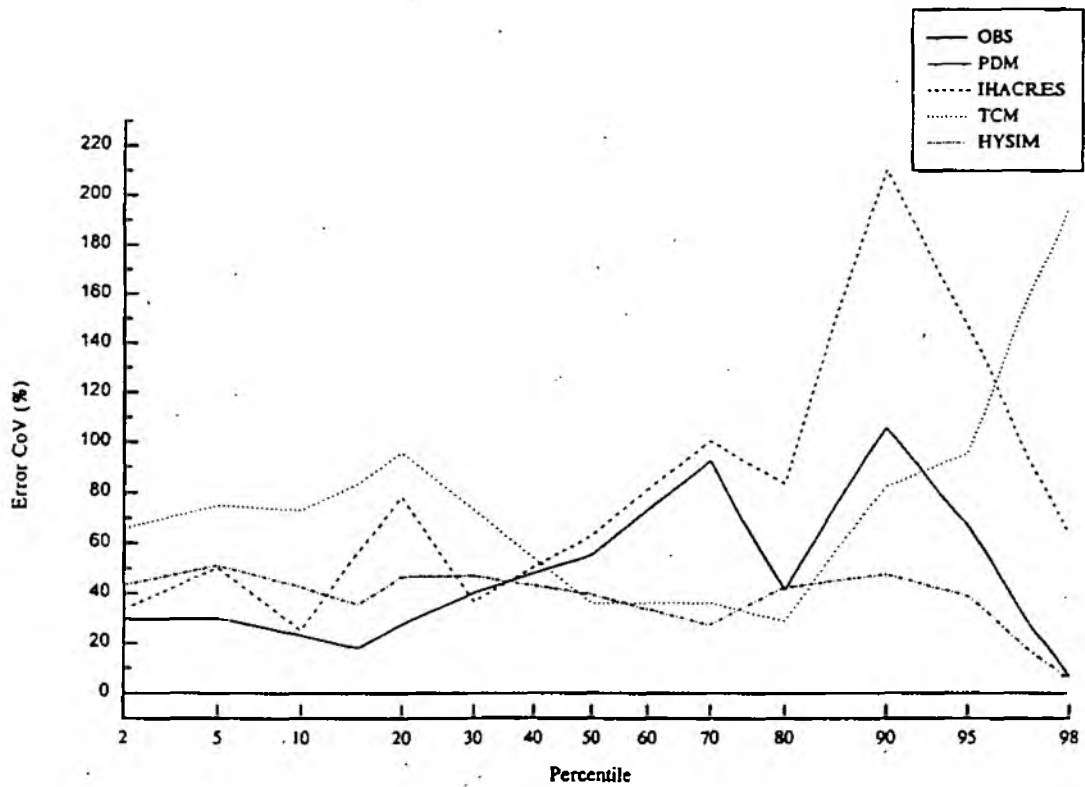


Figure A2.4: Calibration period: CoV for simulation errors at key percentile points

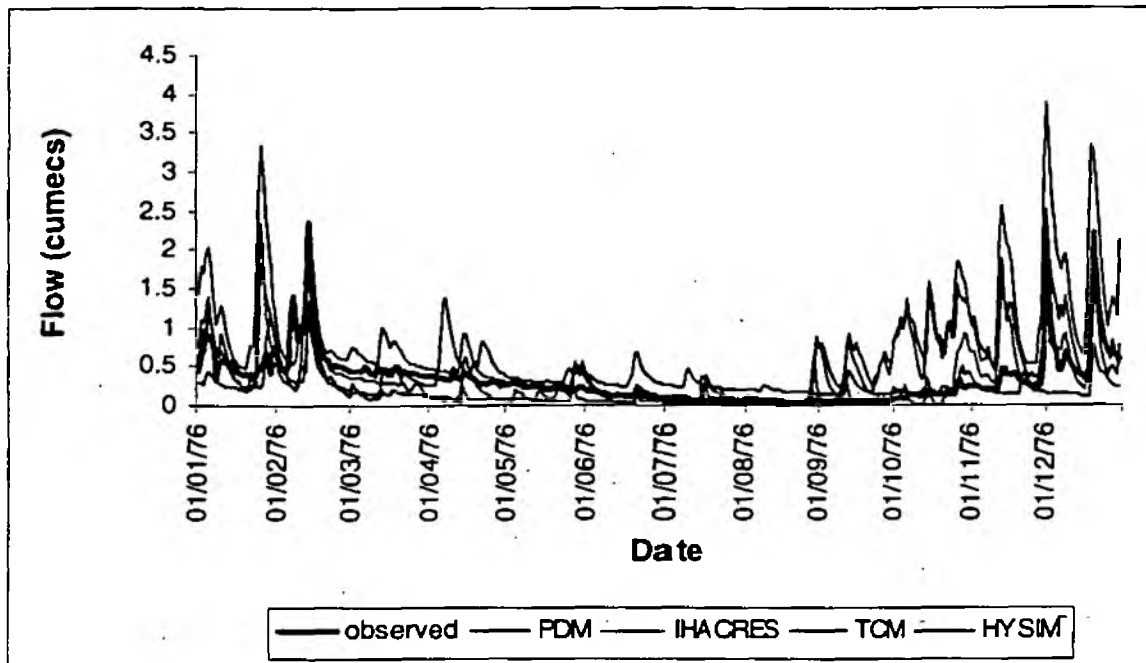


Figure A2.5: Evaluation period: observed and simulated hydrographs for 1976

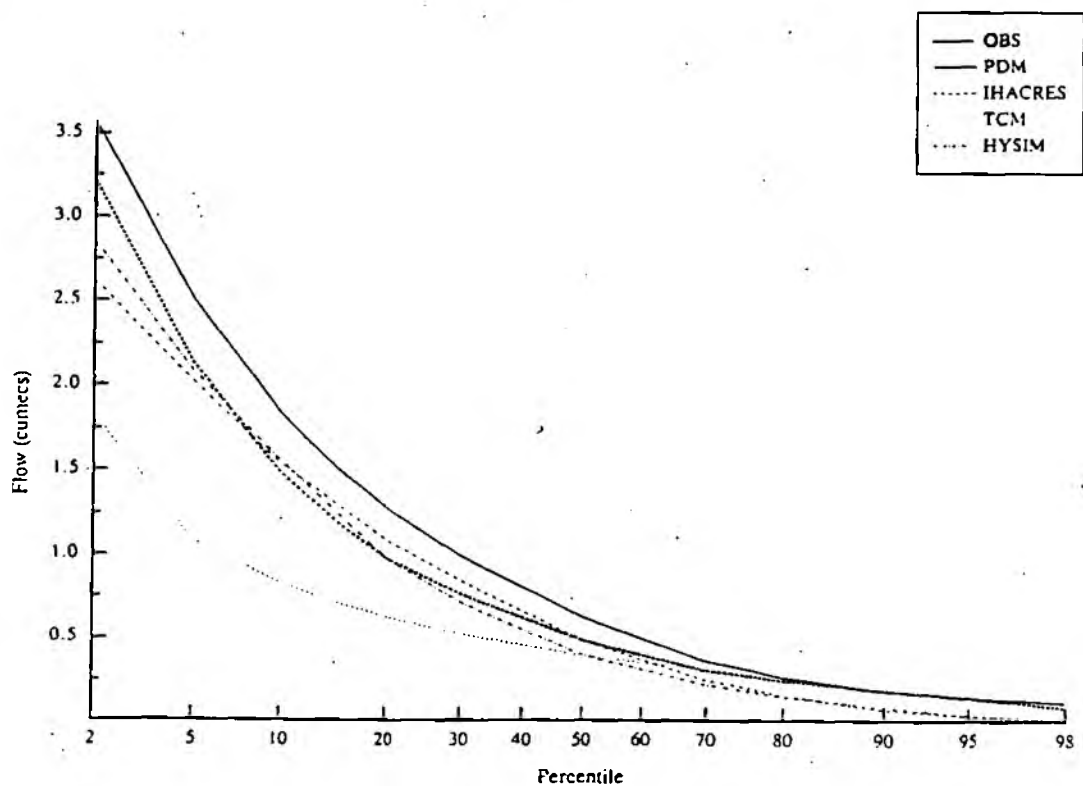


Figure A2.6: Evaluation period: simulated and observed flow duration curves

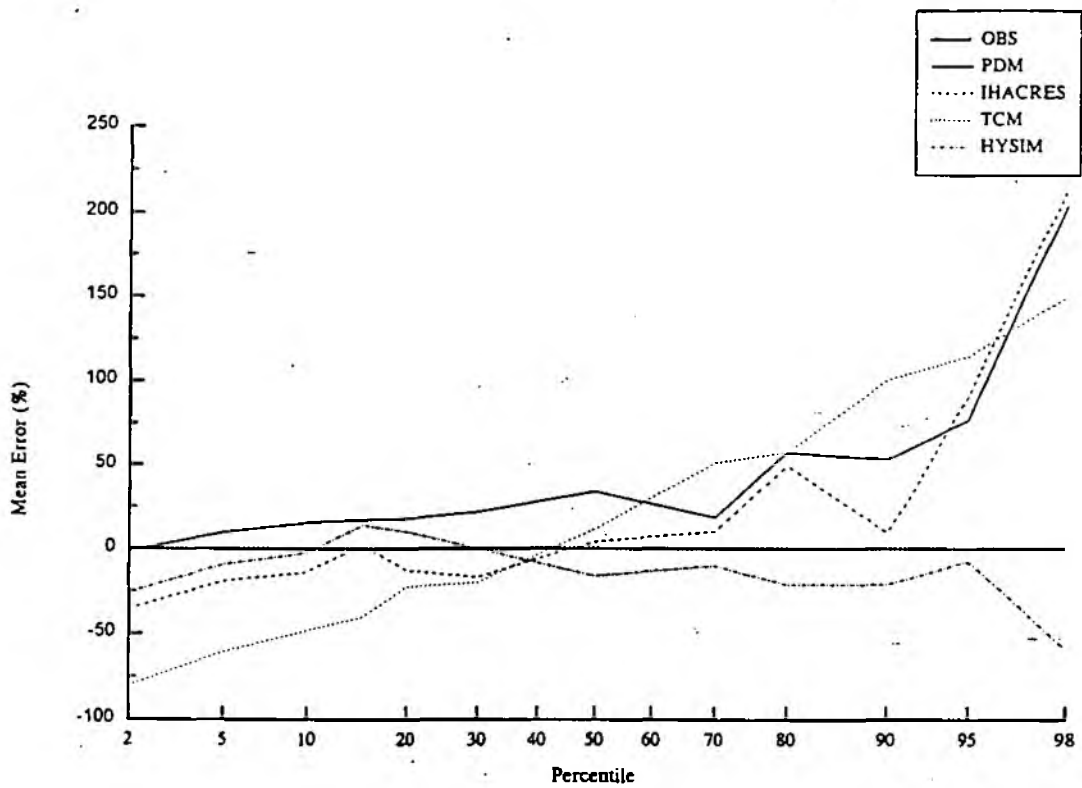


Figure A2.7: Evaluation period: mean simulation errors at observed percentile points

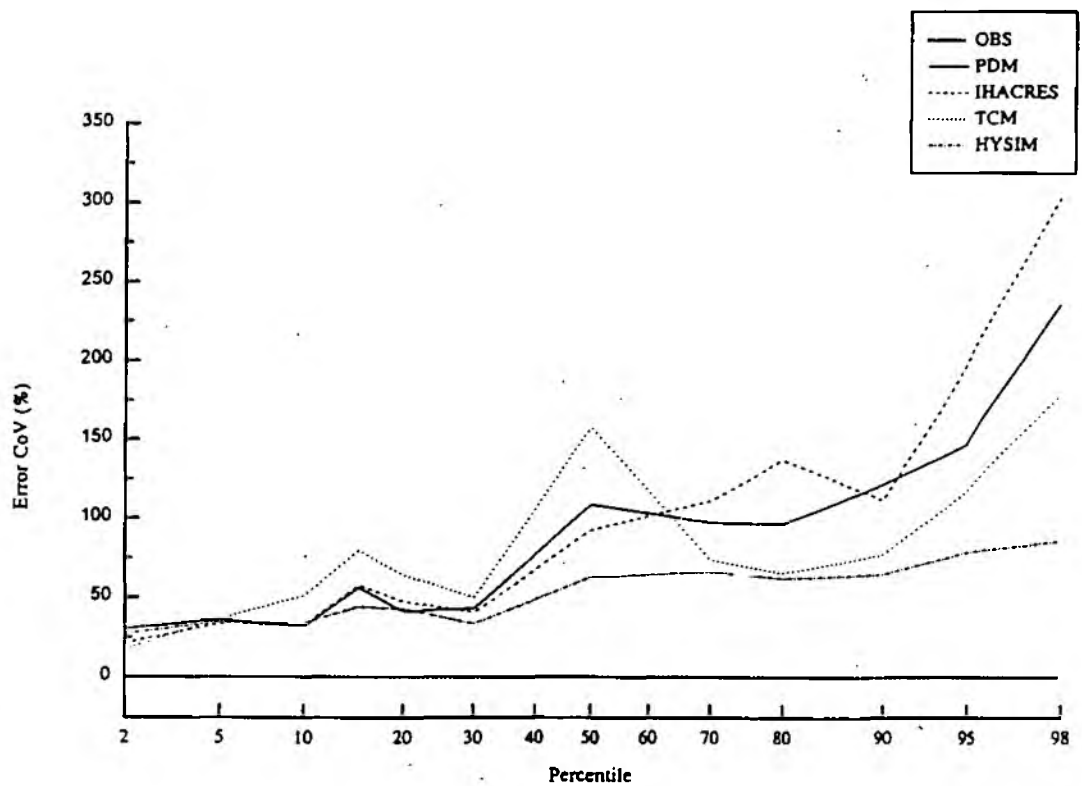


Figure A2.8: Evaluation period: CoV for simulation errors at key percentile points

A3 The Nene at Orton

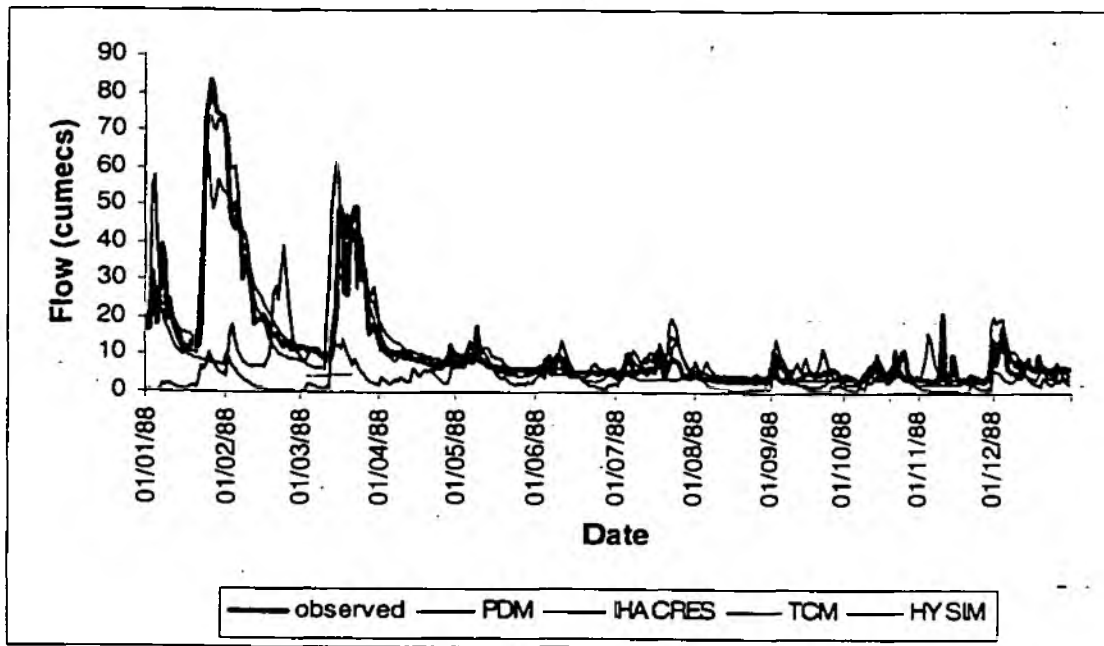


Figure A3.1: Calibration period: observed and simulated hydrographs for 1988

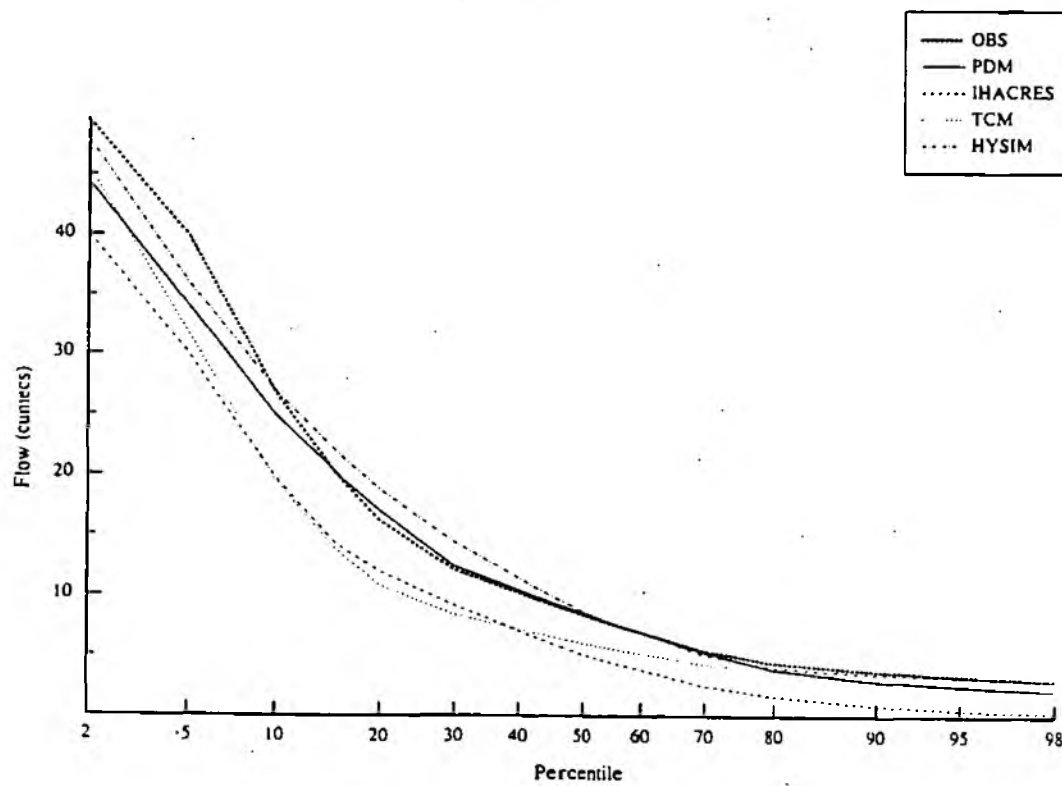


Figure A3.2: Calibration period: simulated and observed flow duration curves

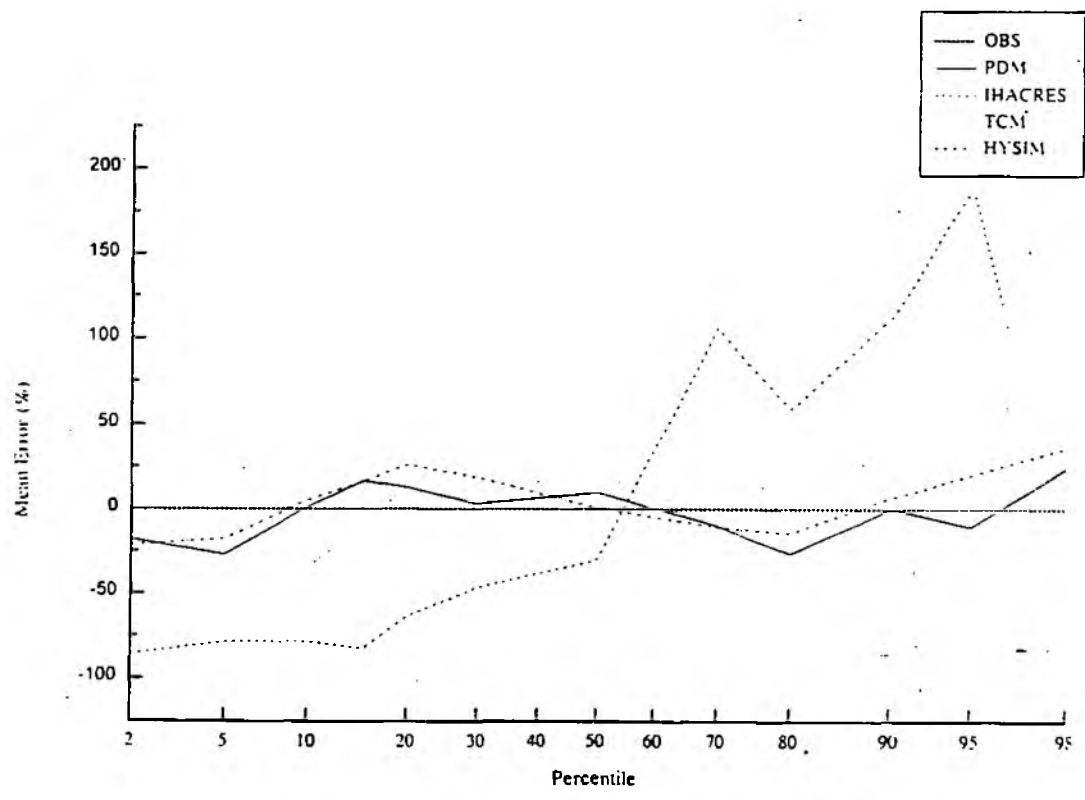


Figure A3.3: Calibration period: mean simulation errors at observed percentile points

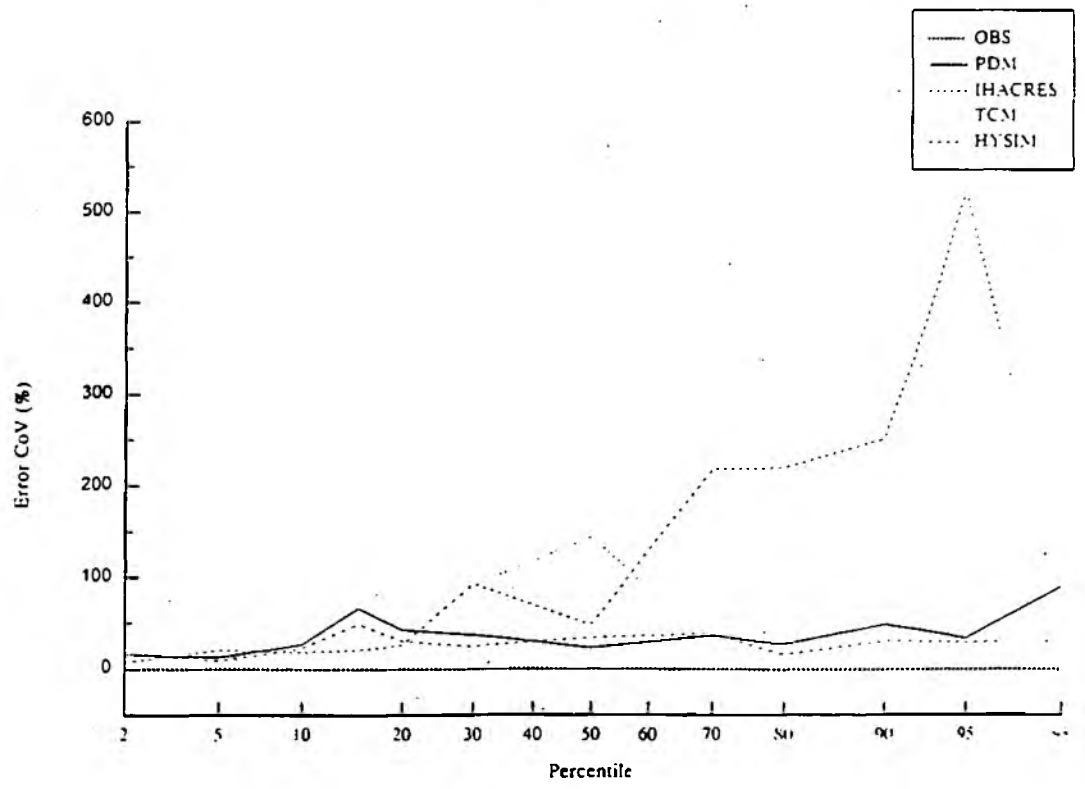


Figure A3.4: Calibration period: CoV for simulation errors at key percentile points

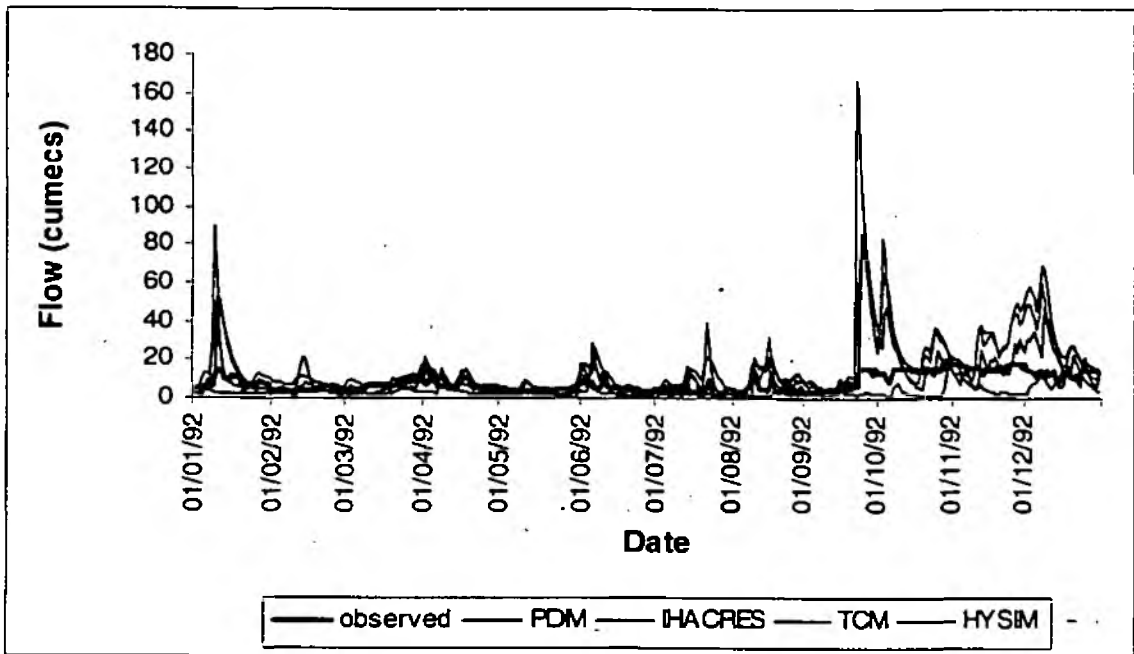


Figure A3.5: Evaluation period: observed and simulated hydrographs for 1992

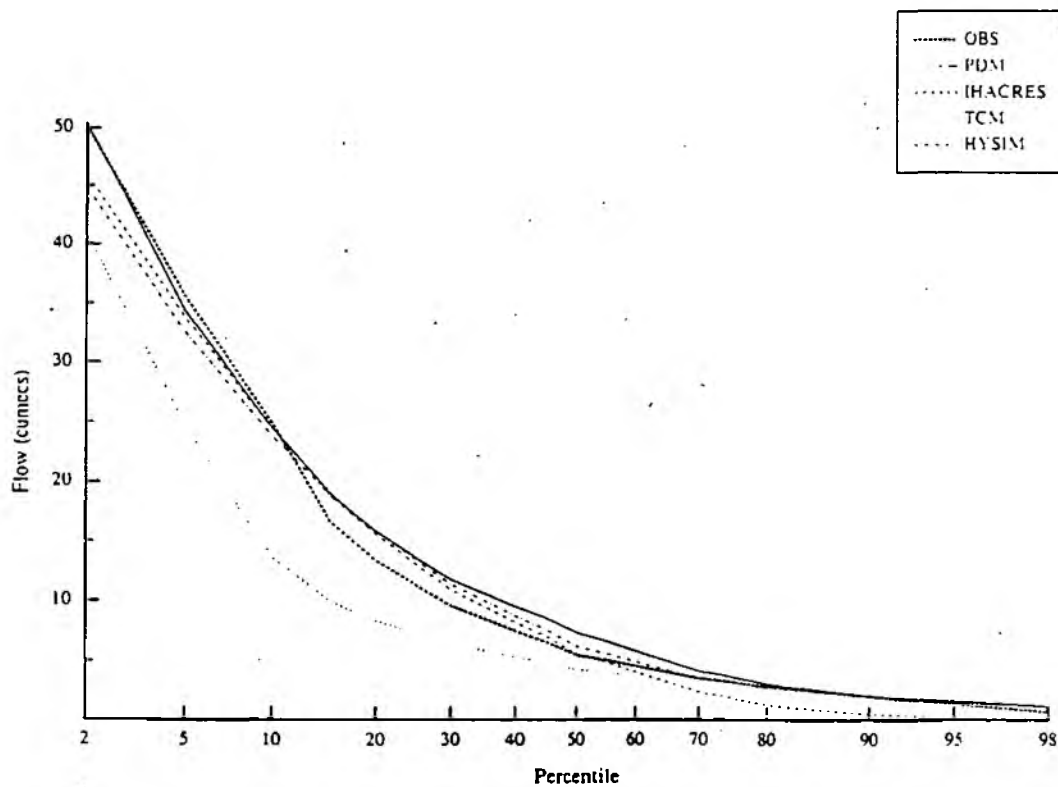


Figure A3.6: Evaluation period: simulated and observed flow duration curves

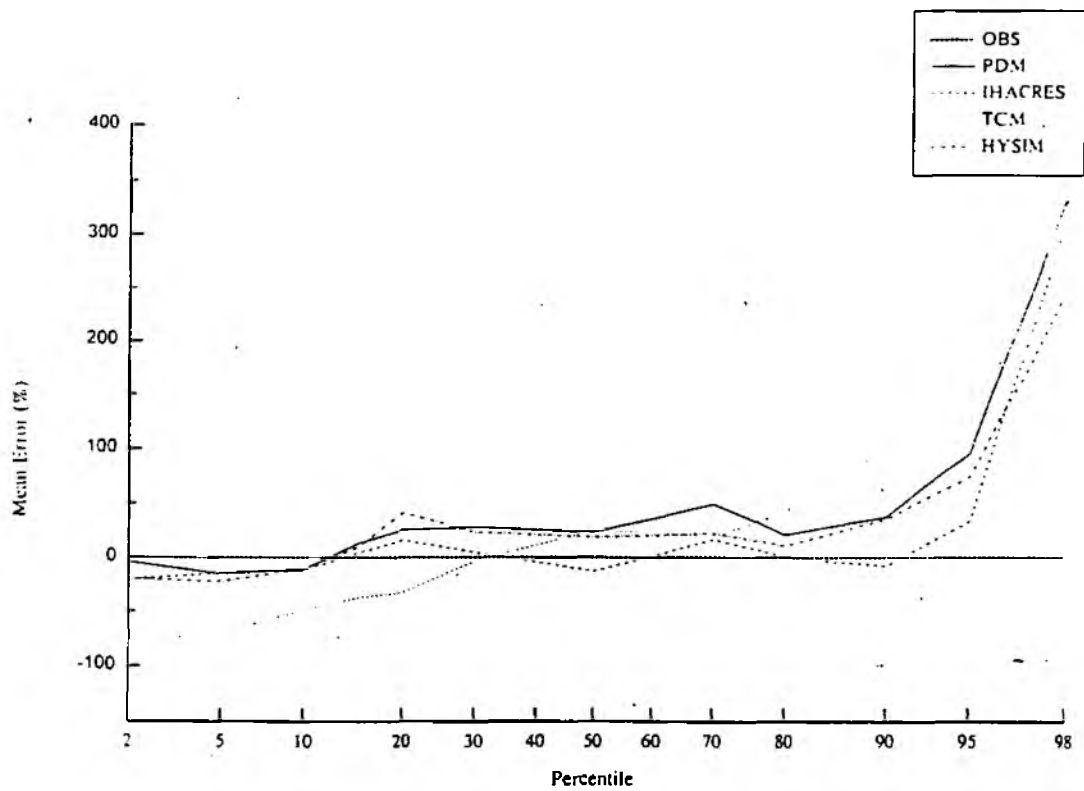


Figure A3.7: Evaluation period: mean simulation errors at observed percentile points

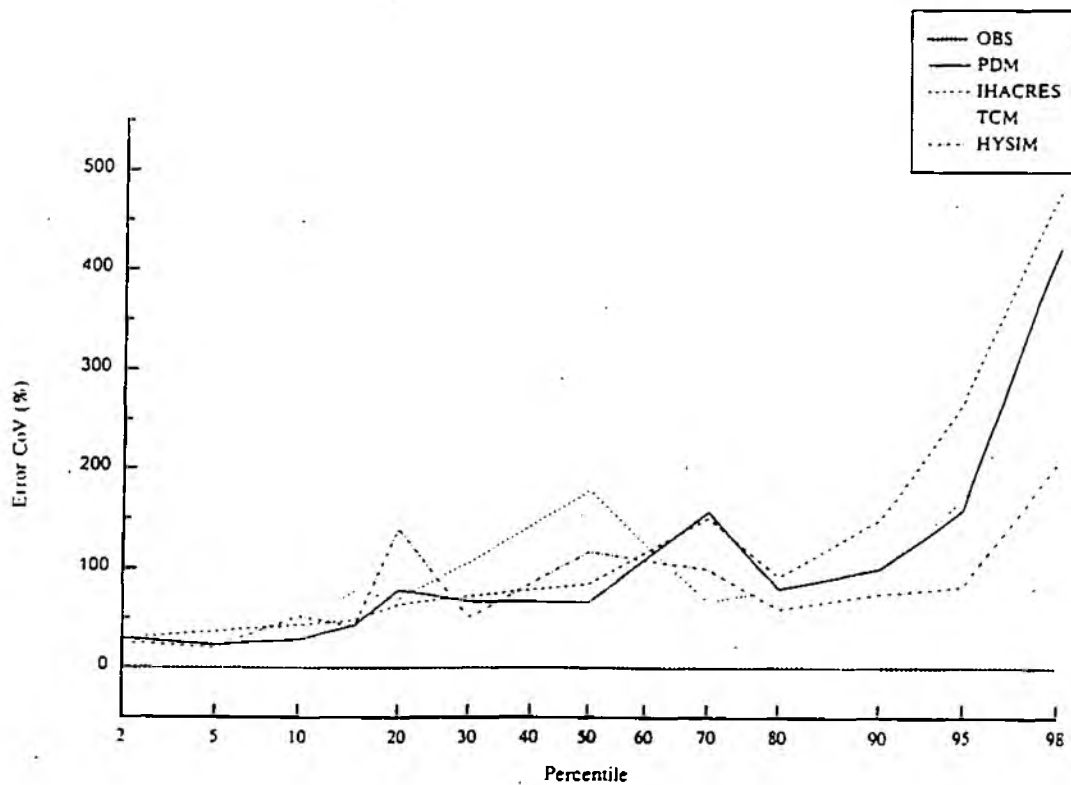


Figure A3.8: Evaluation period: CoV for simulation errors at key percentile points

A4 The Blackwater at Appleford Bridge

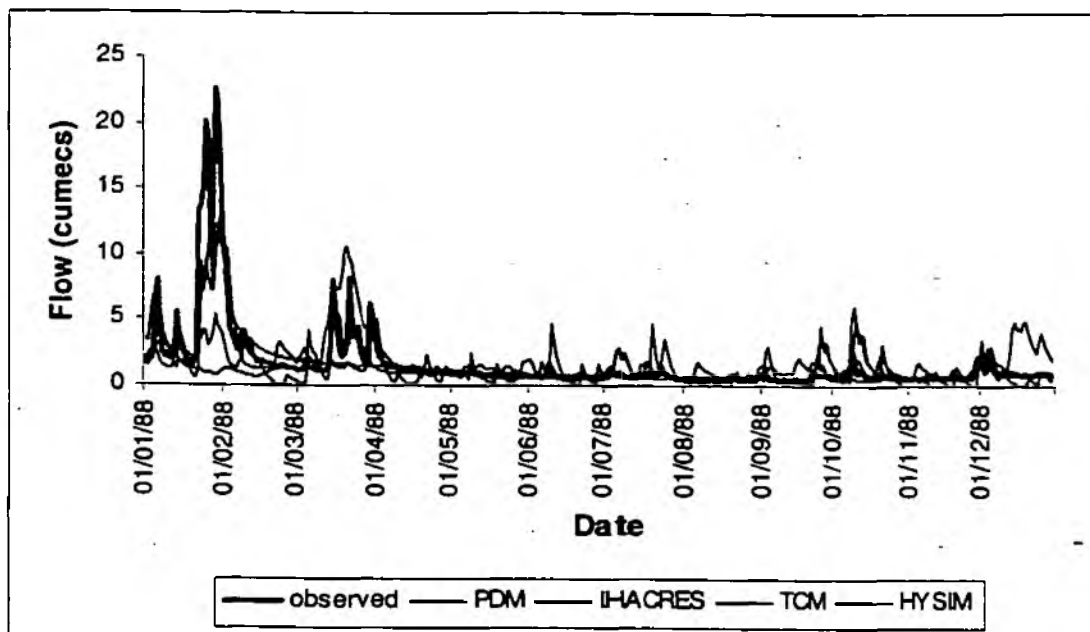


Figure A4.1: Calibration period: observed and simulated hydrographs for 1988

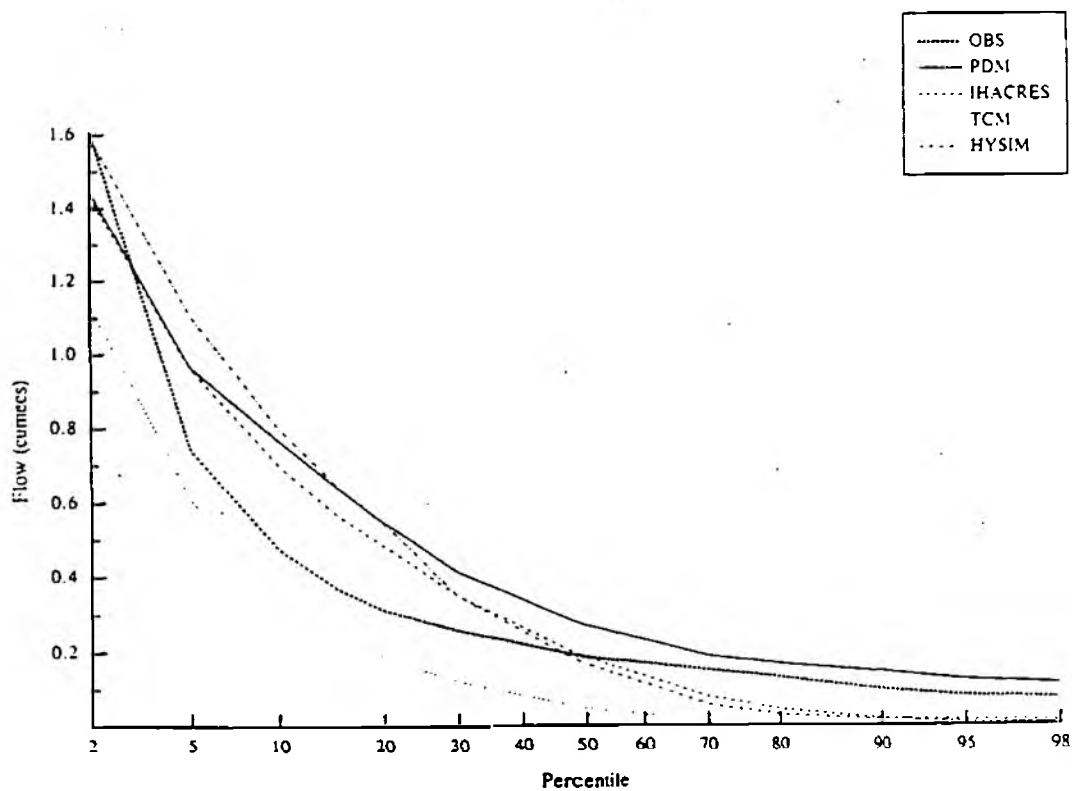


Figure A4.2: Calibration period: simulated and observed flow duration curves

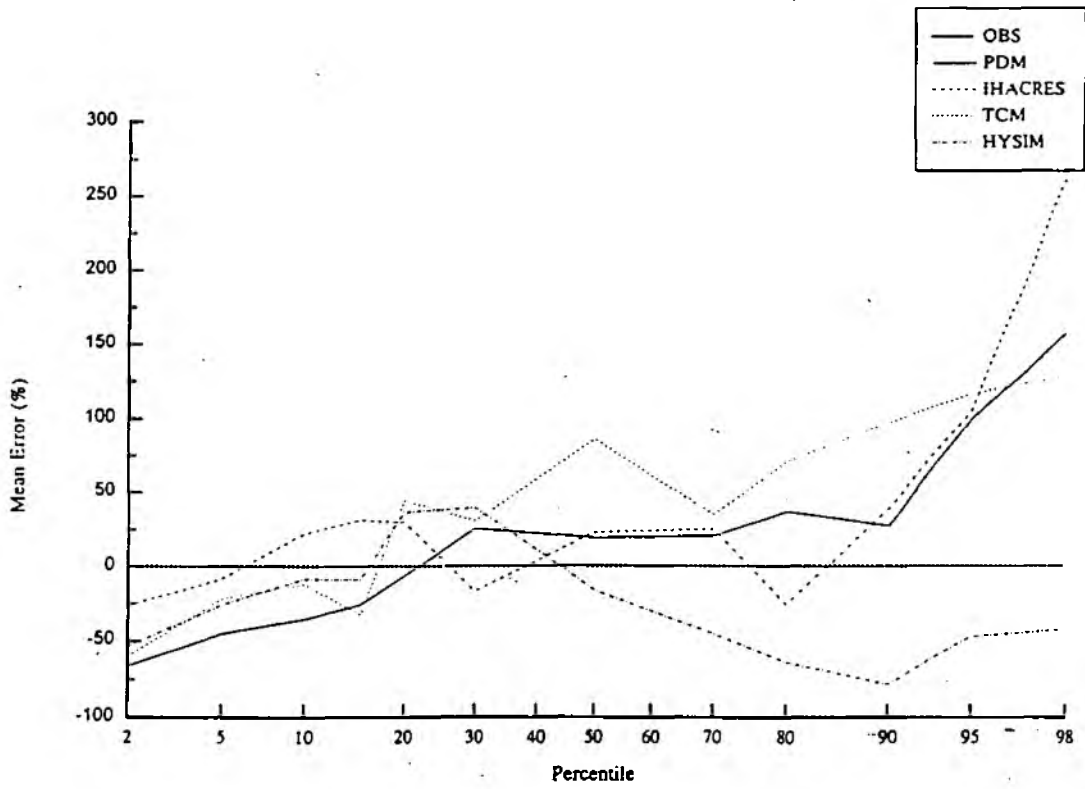


Figure A4.3: Calibration period: mean simulation errors at observed percentile points

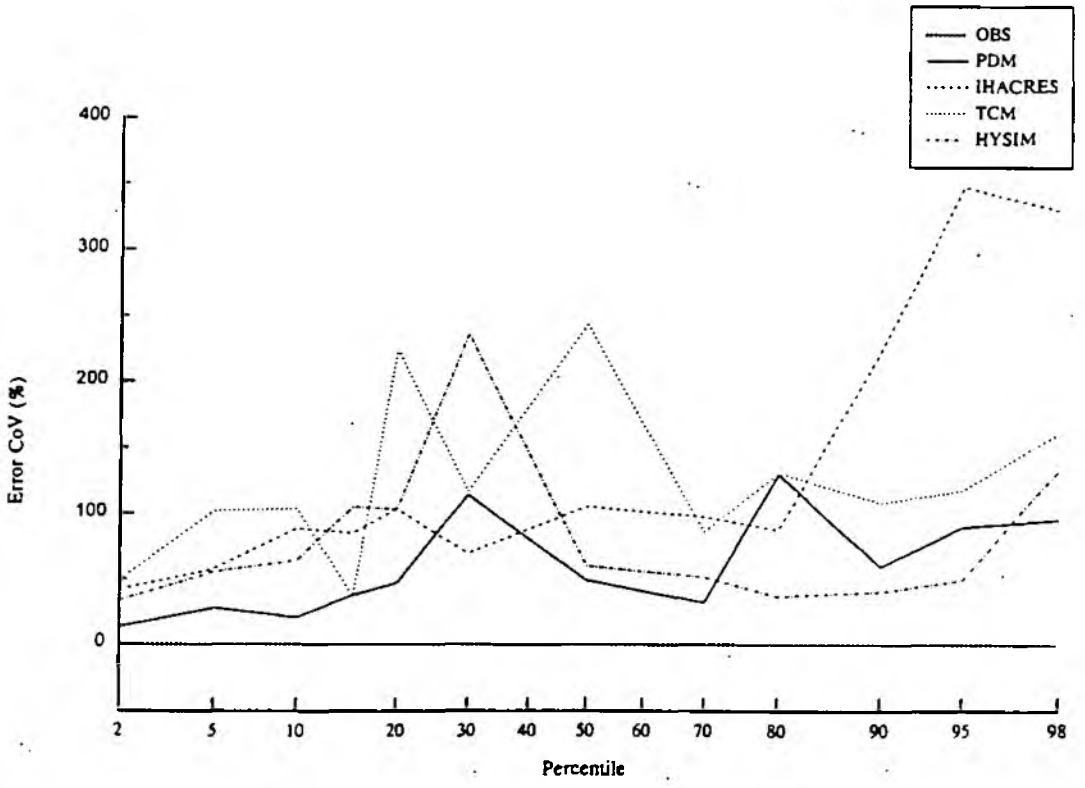


Figure A4.4: Calibration period: CoV for simulation errors at key percentile points

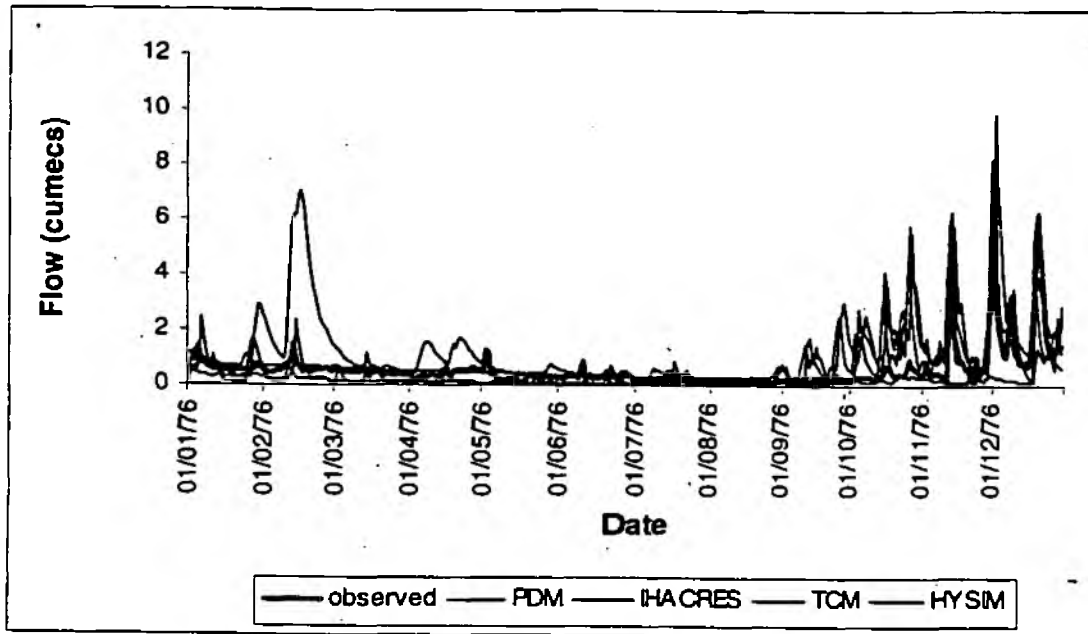


Figure A4.5: Evaluation period: observed and simulated hydrographs for 1992

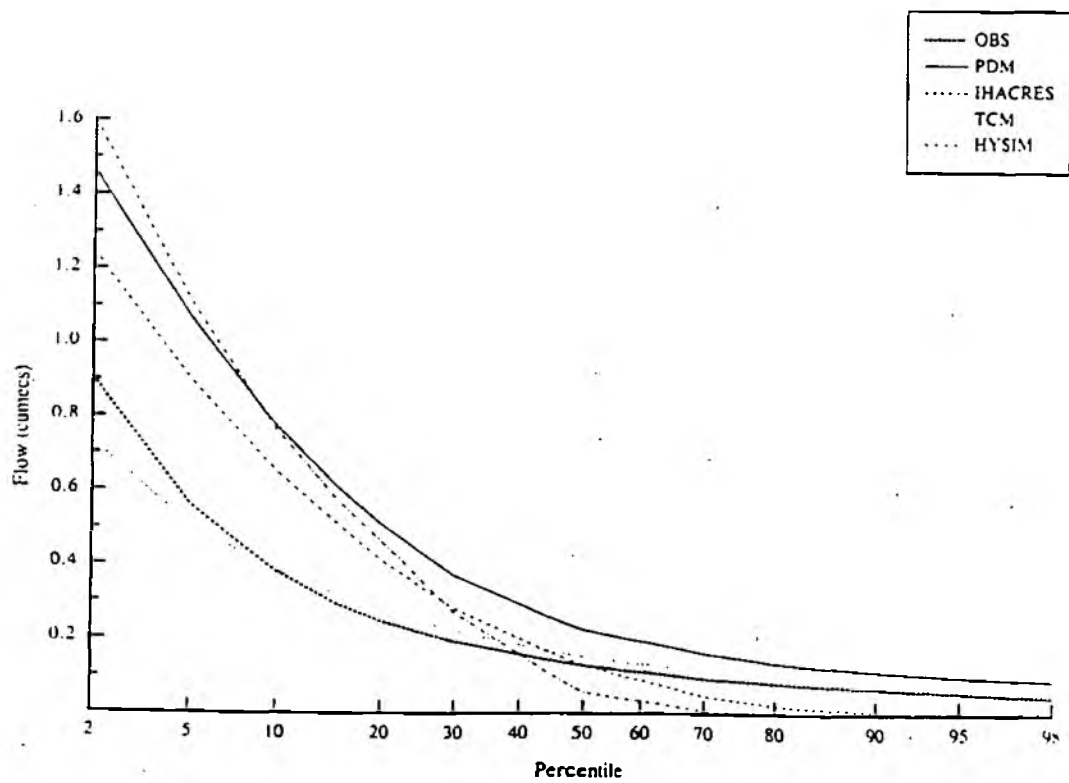


Figure A4.6: Evaluation period: simulated and observed flow duration curves

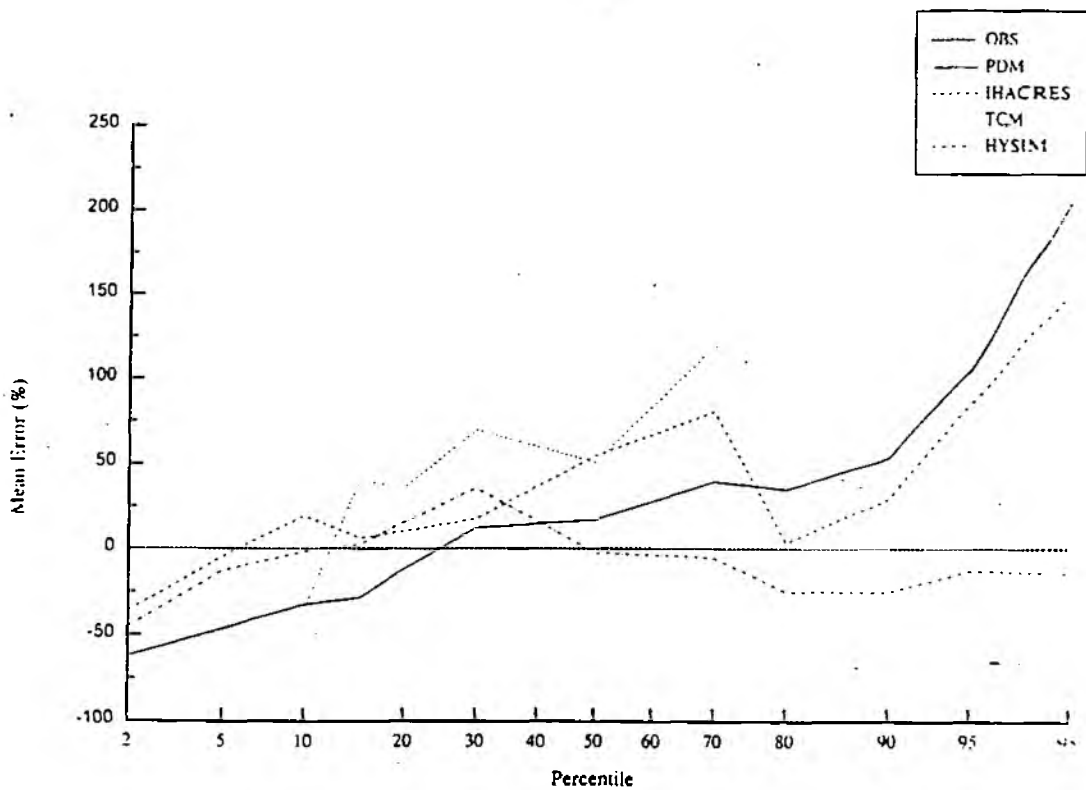


Figure A4.7: Evaluation period: mean simulation errors at observed percentile points

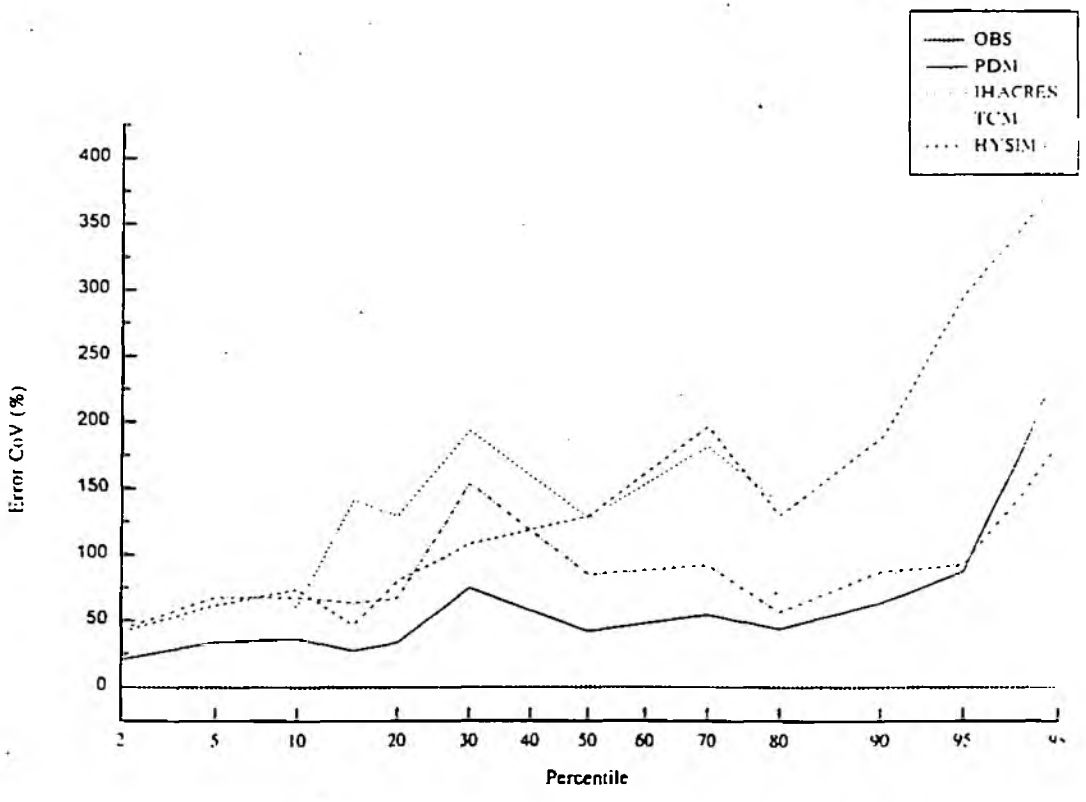


Figure A4.8: Evaluation period: CoV for simulation errors at key percentile points

A5 The Box at Polstead Bridge

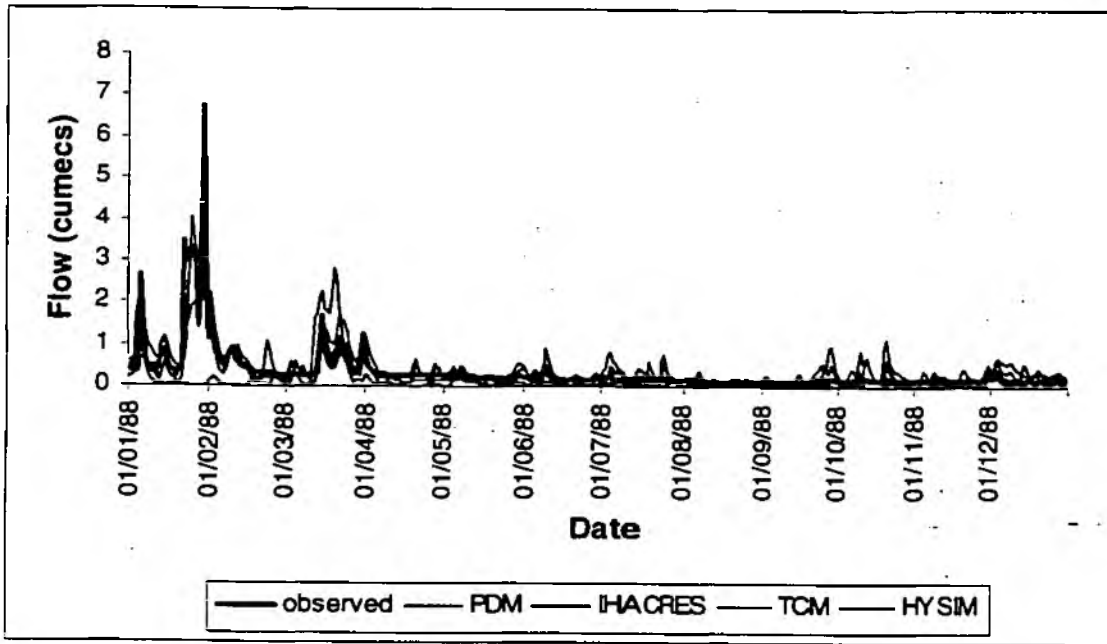


Figure A5.1: Calibration period: observed and simulated hydrographs for 1988

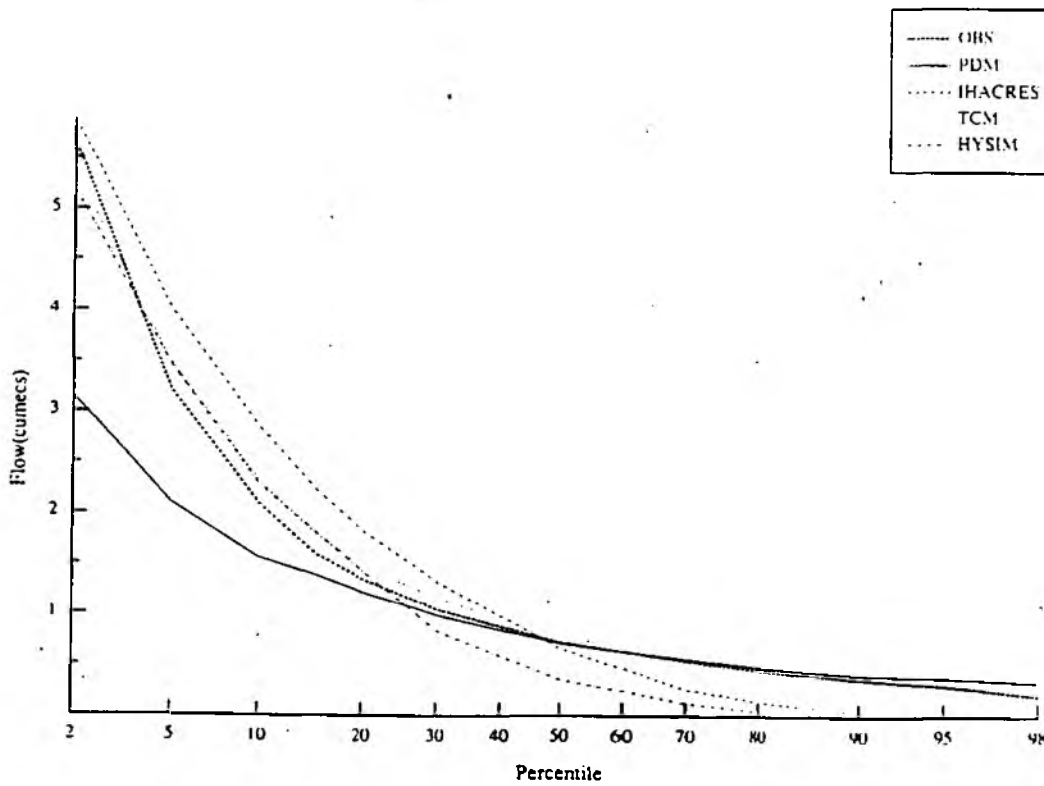


Figure A5.2: Calibration period: simulated and observed flow duration curves

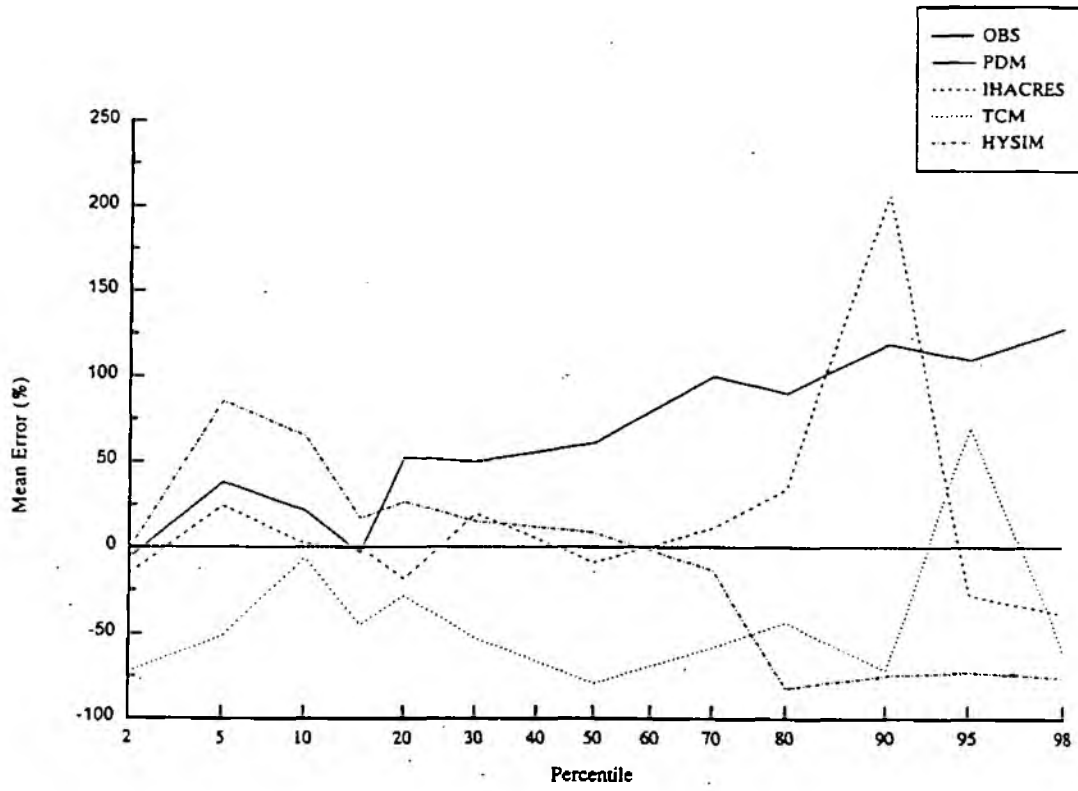


Figure A5.3: Calibration period: mean simulation errors at observed percentile points

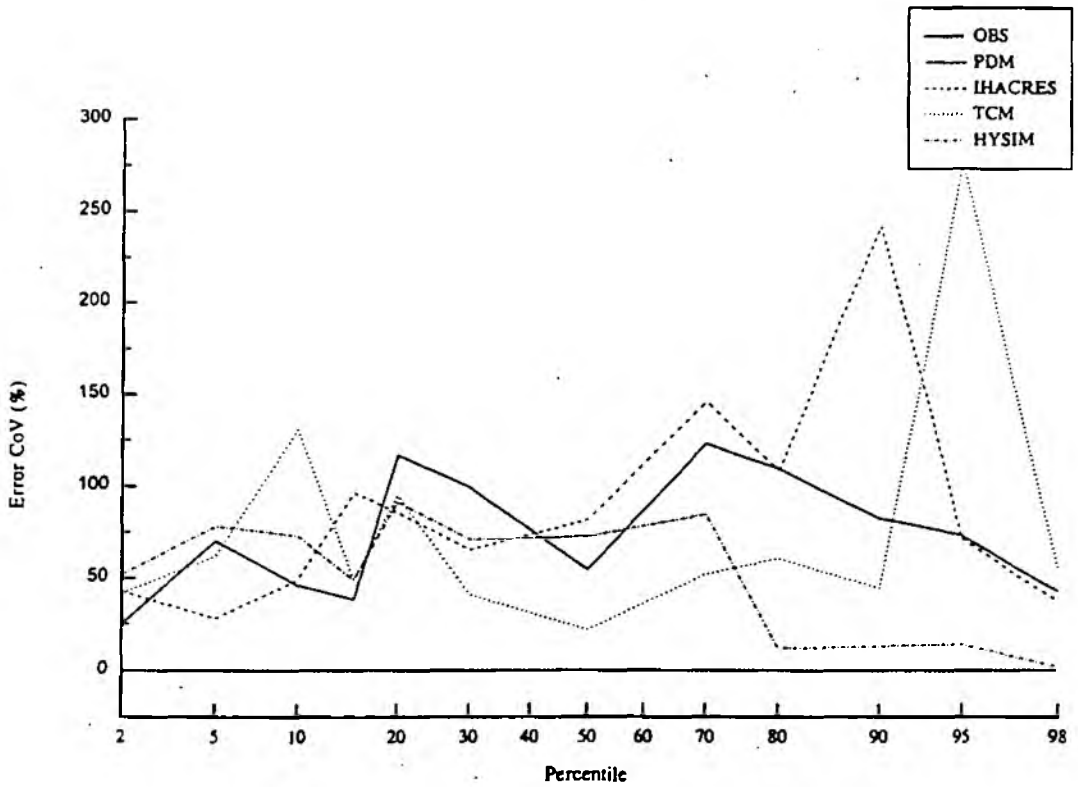


Figure A5.4: Calibration period: CoV for simulation errors at key percentile points

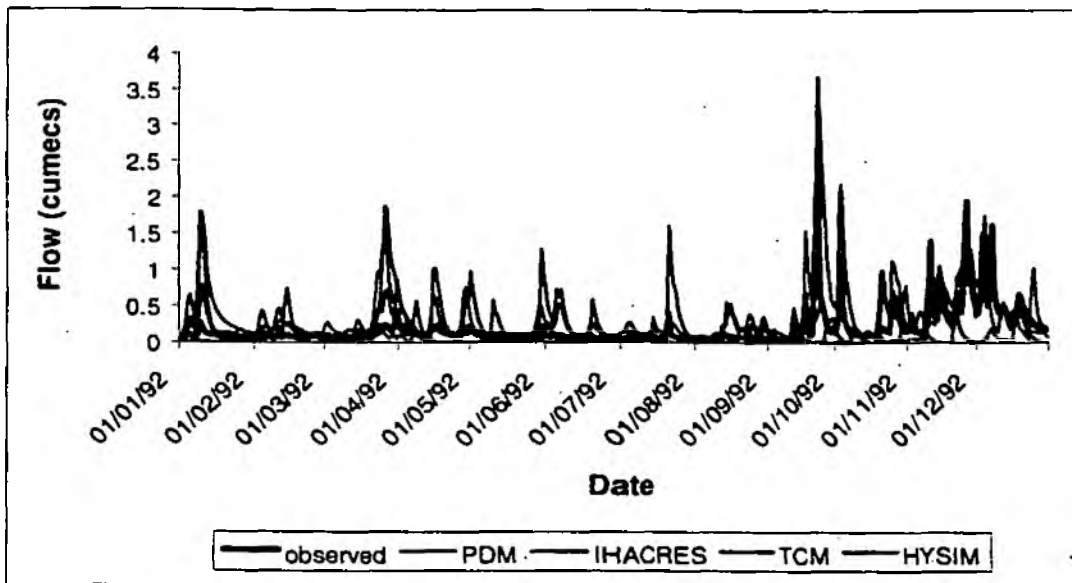


Figure A5.5: Evaluation period: observed and simulated hydrographs for 1976

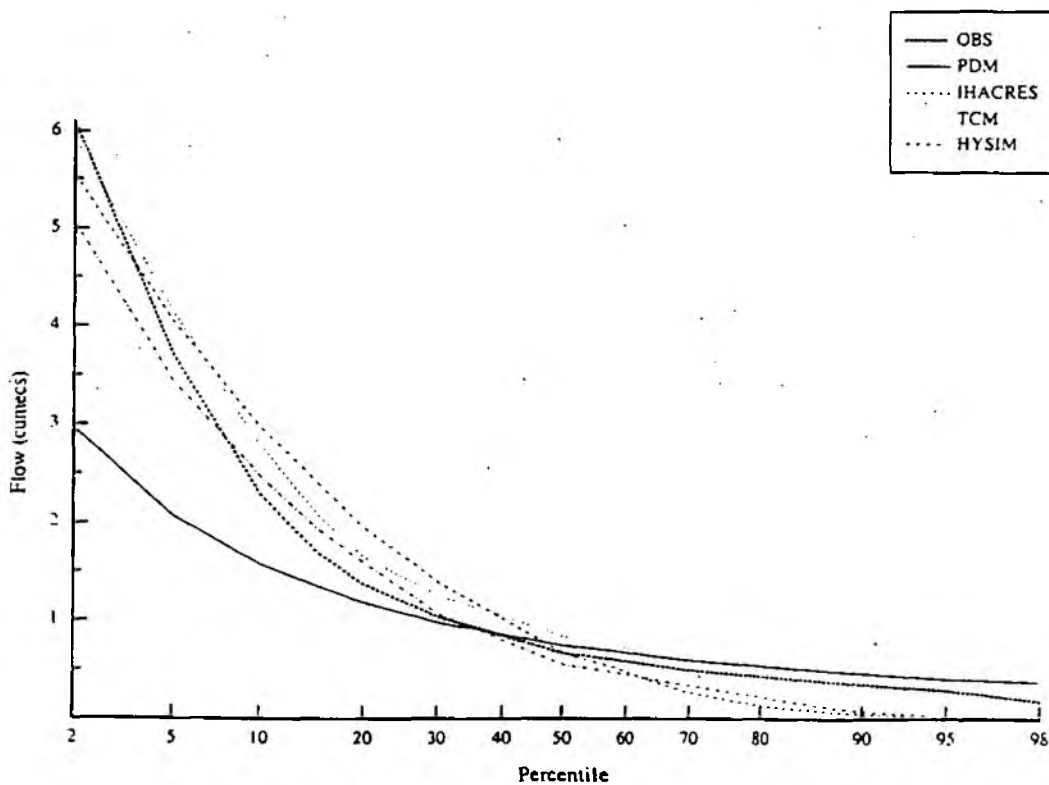


Figure A5.6: Evaluation period: simulated and observed flow duration curves

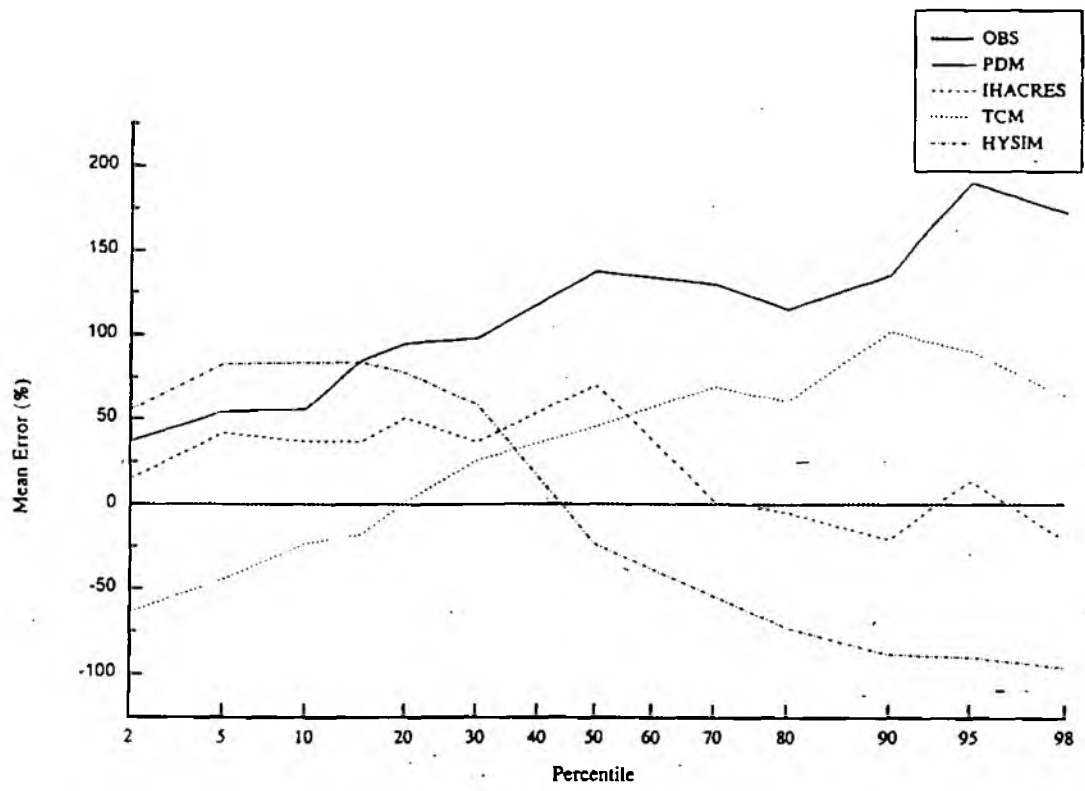


Figure A5.7: Evaluation period: mean simulation errors at observed percentile points

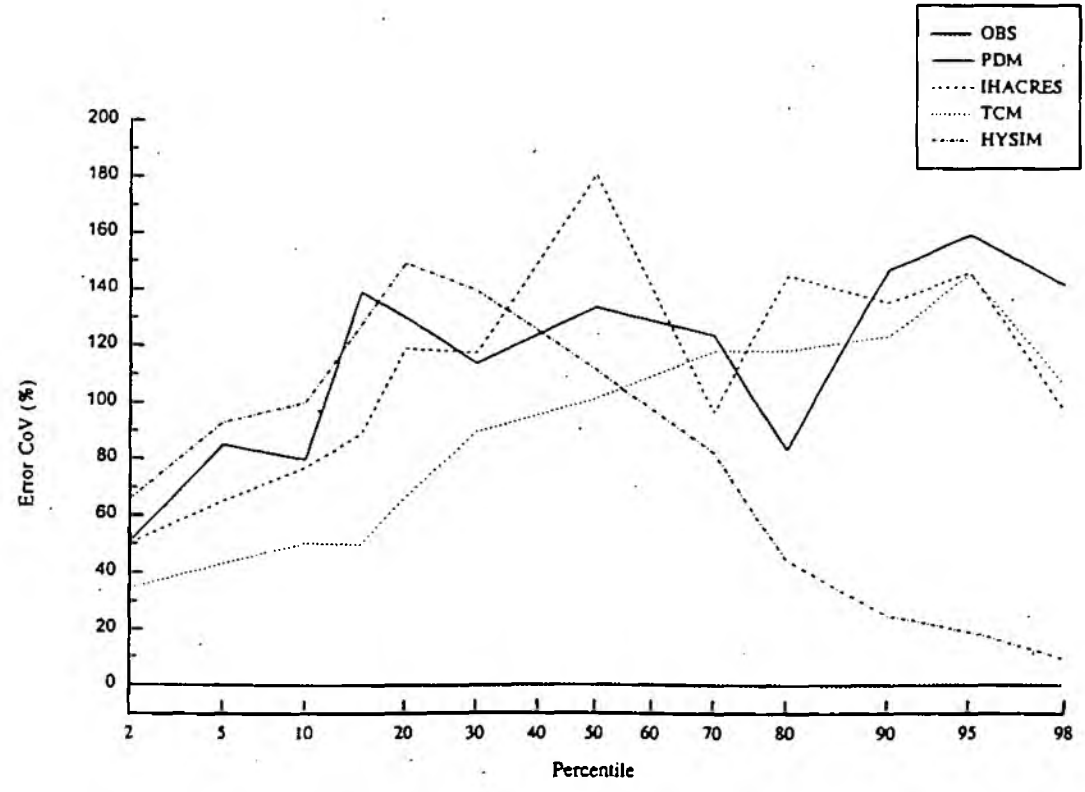


Figure A5.8: Evaluation period: CoV for simulation errors at key percentile points